DISSERTATION FOR THE DEGREE OF DOCTOR OF PHILOSOPHY (PHD)

Mechanisms and Consequences of Chronic Astrocytic and Neuronal Activation of Murine Mesopontine Regions

by Baneen Maamrah

UNIVERSITY OF DEBRECEN
DOCTORAL SCHOOL OF MOLECULAR MEDICINE

DEBRECEN, 2025

DISSERTATION FOR THE DEGREE OF DOCTOR OF PHILOSOPHY (PHD)

Mechanisms and Consequences of Chronic Astrocytic Activation in the Murine Mesopontine Regions

by Baneen Maamrah

Supervisor: Dr. Balázs Zoltán Pál

UNIVERSITY OF DEBRECEN
DOCTORAL SCHOOL OF MOLECULAR MEDICINE

DEBRECEN, 2025

Table of Contents

List of abbreviations:

AAV	Adeno-associated Virus
ChAT	Acetyltransferase
BG	Basal ganglia
ATP	Adenosine triphosphate
AD	Alzheimer's disease
AMPA	α-amino-3-hydroxy-5-methyl- 4-isoxazole propionic acid
BBB	Blood-brain barrier
BM	Barnes Maze
DREADD	Designer receptors exclusively activated by designer drugs
EPSCs	Excitatory postsynaptic currents
GABA	Gamma-aminobutyric acid
GFAP	Glial Fibrillary Acidic Protein
GPCRs	G protein-coupled receptors
GluN2B	A subunit of the NMDA receptor, involved in synaptic plasticity
CnF	cuneiform nucleus
hM3	Human muscarinic receptor
IHC	Immunohistochemistry
NeuN	Neuronal nuclear protein
NMDA	N-methyl-D-aspartate
PD	Parkinson disease
PPNc	Pars compacta
RAS	Reticular activating system
PPNd	Pars dissipata
PPN	Pedunculopontine nucleus
PrCnF	precuneiform nucleus
PSP	Progressive supranuclear Palsy
SCP	Superior cerebellar peduncle
SICs	Slow inward current
VTA	Ventral tegmental area
IPSCs	Inhibitory postsynaptic currents
MWM	Morris Water Maze
NFIA	Nuclear factor-I A
mGluR	Metabotropic glutamate receptor

1. Introduction

The mesencephalic locomotor region (MLR) acts as a crucial conduit, that link the brain's higher motor control centers to the lower motor neurons that facilitate movement. The main excitatory elements within the MLR, include the pedunculopontine nucleus (PPN), which is the largest component of MLR, and extended nuclei to it, and their activation has been proposed to produce different forms of movement. In previous studies, scientists found the MLR by demonstrating that electrical activation of this brain region could make decorticated cats walk (Shik et al., 1966). Recent researches using optogenetic techniques has shown that the motor action of the MLR depends on excitatory signals from glutamatergic neurons (Roseberry et al., 2016; Caggiano et al., 2018). MLR neurons regulate various aspects of movement. The cholinergic neurons of the PPN affect on muscle tone and modulate the acoustic startle response (Takakusaki et al., 2016; Vitale et al., 2019), while the glutamatergic neurons of the PPN are linked to exploration movements; additionally, the activity of glutamatergic neurons in the CnF correlates with movement velocity (Dautan et al., 2021; Huang et al., 2024). The PPN is an important part of the reticular activating system, which regulates activity cycles and overall brain states associated with REM sleep as well as consciousness by sending cholinergic and non-cholinergic projections to many subcortical regions (Mena-Segovia and Bolam, 2017). The changes observed can be related to the lesions of non-cholinergic neurons, as the targeted lesion of cholinergic neurons did not lead to learning impairments or modifications in the locomotor response to nicotine (MacLaren et al., 2016), Instead developed of sensorimotor and gait deficits (MacLaren et al., 2018).

Our previous study indicated that neuromodulatory effects on astrocytes produce tonic excitability changes depending on metabotropic glutamate and N-methyl-D-aspartate receptors in the mesopontine region. Although these effects were significant in in vitro studies, but in vivo impact has not been examined (Kovács and Pál, 2017).

Following to investigated the pathophysiological significance of regional astrocytic

tau protein expression and a reduction in cholinergic neuronal number in the region result in reduced startle response amplitude and gait abnormalities (MacLaren et al., 2018; King et al., 2021). These findings effectively modeled the brainstem-related symptoms observed in progressive supranuclear palsy (PSP).

2. Literature background

2.1. Astrocytic diversity: morphology and function in CNS

There are many different glial cell types in the adult central nervous system (CNS), such as astrocytes, oligodendrocytes, and microglia (Krencik et al., 2011). Astrocytes are one of the most common cell types in central nervous system. They play vital roles in maintaining the CNS and stability, including buffering ions, recycling neurotransmitters, maintaining the blood-brain barrier, and releasing gliotransmitters (Phatnani and Maniatis, 2015). However, different groups of astroglia perform these functions differently (Zhang and Barres, 2010).

2.1.1. Astrocyte-neuron interactions of brain function and dysfunction

The functions of glial cells, especially astrocytes, have been reconsidered for several decades. An increasing amount of research suggests that astroglial cells are significant not only in trophic support (Volterra and Meldolesi, 2005), but also in the brain's information processing and cognitive processes (Verkhratsky and Nedergaard, 2018; Kol et al., 2020). Gap junctions facilitate connections between astrocytes, forming astroglial networks that provide metabolic support to neurones. Studies conducted in the recent few years have demonstrated the role of disorders in astroglial connections in pathological nervous system lesions. It is of significant interest to study the morphological and functional modifications of astrocytic networks due to aging, diseases, or exposure to stress stimuli (Ridet et al., 1997; Charvériat et al., 2017). First, Rudolf Virochow described glial cells as a homogenous connective tissue that supports neuronal components. Later studies on the cell composition of the brain by Cajal et al. revealed that different parts of the brain include morphologically unique types of glia and neurones. In the last century, astrocytes have evolved into an important link between neurons and the external environment, supporting different physiological functions in the blood-brain barrier (BBB) formation, neuronal development, neural network function, neurotransmission, and metabolic assistance. Astrocytes maintain homeostasis in the brain by regulating the uptake of neurotransmitters, water, and amino acids. The end-feet structure of astrocytes forms the

neurovascular unit between endothelial cells and neurons. Astrocytes have complex processes for making tripartite synapses and covering synapses and can monitor the ongoing synaptic circuit local activities and regulate homo/heterosynaptic in several ways.

The neurotransmitter receptors expressed on astrocytes recognise and respond to synaptic activity by raising intercellular Ca^{2+} from astrocytes and producing neuroactive gliotransmitters which regulate synapses. Different approaches, including electrophysiological recordings, molecular biology methods, optogenetic and chemogenetic tools, and imaging by confocal microscopy, play a role in the study of astrocytes. By obtaining a deeper understanding of these cells, researchers have sought to understand their complexity and use their capacity to develop treatments for neurological disorders.

2.1.2. Astrocyte-neuron interactions and their role in brain homeostasis

Astrocytes in the brain are the primary regulatory glial cells that play a variety of roles in maintaining brain homeostasis. These roles include preventing increase of extracellular potassium producing and storing gliotransmitters, providing growth factors, nutrients, and antioxidants to neurons, and regulating the immune response and iron homeostasis in the brain (Jha et al., 2018).

The production and upregulation of numerous gliotransmitters, including ATP, D-serine (Takano et al., 2007), and glutamate, by astrocytes modulate paracrine signalling between astrocytes and neurons, pericytes, microglial cells, and endothelial cells. Cellular crosstalk (Fig.1) between microglia, astrocytes, oligodendrocytes, pericytes, endothelial cells, and neurons has pathophysiological significance in the pathogenesis of neurodegeneration (Abbott, 2002; Lo and Rosenberg, 2009; Choi et al., 2014).

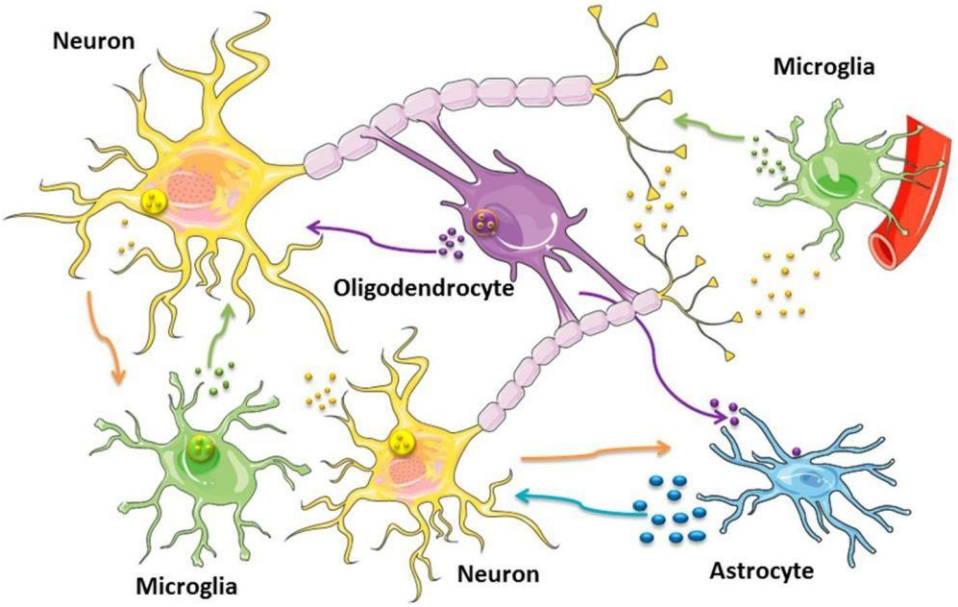

Fig. 1. An overview of astrocytic functions: By supplying energy sources, strengthening antioxidant defense, and astrocytes-neuronal function. Their capacity to sense cytokines released by microglia and engage in neurovascular connections makes are crucial part of the interactions between different types of brain cells during the immune response (Riva et al., 2019).

Glutamate is a gliotransmitter and the most common excitatory amino acid neurotransmitter in the central nervous system, which mediates rapid excitatory transmission by activating metabotropic glutamate receptors (mGluRs) as well as ionotropic receptors like AMPA (α-amino-3-hydroxy-5-methyl-4-isoxazole propionic acid, NMDA (N-methyl-D-aspartate), and kainate receptors. Astrocytes play a crucial role in maintaining extracellular glutamate levels (Rose et al., 2018). Astrocytes that surround the glutamatergic synapse show significant amounts of excitatory amino acid transporter-1 (EAAT-1), glutamate reuptake transporters, and EAAT-2. Astrocytes remove approximately 90% of the glutamate existing in the synaptic cleft via EAAT-1 and -2 transporters to prevent glutamate accumulation and excitotoxicity (Lewerenz and Maher., 2015; Gonçalves et al., 2019).

Astrocytes can control neuronal function in different ways, and the regulation of tonic inhibition might be particularly crucial. The gamma-aminobutyric acid (GABA)-related suppression of neuronal activity consists of both tonic and phasic components. When the

vesicular is released from the presynaptic axon terminal, transient and discrete inhibitory postsynaptic currents (IPSCs) form the phasic component. Low-affinity $GABA_A$ receptors in synapses mediate these currents. In contrast, high-affinity, slowly desensitising extrasynaptic $GABA_A$ receptors exposed to low ambient GABA concentrations mediate persistent tonic GABAergic inhibition (Belelli et al., 2009). It has been shown that tonic inhibition is very crucial. Tonic inhibition significantly affects the excitability of both individual neurones and networks by modifying the membrane conductance of the postsynaptic neurons (Semyanov et al., 2004). Furthermore, tonic inhibition has become increasingly common in the treatment of pathophysiological disorders such as stroke (Clarkson et al., 2010) and epilepsy (Cope et al., 2009).

Many studies have explained the interaction between cellular and subcellular GABAergic and glutamatergic systems (Héja et al., 2006; Liang et al., 2006; Somogyi, 2006; Gutierrez and Heinemann, 2006; Eulenburg and Gomeza, 2010), and previous research has demonstrated that glutamatergic and GABAergic neurotransmission directly interact at the molecular level. They discovered that the absorption of Glu increases the extracellular level of GABA both in vitro and in vivo. The direct connection between excitatory and inhibitory neurotransmitter transporters was found to be independent of glutamate decarboxylase activity, external Ca^{2+} presence, or depolarization mediated by the Glu receptor. It was eliminated when glial Glu or GABA transporter non-transportable blockers were found, suggesting that the process was driven by the concerted action of these transporters (Héja et al., 2009). Glutamate is coupled with the subsequent reversal of glial GABA transporters, which elevates the amount of extracellular GABA (Fig.2). As a result, they were able to show GABA signals resulting from glial Glu uptake for the first time. By measuring GABA uptake and release in rat brain slices and cultured mouse neurones, the presence of this Glu- GABA exchange pathway has been found both in vitro and in vivo in the rat hippocampus using brain suspensions from various parts of the rat or human brain, including the choroid plexus, spinal cord, corpus callosum, cortical gray and white matter, and hippocampus.

They showed that all the identified Glu transporter substrates could cause the release of GABA, but not non-transportable inhibitors (Héja et al., 2009).

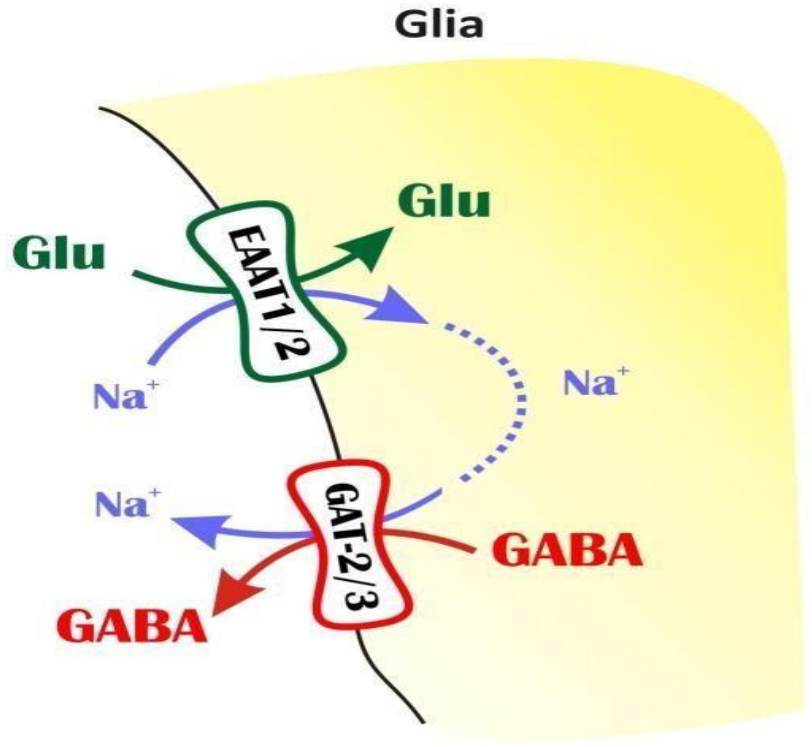

Fig. 2. Graphical representation of the hypothesised glutamate-GABA exchange mechanism (Héja et al., 2009).

2.1.3. The active role of astrocytes in synaptic communication

Astrocytes control the growth and plasticity of synapses by a range of secretory and contact-mediated signals (Araque et al., 1999). Astrocytes are believed to regulate the development of excitatory synapses and synaptic activities in the developing and adult brain as a component of tripartite synapses, including postsynaptic and presynaptic terminals (Araque et al., 2014; Adamsky et al., 2018). Many studies have demonstrated that astrocytes in different areas of the brain are not the same, and that astrocytes located next to each other in the same brain region could have differences.

Research has indicated that astrocytes can modulate firing synaptic structure and function, as well as synaptic transmission, by releasing gliotransmitters as a result of Ca^{2+} influx, such as D-serine and glutamate (Araque et al., 2014). Through both ionotropic and metabotropic signalling cascades, astrocyte receptors are connected to intracellular ionic signalling and astrocyte metabolism. Astrocytes receive neurotransmitter and neuromodulator signals from

synapses through a variety of receptors. The expression of these receptors is likely regulated by the local neurotransmitter environment (Verkhratsky and Nedergaard, 2018). The CNS contains a variety of cell types which express metabotropic glutamate receptors (mGluRs) in different ways. Three subgroups have been identified based on sequence homology and cellular signalling activation (Gerber et al., 2007), and eight different mGluR subtypes have been identified.

As glutamate regulates both neuronal cell excitability and synaptic transmission via the second messenger signalling pathway, mGluRs are significantly associated with the control of neuronal firing and synaptic transmission throughout the CNS (Sladeczek et al., 1985; Sugiyama et al., 1987). They control the metabolism of energy to maintain neuronal activity, particularly those involved in memory formation (Henneberger et al., 2010; Bazargani and Attwell, 2016). Additionally, memories can be categorised according to the kind of information that is transmitted and stored, which divides memories into two categories: implicit (non-declarative) and explicitly referred to as declarative in humans (Squire, 2004). In general, astrocyte Ca^{2+} dynamics stimulated and downstream effects on learning and memory can be investigated by activating Gi or Gq-GPCR signalling with hM4Di and hM3D(Gq) DREADDs or (Gq-coupled melanopsin) (Roth, B. L. 2016; Mederos et al., 2020). Using hM3D(Gq) DREADD like, indicates that improving astrocyte Ca signalling enhances spatial and T-maze, and fear conditioning tests show context-dependent memory formation. Furthermore, the role of hippocampal astrocytes in spatial memory has been demonstrated using a melanopsin-based method to temporally trigger Gq activation in astrocytes (Adamsky et al., 2018; Nagai et al., 2021). Alternatively, in a learning by association test including initiated fear conditioning, triggering the Gq-GPCR pathway in the central amygdala through astrocytes using the same hM3Dq method decreases the firing of neurons by astrocyte-derived ATP release along with reduced fear reactions (Martin et al., 2017).

The role of astrocytic Gs-GPCR signalling in learning and memory has also been studied in association with aging and dementia in mice. It has been discovered that memory

impairments are coupled with higher levels of ATP, A2A in hippocampus astrocytes in Alzheimer's disease patients, and mice used as Alzheimer's disease models. In mice, both young and old, learning is not affected by the expression and activation of the human Gs-coupled 5-HT4b serotonin receptor Rs1, which leads to a decrease in long-term memory retention. Conversely, adult wild-type and old AD mice have improved memory when astrocytic A2A receptors are genetically reduced (Orr et al., 2015).

2.1.4. Astrocyte and gliotransmitters contribution in excitotoxicity function

Glial cells, such as astrocytes, are completely integrated into networks of neurons to form a single, functional regulatory circuit that is necessary for brain activity. This has led to a significant advancement in the field of neuroscience regarding how the brain processes information; although astrocytes lack electrical excitability across their membrane, they effectively handle ions in response to various stimuli, which is necessary for the proper control of the physiological processes that are regulated by the brain (Verkhratsky and Nedergaard, 2018). The astrocyte volume changes are related to Cl^{-1} permeability, whereas internal K^{+1}, Na^{+1}, Ca^{2+}, and H^{+1} fluctuations are associated with enhanced synaptic activity. Strong evidence indicates that the connection between astrocytes and neurons is Ca^{2+} dependent (Araque et al., 2014; Savtchouk and Volterra., 2018). Two important methodological that have facilitated the understanding of gliotransmission, other astrocytic functions (calcium imaging), and advanced optical microscopy (Li et al., 2013).

Gliotransmitters can modulate synaptic transmission and plasticity, including glutamate, neurosteroids, adenosine triphosphate (ATP), inflammatory mediators, and GABA, can modulate synaptic transmission and plasticity. Synaptic transmission, neuronal networks, cerebral blood flow, synchronisation, and immunoinflammatory responses in the brain are all regulated under physiological conditions and the release of gliotransmitters (Volterra and Meldolesi, 2005).

2.1.5. Astrocytes as therapeutic targets in neurodegenerative diseases

Astrocytes play an essential role in the regulation of gliotransmitters, and neurotransmitters are involved in excitatory neurotransmission (mostly glutamate), which is required for the control of both long-term potentiation and long-term depression, and is important for both synaptic transmission and plasticity, leading to astrocyte participation in cognition and related memory functions (Dallérac and Rouach, 2016). Additionally, synaptic structural remodelling and functional plasticity are mediated by astrocytes (Santello et al., 2019). These findings, astrocytes may be promising new therapeutic targets for restoring cognitive function before dementia develops (Dallérac and Rouach, 2016).

Studies discussing the transcriptional patterns of astrocytes in multiple regions of the brain have indicated that astrocytes exhibit significant molecular heterogeneity. While the functional implications of these variations remain unclear, understanding astrocytic subtypes is helpful in directing the development of astrocyte-based therapeutics (Krencik and Zhang, 2011). The process known as "reactive astrogliosis," which is characterised by elevated levels of GFAP and inflammatory pathways triggers astrocyte activation in the early stages of many neurological disorders, leading to an increased release of inflammatory cytokines and changes in astrocyte morphology (Colangelo et al., 2014).

Astrocytes undergo changes with ageing. Despite changes in their structural shape and branching (Robillard et al., 2016; Popov et al., 2021), studies have shown changes and how they function. Specifically, the propagation of calcium signals and a reduction in how astrocytes respond have been observed along with modifications in their electrical membrane characteristics (Popov et al., 2021). In aged rodents, the connection between astrocytes and neurons that use glutamate decreases, similar to the general degradation of neural function. The ability of astrocytes to remove glutamate, their response when mGluR5 receptors are activated, and the strength of excitatory postsynaptic currents (EPSCs) decrease with age. Simultaneously, the concentration of glutamate outside the cells increased. However, researchers did not find any age-related changes in astrocytic calcium waves or in neuronal

responses that depend on NMDA receptors when astrocytes are activated (Gómez et al., 2017). Our previous study showed that slow inward currents (SICs), which are excitatory events in neurons, are elicited when astrocytic glutamate activates extrasynaptic NMDA receptors, that exist in mice at all ages, showing a gradual decline with age. These SICs can induce spike timing-dependent plasticity (STDP) in mice. In humans, SICs exhibit slower dynamics and a larger transfer of charge compared to mice. Age-related changes in SICs are stronger in humans, as they are undetectable in samples from patients over 70 years of age. Moreover, human SICs appear to contribute to synaptic plasticity. The effect of slow inward currents (SICs) on synaptic plasticity differs between humans and mice. In mice, the effects of SICs on synaptic plasticity are affected by aging. This might be from reduced mGluR5 signalling or age-related changes in NMDA receptors. However, in humans, SICs themselves are affected by age (possibly through changes in glutamate release or uptake or in NMDA receptors).

This finding showed a moderate but significant reduction in the density of GluN2B subunits, which could contribute to the decrease in SIC activity and how synapses respond to SICs (Fig.3). However, this limited decrease suggests that other factors are also involved. These observations demonstrate the significant differences in brain aging between mice and humans (Csemer et al., 2023).

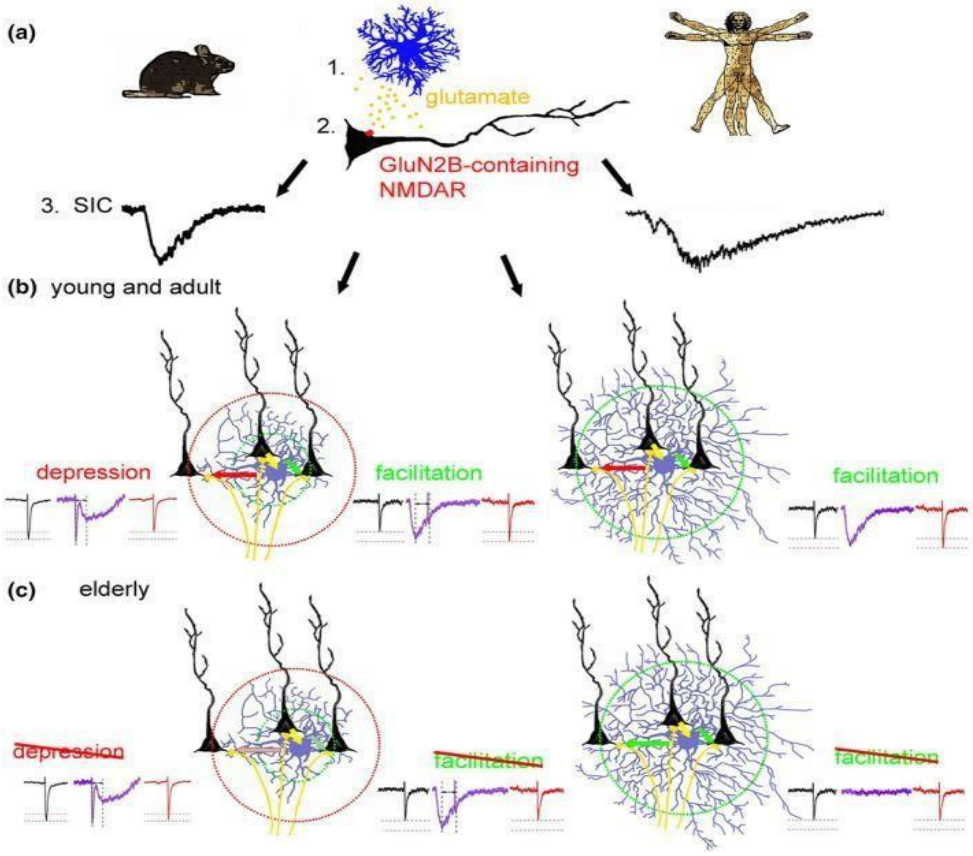

Fig. 3. Comparison of human and murine SICs. (A). Slow inward currents (SICs) in both mice and humans arise from astrocytic glutamate release and subsequent activation of (1) neuronal GluN2B-containing NMDA receptors (2), although their amplitude and kinetic properties vary between species (3). B. These SICs play a role in synaptic plasticity: young and adult mice (left) exhibit either timing-dependent synaptic depression or potentiation, potentially influenced by the synapse's proximity to astrocytic glutamate release, whereas humans (right) demonstrate only potentiation, possibly because of their more complex astrocyte morphology. C. furthermore, aging impacts this process, reducing SIC-mediated synaptic plasticity in mice due to altered synaptic responsiveness, whereas in humans, the SICs themselves are directly affected by aging. (a) Slow inward currents (SICs) resulting from the release of glutamate by astrocytes (1) and the activation of neuronal NMDA receptors containing GluN2B subunits (2) in both mice (left) and humans (right; indicated by symbols). Murine and human SICs exhibit variations in their size and speed-related characteristics (3). B. In young and adult mice (left), synaptic weakening or strengthening, which depends on the timing of signals, occurs, possibly related to how far synapses are located from where astrocytes release glutamate. In humans (right), only strengthening of synapses was observed, which might be due to the intricate structure of the astrocytes. C. In aged mice (left), synaptic plasticity induced by SICs decreases because of alterations in the synapse response. In contrast, in humans (right), SICs are affected by the aging process (Csemer et al., 2023).

Aged astrocytes may cause inflammation and have a direct effect on the health and function of other CNS cell groups according to their interactions with them. Many age-related diseases, such as neurodegenerative disorders, have become more common with increasing age. Several characteristics of neurodegeneration and aging are similar, including gliosis, myelination loss, cognitive impairment, memory function loss, and astrocyte disruption (Palmer & Ousman, 2018) (Fig.4).

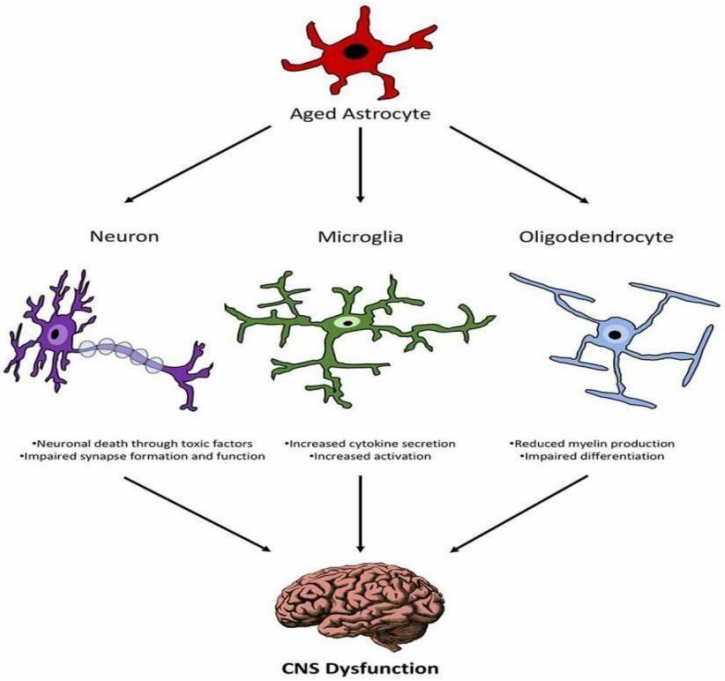

Fig. 4. Schematic showing the interaction between astrocytes and other central nervous system cells during aging (Palmer and Ousman, 2018).

2.1.6. The astrocytic overstimulation methods

Experimental animal models of human neurological conditions provide excellent experimental in-vivo tools that facilitate the study of many different aspects of these disorders. These models enable the development of disease states by disrupting specific biological processes. Optogenetics and chemogenetics provide new opportunities that are not possible using other animal models of human brain disorders. These strategies allow researchers to induce neuropathological conditions that vary in severity, from acute to chronic (Viktoriya et al. 2024).

Optogenetics is a new biological approach that uses several light-sensitive proteins known as

opsins, including microbial ion channels, ion pumps, and engineered G protein- coupled receptors (GPCRs) (Boyden et al., 2005; Tye and Deisseroth. 2012). After absorption of a specific wavelength of light, opsin undergoes a conformational change that causes several biological processes in cells that express opsin. Some opsins cause ions to move across the cell membrane, whereas others activate internal signalling pathways, such as those involving G proteins. Since the absence of most of these opsins in experimental model organisms and the low effect of photo-stimulation on cells and tissues, optogenetics has been used as a powerful technique for manipulating specific cell populations both in vitro and in vivo through a combinatorial strategy involving cell type-specific promoters as well as in genetic modifications (Fig.5).

This method allows the modification of cellular activity with millisecond-scale temporal precision. This precise stimulation has made it possible to show direct cause-and-effect relationships between manipulated cell activity and what happens as a result, especially when studying the brain circuits that control specific behaviours (Boyden et al., 2005).

Chemogenetics depends on modified proteins, including GPCRs and ligand-gated ion channels, that are no longer responsive or only very weakly responsive to their endogenous ligands but strongly respond to synthetic chemical ligands that are biologically inert (Armbruster et al., 2007; Dong et al., 2009; Nichols and Roth. 2009). The definition of hM3Dq, is a designer receptor exclusively activated by designer drugs (DREADDs), is produced through several cycles of randomised mutagenesis of the human M3 muscarinic receptor associated with the Gq protein (Armbruster and Roth. 2005). It is neither responsive to the endogenous muscarinic cholinergic receptor ligand acetylcholine, nor is it constitutively active; however, it is significantly activated by the synthetic ligand CNO (Armbruster et al., 2007; Dong et al., 2009). When CNO binds to hM3D(Gq), it can make neurons more excitable, leading to burst-like firing (Alexander et al., 2009; Krashes et al., 2013). Therefore, it is the most employed chemogenetic tool for neuronal activation. hM4Di, another DREADD

molecule, is a modified of the Gi-coupled human M4 muscarinic receptor that is activated by CNO (Armbruster et al., 2007; Nawaratne et al., 2008; Atasoy et al., 2012). When this CNO binds to hM4Di, it activates the Gβγ subunit of the Gi protein, which later stimulates the G protein to inwardly rectify potassium channels, leading to potassium efflux and significant hyperpolarisation when expressed in neurones (Reuveny et al., 1994; Kunkel and Peralta. 1995). That means hM4Di has been used to inhibit both spontaneous and depolarization-induced neuronal activity (Armbruster et al., 2007).

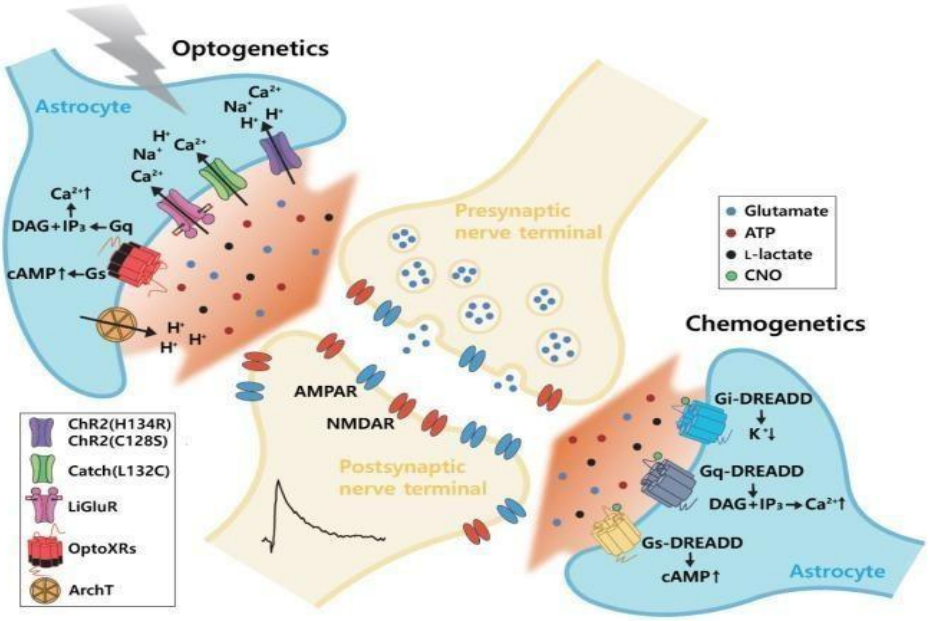

Fig. 5. Comparative mechanisms of optogenetics and chemogenetics in astrocytes and neuronal modulation. Scientists use optogenetic (left) and chemogenetic (right) methods to stimulate astrocytes by employing various genetically encoded molecules that can affect the levels of ions (H^{+1}, Na^{+1}, Ca^{2+}, and K^{+1}) and signalling pathways (Gq, Gs, DAG, IP3, and cAMP) inside these cells. (1) These changes within astrocytes, such as increased calcium and acidity, cause them to release signalling molecules called gliotransmitters (glutamate, ATP, and L-lactate). (2) These gliotransmitters can change how excitable nearby neurons are and how they communicate at synapses. (3) Optogenetic tools are activated by specific types of light, whereas chemogenetic tools are activated by artificial molecules such as CNO. Some examples of these tools include: ChR2 (channelrhodopsin-2), CatCh (calcium translocating channelrhodopsin), LiGluR (light-gated ionotropic glutamate receptor 6), ArchT (archaerhodopsin), OptoXRs (light-driven chimeric G protein-coupled receptors) for optogenetics; and Gi-DREADD (Gi-coupled designer receptors exclusively activated by designer drugs), Gq-DREADD (Gq-coupled DREADD), and Gs-DREADD (Gs-coupled DREADD) for chemogenetics, which are activated by CNO (clozapine-N-oxide). The released gliotransmitters can then interact with receptors on

neurons, such as the N-methyl-D-aspartate receptor (NMDARptor) and α-amino-3-hydroxy-5-methyl-4-isoxazolepropionic acid receptor (AMPAR). Other signalling molecules involved include adenosine triphosphate (ATP), IP3 (inositol 1,4,5-trisphosphate), diacylglycerol (DAG), and cAMP (cyclic adenosine monophosphate). (Alexander et al., 2009; Krashes et al., 2013).

2.2. The pedunculopontine nucleus in health and disease

The pedunculopontine nucleus (PPN) and the nearby cuneiform nucleus (CnF) comprise the mesencephalic locomotor region (MLR), which is the first locomotor region to be identified and present in all classes of vertebrates (Shik et al., 1966; Shik, Severin and Orlovskiĭ, 1966). In addition, the PPN is also part of the reticular activating system regulating global brain states (Mena-Segovia and Bolam, 2017).

The PPN has been involved in motor function in many different independent investigations conducted over the past few decades, both in humans and in animal models. It has been suggested that this nucleus could be a potential new target for treating motor symptoms in Parkinson's disease (PD) was first raised in 1989 (Mitchell et al., 1989), specifically because of altered PPN activity in a parkinsonian model of non-human primates, which has crucial therapeutic implications. The PPN is considered to regulate both waking and rapid eye movement (REM) sleep. It is recognized that the PPN is an important part of the reticular activating system (RAS) (Mena- Segovia and Bolam, 2017). Pars compacta (PPNc) and pars dissipatus (PPNd) are the two subnuclei that comprise the human PPN. Small- and medium-sized neurons are spread across the superior cerebellar peduncle (SCP), and central tegmental tract, forming the PPNd, which consists of a compact cluster of massive neurons (Olszewski and Baxter, 1995). Although cholinergic neurons also contain neuropeptides and a novel neuromodulator, the PPNc and PPNd also have GABAergic inhibitory neurons (Vincent et al., 1983; Bevan and Bolam, 1995).

2.2.1. Astrocytes and neuromodulatory mechanisms in the PPN

As reviewed by Katona and Freund (2012), endocannabinoids modulate multiple signalling pathways and synaptic connections, which have different effects on brain activity.

Cannabinoid type 1 (CB1), receptor stimulation may affect sleep-wake cycles, among other factors. The prototypical endocannabinoid anandamide administered intracerebroventricularly or directly to the PPN, reduced wakefulness and increased both Slow-Wave Sleep and REM sleep, based on in vivo animal studies. Although anandamide's effect on sleep may be reversed by CB1 receptor antagonists, it is believed that these endocannabinoids affect sleep modulation by acting on CB1 receptors (Herrera et al., 2010; Murillo, 2008).

Our laboratory previously showed the presence of SICs after astrocytic activation in the PPN, resulting in stimulation of a population of neurones, inhibition of another population, and no change in the third population (Fig.6). Several neurons synchronise the slow inward currents (SICs) that are produced in the brain cortical areas, but this synchronisation has not been observed in brainstem areas such as the PPN (Kovács and Pál, 2017).

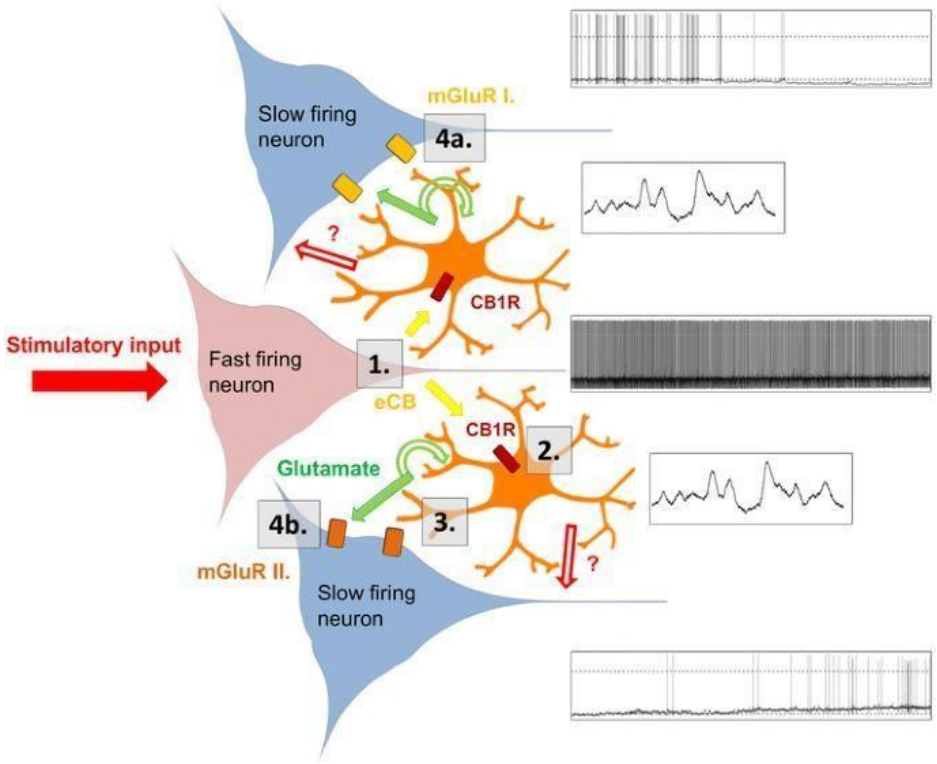

Fig. 6. Diagram showing the endocannabinoid signalling hypothesis for PPN. (1) Endocannabinoids (ECB) are produced by the active PPN neurones. (2) CB1 receptors in astrocytes are activated by endocannabinoids. In addition, astrocytes release gliotransmitters such as glutamate and increase the frequency of their calcium waves. Glutamate can either hyperpolarizes neighbouring neurones by activating group I metabotropic glutamate receptors (4a) or depolarizes neurones through group II mGluRs (4b). Astrocytic glutamate receptors (hollow

green arrows) may also be activated by Glu. Therefore, these astrocytic mGluRs may cause changes in gliotransmitter release ((Kõszeghy et al., 2015).

We have shown that both neurons and glial cells within the PPN respond to agonists that activate CB1 receptors (Kõszeghy et al., 2015). The response in neurons can be either depolarization or hyperpolarization (Fig.7), whereas astrocytes show a greater frequency of calcium waves, and none of these effects is observed in mice deficient in the CB1 gene. The hyperpolarization is prevented by blocking group I metabotropic glutamate receptors (mGluRs), whereas blocking group II mGluRs prevents depolarization.

The neuromodulatory agents, whether sleep- or wake-promoting, might change SICs based on the neural activity background when used for PPN function during sleep/wakefulness. This could potentially stabilisethe desynchronized state required for PPN neuron firing during wakefulness and sleep regulation (Kovács and Pál, 2017). This balanced level of desynchronisation is important for wakefulness, attention, and associated learning and active memory, and possibly for other PPN functions such as sensory gating, reward, and locomotion. Therefore, what remains to be done is to observe behavioural changes in response to astrocyte overstimulation and relate them to known functions of the PPN. In conclusion, we found that PPN neurons react heterogeneously to CB1 receptor stimulation by activating astrocytic CB1 receptors, which change their membrane potential and action potential firing frequency. PPN neurons appear to be efficiently regulated by this indirect cannabinoid signalling pathway, which probably plays a significant role in the oscillatory activity of neurons.

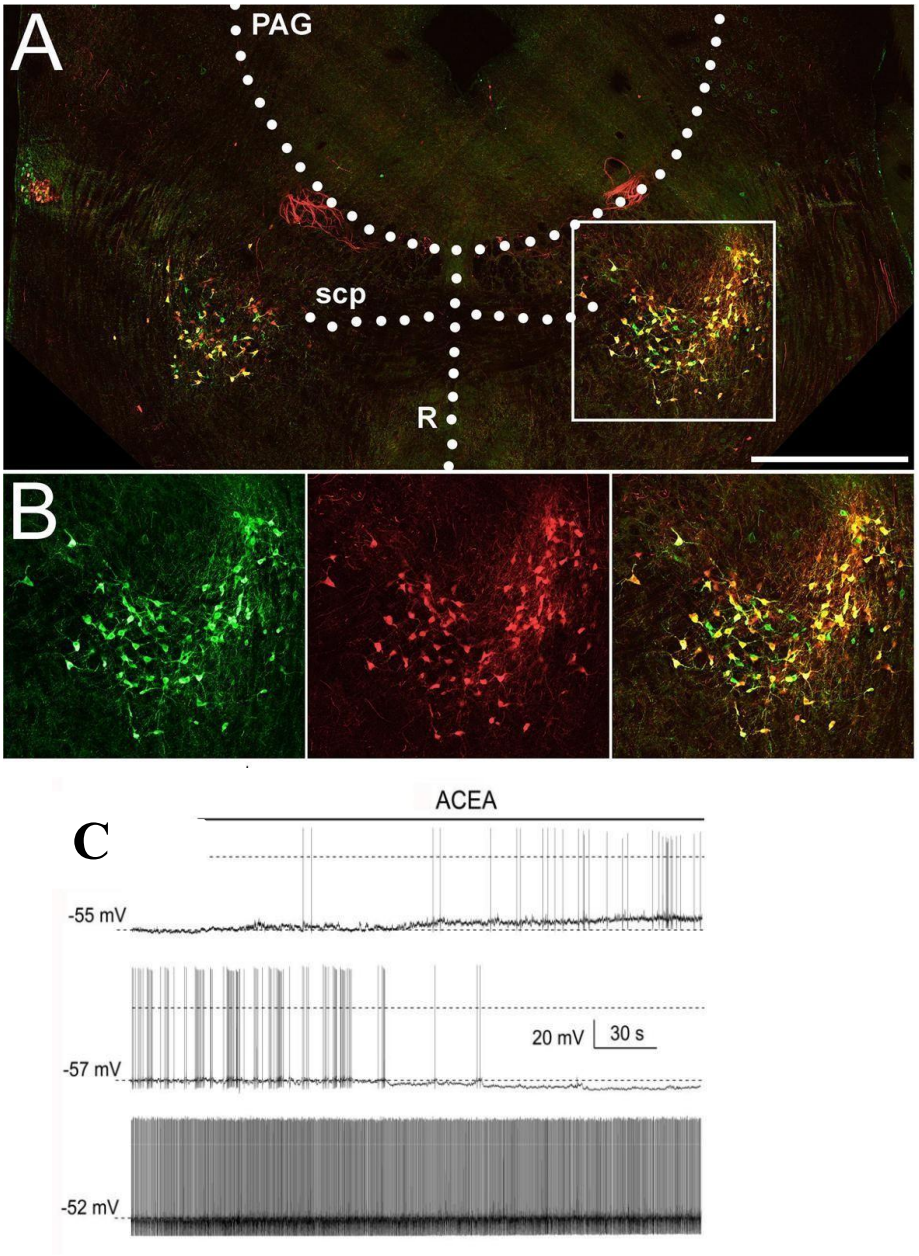

Fig. 7. (A) an overview of a coronal section from a ChAT-tdTomato animal. It shows tdTomato in red and ChAT immunohistochemistry in green, and highlighting brain regions (periaqueductal gray matter (PAG), superior cerebellar peduncle (scp), and dorsal and median raphe nuclei (R)). A scale bar of 1 mm is provided.

(B) it presents magnified views of the area outlined by the white square in panel A. (C) Alterations in action potential firing by the CB1 receptor agonist ACEA. One population is depolarized (top), another is hyperpolarized (middle), and a third has no change (bottom). This reflects the heterogeneity of neuron and astrocyte activity within the PPN.

2.2.2. The role of PPN pathological conditions

The PPN has been shown to be able to regulate motor initiation, duration, rhythm, and frequency in a variety of studies that have investigated its impact on locomotion using in vivo electrical monitoring, neuromodulation, and pharmacological interventions (Kelland and Asdourian, 1989; Dautan et al., 2021).The PPN that have extensive decline in neurons in the earliest stages of neurodegenerative diseases, including multiple system atrophy (MSA), dementia with Lewy bodies (DLB), Parkinson's disease (PD), and PSP, and express the neurotransmitter acetylcholine (ACh) in the PPNs of humans, non-human primates, and rodents (Hirsch et al., 1987; Pienaar et al., 2015), glutamate and gamma-aminobutyric acid (GABA) (Wang and Morales, 2009; Martinez et al., 2011), and glycine (Pienaar et al., 2015). The most frequently studied cholinergic neurons are those that produce ACh; and recent research has revealed previously unidentified parcellation of cholinergic inputs to the dopamine containing midbrain neurons (Fig.8). Furthermore, to the striatum's direct cholinergic projections (Dautan et al., 2014; Dautan et al., 2016). The PPN has also been found to be involved in modulating multiple types of locomotion; dystonia may be the source of abnormal locomotion produced by PPN intervention (Jankovic and Tintner, 2001).

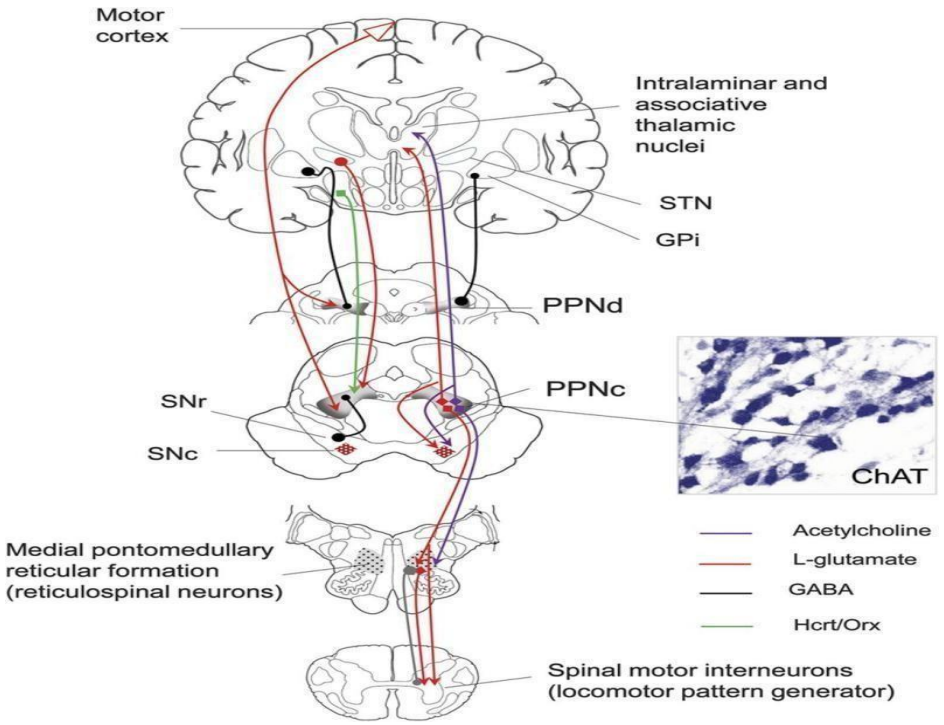

Fig. 8. Neural circuitry and modulation pathways of the pedunculopontine nucleus (PPN). This diagram showing the pedunculopontine nucleus (PPN) is divided into two separate areas: the pars compacta (PPNc), which contains neurons that synthesise l-glutamate, γ-aminobutyric acid (GABA), and acetylcholine, and the pars dissipata (PPNd), which is found across the rostrocaudal region across the nucleus. PPNc is mostly composed of cholinergic neurons, which are characterised by the expression of choline acetyltransferase (ChAT). The pallidus globus internus (GPi) and substantia nigra pars reticulata (SNr) provide GABAergic inputs to the PPN, whereas the subthalamic nucleus (STN) and deep cerebellar nuclei provide direct glutamatergic inputs. Ascending and descending projections are provided by cholinergic and noncholinergic neurons within the PPN. The substantia nigra pars compacta (SNc), GPi, and intralaminar and correlated nuclei of the thalamus are the main targets of ascending projections. The spinal cord, which regulates muscle tone and movement, as well as pontine and medullary reticular formation, receives descending projections (Benarroch, 2013).

The PPN and its connections with basal ganglia are complex networks containing forebrain nuclei which are important for motor control. It has been provided that a variety of neurodegenerative diseases, including Parkinson's disease (PD), may be directly related to any damage or instability of the BG (Pisani et al., 2007).

Patients with Parkinson's who have reduced thalamic ACh metabolism and recapture are more likely to experience falls and FOG (Bohnen et al., 2009, 2019). where the main supply of ACh is the PPN. The GPi and SNr's synaptic inhibition and cell death are probably responsible for the decline in cholinergic tone. Additionally, in certain patients with PD, cholinesterase therapies reduce falls which block the breakdown of acetylcholine (Chung et al., 2010). As a result of its importance in movement, deep brain stimulation (DBS) has been recommended as a possible therapy for postural instability, falls, and FOG in PD and atypical Parkinsonism. This method has produced a range of results. PPN-DBS have shown in numerous PPN-DBS improves general gait parameters and FOG in patients with PD (Pereira et al., 2008; Mestre et al., 2016). The PPN is a component of the reticular activating system (RAS), which consists of nuclei that control attention and consciousness. In order to regulate the tone of muscles during sleep and waking, the PPN receives SNr GABA and lateral hypothalamic orexin inputs (Takakusaki et al., 2016), REM sleep is suppressed when GABAB receptors are attached

(Sakai and Koyama, 1996; Datta and Maclean, 2007). Through thalamic projections that control cortical activity, PPN cholinergic neurons facilitate EEG desynchronization and alterations in consciousness (Hallanger et al., 1987; Kotagal et al., 2012). PPN cholinergic neurons demonstrate resting alpha activity and gamma oscillations associated with awake behaviour, respectively, during REM sleep and wakefulness (Steriade et al., 1991; Kezunovic et al., 2011). For Parkinsonian patients with severe gait disorders, postural dysfunction, and falls, including those with PSP and idiopathic Parkinson's syndrome (IPS), the PPN has been suggested as a therapeutic target for DBS. It has been proposed that DBS excites the PPN and increasing the ratio of signal to noise may modify the defective movements associated with Parkinsonian illnesses. This leads to the design of neuronal processing in the basal ganglia, and particular processes could include the release of dopamine by the substantia nigra compacta in response to direct cholinergic input of the PPN to the cortex, thalamus, and basal ganglia (Plaha and Gill, 2005).

In 1964, Drs. Steele, Richardson, and Olszewski first described the clinicopathological syndrome of PSP, describing a group of patients with postural instability, ocular motor abnormalities, facial and cervical dystonia, dementia, and other characteristics (Steele et al., 1964). Research suggests that some PSP symptoms, particularly those associated with posture, gait, and balance, may be caused by degeneration of the PPN. PPN dysfunction may be a factor in the movement coordination difficulties observed in patients with PSP, as the PPN is involved in the control of motor functions. It is believed that PSP and IPS reflect different disease entities even though they have similar clinical characteristics. Compared with IPS, PSP usually corresponds to a greater rate of progression of disease and more severe axial symptoms, such as gait disturbance (Jellinger, 1988). Patients with both PSP and IPS have been reported to have degeneration of the PPN (Hirsch et al., 1987). Histopathological investigations have shown that patients with severe gait dysfunction have more declared degeneration of cholinergic neurons, and PSP patients have a higher neuronal loss than IPS patients. Additionally, recordings from two PSP patients had less recognized neuronal groups

than recordings from five IPS patients, which is similarly with a higher loss of PPN neurons in PSP as compared to IPS (Weinberger et al., 2008).

In 98% of patients with PD, sleep disruptions cause excessive sleepiness during the day (Comella, 2007). Although the frequency of sleep abnormalities associated with Parkinson's disease (PD) is worrisome in and of itself, REM sleep behaviour disorder (RBD) is associated with a higher risk of cognitive impairment in PD patients (Marion et al., 2008). RBD may play a pathophysiological role in PPN-ACh and Substance-P-expressing neurones. Cortex and thalamus cholinergic transmission are reduced in PD individuals with RBD compared to those without RBD, despite equal illness duration and age of onset (Kotagal et al., 2012; Bedard et al., 2019). Additionally, RBD symptoms are reduced by AChE inhibitors, suggesting that cholinergic tone loss may be the cause of RBD (Ringman and Simmons, 2000).

2.2.3. KCNQ4 contribution to neuronal excitability and synchronization in the PPN

In the central nervous system, multiple brain regions express KCNQ2, KCNQ3, and KCNQ5, while KCNQ4 is limited to specific nuclei within the auditory brainstem, including the cochlear nuclei, nuclei of the lateral lemniscus, and the inferior colliculus (Kharkovets et al., 2000; Delmas and Brown, 2005; Brown and Passmore, 2009). Additional brainstem areas where KCNQ4 is expressed are the principal and spinal trigeminal nuclei, as well as components of the reticular activating system (RAS) such as the raphe nuclei and the ventral tegmental area (VTA) (Kharkovets et al., 2000; Hansen et al., 2008). Previously, we found in our lab that cholinergic neurons, but not glutamatergic ones, in the PPN have the M-current. Activation of cholinergic inputs to the PPN can reduce this current. The M-current helps synchronise nearby neurons, uses different methods to show that a subgroup of cholinergic neurons express KCNQ4. Mice lacking KCNQ4 showed changes in their activity cycle. Our findings suggest new roles for KCNQ4 in CNS, specifically in determining the makeup of KCNQ channels in RAS. This, in turn, affects the RAS's electrical properties, which then influences the activity cycles. As KCNQ4 is mainly found in specific brainstem areas, drugs that target this subunit could be potential treatments for sleep-wake cycle problems

(Bayasgalan et al., 2020).

KCNQ4 is also found in some places outside the brain, notably in the outer hair cells of the cochlea (Kharkovets et al., 2000, 2006; Carignano et al., 2019). When this subunit has a dominant negative mutation, it causes hereditary hearing loss that is not linked to other conditions (DFNA2) (Kharkovets et al., 2000, 2006). This condition involves the gradual breakdown of outer hair cells as people age (Carignano et al., 2019). Interestingly, where KCNQ4 is expressed overlaps a lot with the brain network responsible for the startle reflex, which is a rapid motor response to strong, potentially dangerous stimuli. In mice, can distinguish between startles triggered by acoustic, vestibular, and tactile stimuli (Koch, 1999) (Fig.9). Problems with the cochlea or the central nervous system can either make the acoustic startle reflex stronger or weaker, and how it's changed can be seen in various diseases or conditions (Bakker et al., 2006; Dreissen et al., 2012; Zhang et al., 2022 a, b).

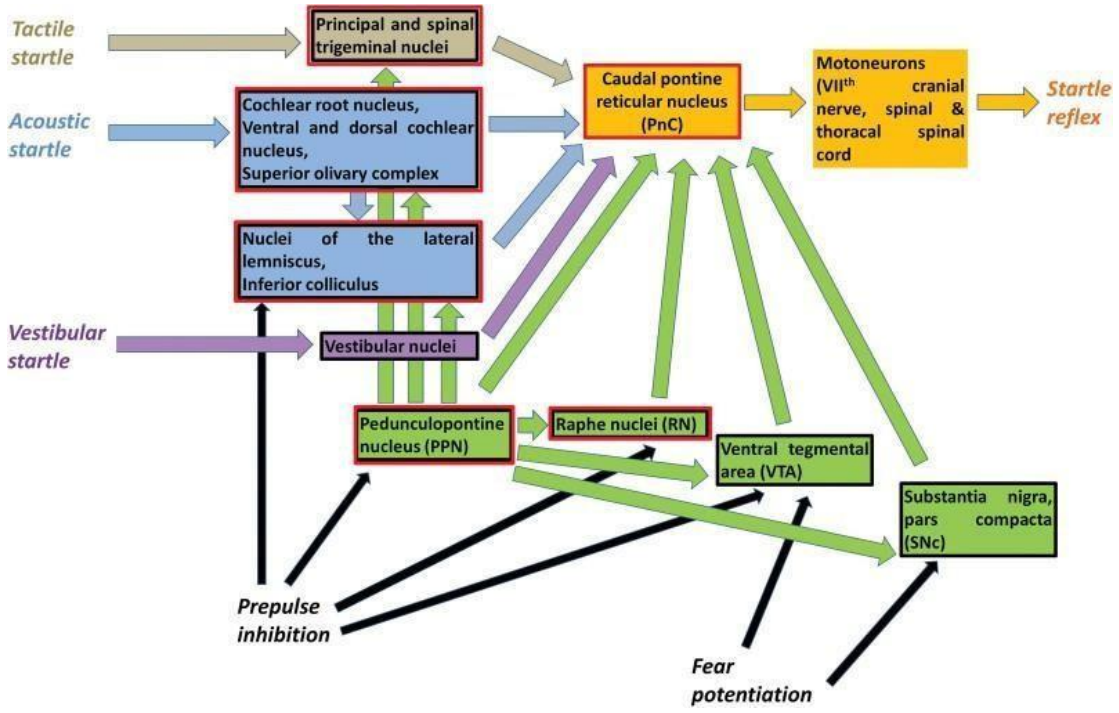

Fig. 9. Neural pathways and mechanisms of the startle reflex. Shows where KCNQ4 is expressed, the pathways involved in the startle reflex, and the brain areas used for chemogenetic stimulation. Black squares indicate the areas where KCNQ4 is present. Red squares show areas expressing mCherry in this study. Yellow symbols represent the main startle reflex pathway. Brown symbols show pathways for the tactile startle. The blue symbols

indicate acoustic startle pathways. Purple symbols represent the vestibular startle pathways. Green symbols show pathways that modify the startle reflex (Koch, 1999; Kharkovets et al., 2000). KCNQ4 stands for potassium voltage-gated channel subfamily Q member 4.

2.3. Behavioral testing in neuroscience research: methods and applications

Behavioural tests play a crucial role in studying neurological disorders, as they provide valuable insights into the functional effects of neurological changes. These tests are designed to assess various aspects of animal behaviour, allowing researchers to link the observed behavioural changes to specific neurological conditions.

The pedunculopontine nucleus is involved in various functions including locomotion, arousal, sleep-wake regulation, and reward processing. Behavioral tests used to evaluate PPN function in neuroscience research typically focus on these domains by understanding how specific biological processes and behaviors are mapped over neural circuitry is one of the main goals in neuroscience.

The circadian rhythm and exercise motivation of rodents can be evaluated using voluntary wheel running. Sleep and psychiatric disorders are associated with deficiencies in these behaviours. Although running wheels require more energy from rodents, they generally increase voluntary activity. This can be beneficial for phenotypic analyses because it amplifies the activity differences between the control and mutant groups. This amplification is especially useful when examining the circadian rhythm of wheel-running activity, as rodents typically only engage in voluntary activity during their active phases (Novak et al., 2012). Rodents clearly perceive wheel running as a reward, and comparative psychologists have long viewed it as classic self-motivated behaviour. Sherwin's review of the evidence demonstrates that various species are often highly driven to run on wheels, even without any external reward is present (Sherwin, 1998). Understanding the neural bases of cognition can be significantly enhanced by connecting behavioural changes that occur at specific times during development with simultaneous shifts in how the brain functions. Among effective tests to evaluate spatial learning and memory deficits in rodents by the Barnes maze (BM) task. It operates on the

principle that an animal, when placed in an unpleasant environment, will learn and recall where an escape box is located under the platform's surface.

Although the Morris Water Maze (MWM) is the primary method for evaluating spatial learning in rodents, the Barnes maze has several notable advantages. A major advantage is that the Barnes maze does not require swimming, thus avoiding potential complications associated with it. Swimming is known to be stressful, with studies showing that MWM training raises plasma corticosterone levels more significantly than the Barnes maze does (Harrison et al., 2009). Additionally, the swimming conditions common in most (MWM) procedures can lower the animal's core body temperature, thereby impacting their performance (Iivonen et al., 2003). Furthermore, rodents frequently begin floating, which is interpreted as a state of behavioral despair and serves as an indicator of "depressive-like" behavior in the widely recognized Porsolt forced swim test (Porsolt et al., 1977). Finally, as previously noted, the Barnes maze provides a clear distinction between the three search strategies employed by a mouse during each trial.

Acoustic startle reflex (ASR), used for anatomical, physiological, and behavioral methods, researchers have identified the pathways responsible for mediating and modulating, which is referred to as the startle response, is an involuntary and natural response to a sudden and unexpected stimulus, like a loud noise or a quick movement (Fig.10). Startle reflex abnormalities have been noted in several clinical applications and understanding these changes can have an impact on both diagnosis and treatment. The startle reflex can be considered a habitual defensive response (in contrast to a directed response). The body becomes habituated to greater startles and reduces the intensity of the startle reflex as the number and frequency of startles increases. This type of response is relative protection of the human body. The ASR is a useful tool for understanding the fundamental functions of the CNS. It is characterised by basic brain circuits, cross-species consistency, and sensitivity to behavioural experiments (Pantoni et al., 2020). Depending on what is categorised as olfactory, vestibular, tactile, visual, or auditory, the olfactory only exists in fish, and the visual is a characteristic of primates.

Among these (ASR) also known as, has been the most widely studied clinical research experiment (Kumru et al., 2009). This could be associated with differences in the stimulus processing times of the recognised sensory modalities, such as sound stimuli, which require less processing time than visual stimuli. This difference may be related to the auditory cortex's shorter distance from the ear and the ear's faster conduction time. Few studies have been conducted on the tactile startle reflex in contrast to the auditory startle reflex, which can frequently result in a local reaction which leads to a specific incubation period and an unexpected response (Ertuglu et al., 2019).

These possibilities and approaches have been made possible by the diagnosis and monitoring of ASR in cases of brain injury, stroke, and psychological disorders. The startle reflex is useful as an indicator of disease; therefore, more research in this area is essential for both detecting and treating clinical conditions. The startle reflex changes in certain disease states, such as those involving the central nervous system traumatic brain damage, stroke, neurodegenerative diseases (Alzheimer's disease and Parkinson's disease), and some mental system diseases (schizophrenia) (Kumru et al., 2009). Hyperekplexia, or hereditary startle diseases, is characterised by an exaggerated startle response to typical stimuli and increased muscular tone in newborns, with origins that can be both psychological (intensified reactions to emotional stimuli) and seizure-related (thought to be astatic seizures) (Dreissen et al., 2012).

Human studies involving physiological aging have indicated a reduction in ASR magnitude, an increase in ASR latency, an inverted U-shaped function of PPI with age (indicating peak PPI amplitude at intermediate ages), and no significant changes in startle habituation (Ellwanger et al., 2003). Reduced habituation to repeated auditory stimuli has been observed in Alzheimer's (Golob et al., 2001). Negative stimuli stimulate the system of defence (aversive states), resulting in the potentiation of the ASR, while positive stimuli engage the appetitive system, leading to a reduction in ASR amplitude (Lang et al., 1990), the positive, negative, and neutral images from the International Affective Picture System produce contrasting effects on startle modulation in older and younger individuals. While younger adults showed

an increase in startle response (reduced inhibition) when viewing negative images compared to positive and neutral images, older adults showed a similar effect when viewing positive images compared to negative and neutral images. This pattern suggests that older adults are more likely to spontaneously inhibit responses to negative stimuli and process positive stimuli than are younger adults (Feng et al., 2011; Le Duc et al., 2016). Older adults also demonstrate better recall of positive information than negative information than younger adults (Sasse et al., 2014).

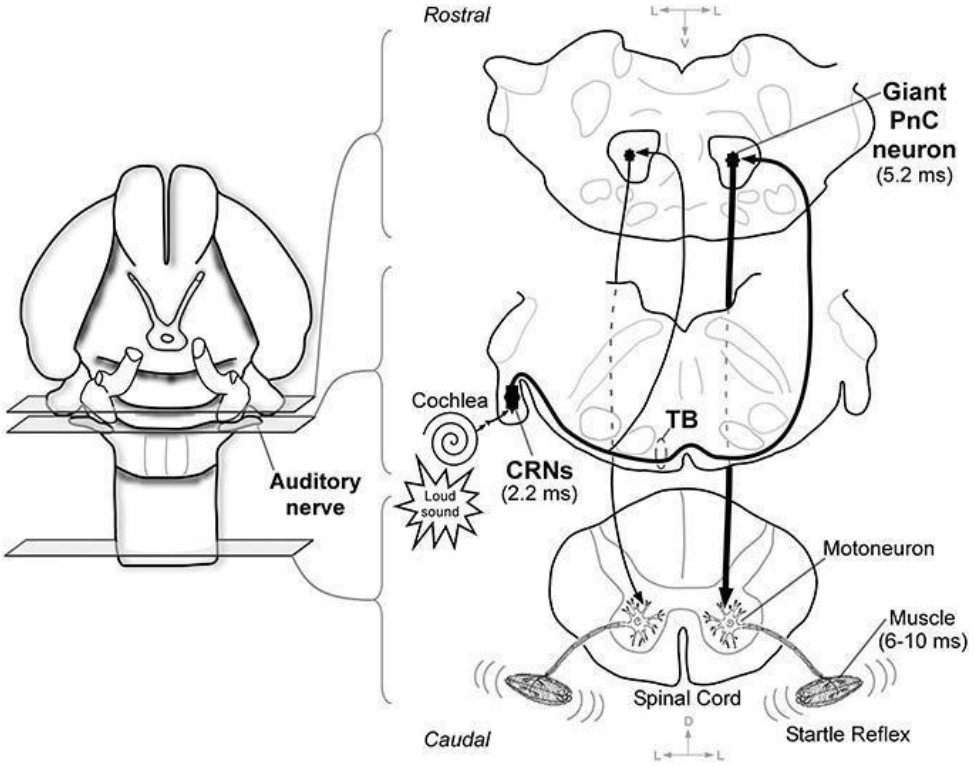

Fig. 10. Major acoustic startle reaction in the mouse brainstem. First, the cochlea's auditory receptors are activated by a sudden, loud sound. Following then, cochlear root neurons, which have first-spike latencies around 2.2 ms and a reliable response, are synaptically connected to auditory nerve fibres (Gómez-Nieto et al., 2013, 2010; Sinex, López and Warr, 2001; López et al., 1999). The large neurons located in the pontine reticular formation (PnC) receive this short-latency acoustic input and respond with 5.2 ms short latency (Lingenhöhl and Friauf, 1994; Lee et al., 1996; López et al., 1999). Lastly, axons from the acoustically driven PnC neurons connect to spinal cord motoneurons to provide an acoustic startle reflex with electromyographic latencies ranging from 6 to 10 ms (Caeser, Ostwald and Pilz, 1989; Davis et al., 198; Ison, McAdam and Hammond, 1973). The line width, which can be observed in coronal brainstem sections, indicates side preponderance within the circuit. The CRN axons mainly target contralateral PnC neurons as they pass through

the trapezoid body (Nodal and López, 2003; López et al., 1999). In this model, projections from cochlear root

neurons to other non-auditory nuclei that take part in the whole expression of the pinna and acoustic responses are not shown (Horta-Júnior et al., 2008; López et al., 1999).

In PSP, which is a sporadic neurological disorder that develops in adult and currently referred to as Richardson's syndrome (PSP-RS), is characterised by postural instability resulting falls early as well as oculomotor abnormalities, mainly affecting vertical more than horizontal eye movements, specifically characterised by saccadic slowness that progresses to supranuclear gaze palsy (Boxer et al., 2017). The absence of startling acoustic stimulus (SAS) induced effects in patients with PSP. The degeneration of pontine nuclei is a common pathological finding in progressive supranuclear palsy (PSP) (Zweig et al., 1987; Malessa et al., 1991; Juncos et al., 1991; Malessa et al., 1994).

Most neurological conditions, including damage to the central and peripheral nervous systems, lead to gait changes. It is generally accepted that understanding the specifics of animal limb movements during walking—both after an injury and during recovery from spinal cord or peripheral nerve damage, when assessed using the right models—is crucial for evaluating these conditions. Gait analysis is an essential method for studying mouse models because it provides measurable behavioural data on how a particular disease, injury, or drug affects an animal's movement. Neurodegenerative diseases cause a gradual decline in brain cells, which eventually leads to death. This progressive loss of neurons impairs neuromuscular control, resulting in issues with balance and walking (known as ataxia) or dementia (Emard et al., 1995; Lewis et al., 2019). In recent decades, researchers in the medical field have focused on gait analysis. Although there is a broad range of neurodegenerative conditions, most research attention has been directed toward gait pathologies associated with Alzheimer's disease, Parkinson's disease, Multiple Sclerosis, Amyotrophic Lateral Sclerosis, Huntington's disease, and various types of dementia (see, Table 1). In addition, PSP is an uncommon neurological disorder that affects on movement, gait, and balance.

The earliest and most disabling symptoms of PSP is impaired gait and balance. Patients with

PSP lose their postural reflexes, coupled with a peculiar unawareness of their balance problems, which often leads to frequent falls and injuries. This significant postural instability has been related to a combination of impaired vision and balance, axial rigidity (stiffness in the trunk), bradykinesia (slow movement), and impaired postural reflexes. Initiating gait is recognised as a highly demanding task for the balance control system and is often used in research to study how the central nervous system controls balance during full-body movements (Isaias et al., 2014, Yiou et al., 2017).

Table 1. shows characteristics of gait in the most common neurodegenerative diseases (Cicirelli et al., 2022).

Neurodegenerative Disease	Gait Characteristics
Alzheimer's Disease (AD)	Decreased walking speed, decreased stride length, increased support time, greater stride-to-stride variability, lower cadence
Parkinson's Disease (PD)	Decreased walking speed, increased cadence, reduced stride length, reduced swing time, higher double support time
Multiple Sclerosis (MS)	Decreased walking speed, shorter step length, reduced cadence, increased double support time
Amyotrophic Lateral Sclerosis (ALS)	Decreased walking speed, increased stride time variability, increased stride length
Huntington's Disease (HD)	Decreased walking speed, decreased step/stride length, increased stance/swing phase, decreased single support time

Aims

- Chronic activation study:

i. Astrocytic overstimulation within the PPN using chemogenetic tools to precisely investigate the functional role of astrocytes within the PPN. The PPN plays a role in reward processing, sleep-wake regulation, arousal, and motor control. Because astrocytes behave differently in different parts of the brain, it is crucial to precisely target PPN astrocytes to investigate their contribution to these important physiological processes. This study employs a chemogenetic approach utilizing the hM3D(Gq) (human muscarinic M3 Designer Receptor Exclusively Activated by Designer Drugs) system. This system offers a powerful tool for selectively manipulating astrocyte activity without directly affecting neighbouring neuronal populations, thereby minimising confounding variables.

ii. To create an animal model of PSP, that causes damage to the PPN. The model will be a beneficial tool for examining the pathophysiology of PSP and identifying potential treatments.

- KCNQ4 study*:*

i. investigated whether KCNQ4 subunit loss is affected by the startle reflex, and whether these changes are caused by brainstem hyperexcitability.

3. Material and methods

3.1. Animals and preparation

All animal experiments followed the rules set by local, national, and international authorities, including EU Directive 2010/63/EU, and were approved by the Hungarian National Food Chain Safety Office (HB/06-ÉLB/129-1/2020; 19/2019/DEMÁB, HB/15-ÉLB/00136-42/2023; 3/2023/DEMÁB).

In this experiment, we used 20 young adult male (2-month-old) mice, of which 16 were wild-type C57Bl6 mice and four were ChAT-tdTomato mice. We labelled the latter mouse a cholinergic neuron by expressing the tdTomato fluorescent marker under the control of the ChAT promoter (Baksa et al., 2019). In the animal facility, the mice were produced in the animal facility by mating homozygous strains of ChAT-cre (B6;129S6-Chat tm2(cre)Lowl/J; Jax number: 006410) and floxed-stop-tdTomato (B6;129S6-Gt (ROSA)26Sor tm9(CAG-tdTomato) Hze/J; Jax mice the accession number: 007905) that were obtained from Jackson Laboratories (Bar-Harbour, ME, USA).

For the KCNQ experiments, Prof. Thomas Jentsch (MDC/FMP, Berlin, Germany) kindly provided the KCNQ4 knockout strain (Kcnq4−/−). In our facility, we bred heterozygous animals using 2-month-old knockout mice and their wild-type littermates (n = 8) and knockouts (n = 14). We used 12 more wild-type mice from the same breeding group for the viral injections. We stereotaxically injected a prepared retrogradely spread adeno-associated virus (AAV) into young adult mice (7–8 weeks old) of both sexes. The mice were housed with their littermates under standard animal facility conditions, which included regular cycles of light and dark. Water and food were accessible to them.

In the study focused on activating astrocytes, 20 mice underwent surgery; 13 of them were in the DREADD experimental group, which showed a specific marker called hM3D-(Gq) and an mCherry tag in their mesopontine astrocytes; the other 7 mice were in the control group, only showing the mCherry tag; and 16 mice were used for behavior tests, not including the

two-bottle preference test. The last 4 mice in the DREADD group were used for the two- bottle preference. Some data were excluded from the analysis because of technical issues during the tests. The remaining 4 mice in the DREADD group were assigned to the two- bottle preference test. Certain measurements were removed from the analysis because of technical problems encountered during the tests. The number of mice used in the behavioral tests is shown in Table 2.

Table2: The Number of animals used for behavioural experiments in both studies.

Chronic activation of Astrocyte	Acoustic startle test	Activity wheel test	Barnes maze test	Footprint test	two-bottle preference test
DREADD (hM3D-(Gq) and mCherry-expression in astrocytes)	8	6	7	9	4
Operated control (mCherry-expression in astrocytes)	7	6	7	6	-
KCNQ4 Knockout	Acoustic startle test	Activity wheel test	Barnes maze test	Footprint test	two-bottle preference test
Wild type KCNQ4 KO strain (Kcnq4−/−)	8	-	-	-	-
Knockouts KCNQ4 KO strain (Kcnq4−/−)	14	-	-	-	-
DREADD Wild-type C3H mice (hM3D-(Gq) and mCherry-expression in neurons).	12	-	-	-	-

3.2. Stereotaxic surgery

For anaesthesia, mice received intraperitoneal injections of xylazine (10 mg/kg) and ketamine (100 mg/kg). Complete anaesthesia, indicated by a lack of flexor and blinking reflexes, was

achieved. All surgical procedures were performed using sterile instruments. Mice were placed on a 37 °C heating pad to monitor their body temperature. The head was secured within a stereotaxic frame (RWD Life Science Co., LTD, Shenzhen, China), and hyaluronic acid eye drops (Vizol S 0.21% eye drop, Penta Pharma Co., Budapest) were administered to the eyes to prevent corneal damage.

Following to the skin incision and trepanation by applying a microdrill (RWD Life Science Co., LTD, Shenzhen, China), a 200 nl viral volume for targeting the PPN in chronic activation of astrocytes (titer: 2 x 10^13 GC/ml for (AAV5)- pAAV-GFAP-hM3D(Gq)- mCherry and 1.7 x 10^13 GC/ml for pAAV-GFAP104-mCherry (AAV5)). For KCNQ study the same volume used (titer: 2 x 10^13 GC/ml for (AAVrg)-pAAV-hSyn-hM3D(Gq)- mCherry and 1.7 x 10^13 GC/ml for pAAV-hSyn-mCherry, (AAVrg) in the caudal pontine nucleus (PNc) was injected through a Hamilton syringe and microinjector (RWD Life Science Co., LTD, Shenzhen, China). The surgical approach aimed to provide bilateral injections were performed using the following stereotaxic coordinates in PPN: 4.96 mm caudal from bregma, 1.25 mm from the midline, and 3.4 mm in depth. Mice were recived a pAAV-GFAP-hM3D(Gq)-mCherry (AAV5) virus vector containing a plasmid that encodes the hM3D(Gq) chemogenetic actuator and mCherry fluorescent tag, both expressed under the GFAP promoter. For the control group was administered a plasmid that only contains the fluorescent marker for mCherry (pAAV-GFAP104-mCherry (AAV5), provided by Edward-Boyden; Addgene plasmid # 58909; http://n2t.net/addgene:58909; RRID: Addgene_58909) for the chronic study.

While the stereotaxic coordinates of KCNQ group was performed bilaterally 6 mm from bregma and 0.6 mm from the midline at 5 mm depth of the caudal pontine reticular nucleus (PnC) and areas projecting to it (Maamrah et al, 2023). Mice recived the pAAV-hSyn-hM3D(Gq)-mCherry virus, including plasmids that encode the mCherry tag and the human M3-muscarinic (hM3D-Gq) chemogenetic actuator (provided by Bryan Roth; Addgene plasmid # 50478; http://n2t.net/addgene:50478; RRID: Addgene_50478), prep #50474-AAVrg; http://n2t.net/addgene:50474; RRID: Addgene_50474. The control contained a

pAAV-hSyn-mCherry, a gift from Karl Deisseroth (Addgene viral prep #114472-AAVrg; http://n2t.net/addgene:114472; RRID: Addgene_114472), that mCherry tag as control expressed in neurons.

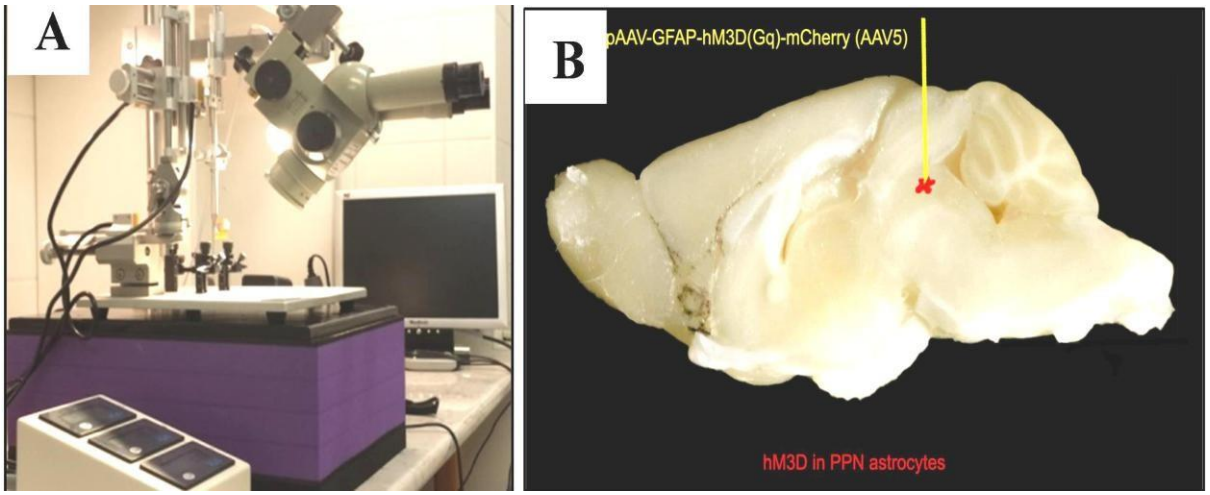

Fig. 11. Stereotaxic surgery setup: (A) Mice were positioned on a platform fitted with stereotaxic instruments to ensure accurate injection into the PPN. (B) AAV viral vector carrying the DREADD construct was delivered at the targeted injection site.

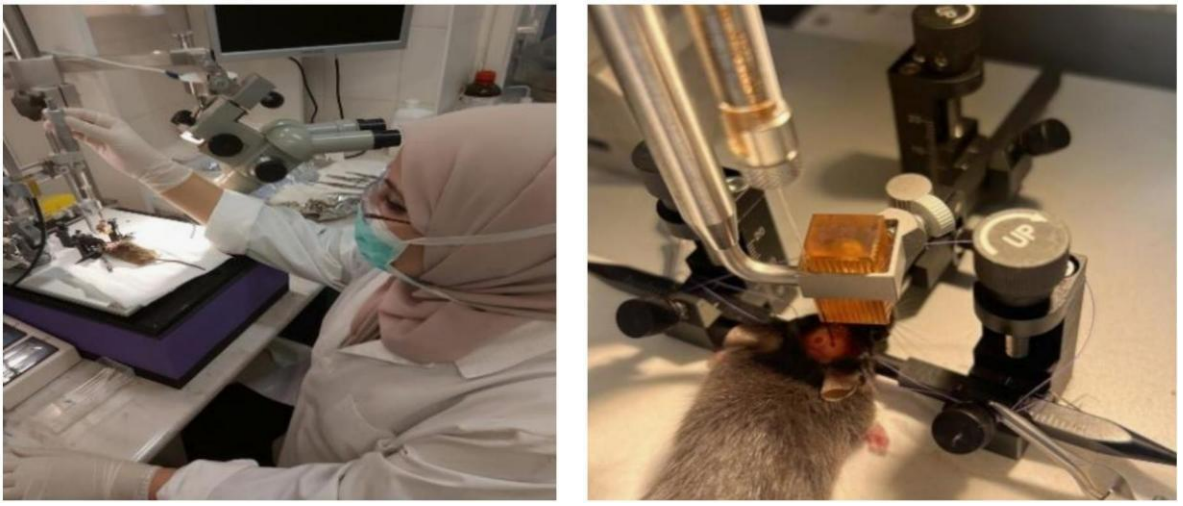

Fig. 12. Stereotaxic surgery of the PPN in mice (A) Mice were placed on a platform equipped with stereotaxic equipment for precise injection into the PPN. (B)Location of injection of AAV viral vector containing DREADD.

After surgery, bone wax was used to close the skull, and the skin was sutured with 5-0 Vicryl (Ethicon). Postoperatively, mice received ibuprofen as a painkiller (30 mg/kg: Nurofen Baby, Reckitt Benckiser Ltd., Budapest, Hungary) at the end of anaesthesia and for the next 2 days after surgery. They were placed in individual, ventilated cages for a duration of 7 days postoperative care.

Clozapine-N-oxide (CNO) was administered in drinking water, and mice were administered to observe chronic actions of astrocytic overstimulation. After recovery, the mice underwent behavioural tests to observe the chronic actions of astrocytic overstimulation in the first group of experiments. While for the KCNQ study, only the acoustic startle reflex was used to assess the same outcome, examining its effect on the startle response in KCNQ4 knockout mice.

3.3. Behavioral tests

All behavioural tests were conducted in the sequential order illustrated in Fig 19, both before and after the 3-week consumption of CNO (Tocris Cookson Ltd., Bristol, UK; 1.04 mg/kg ingested; 4 µg/ml, 9.6 µM in drinking water). The dosage was calculated based on the average water consumption measured during the drinking experiments using a two-bottle preference test (see below).

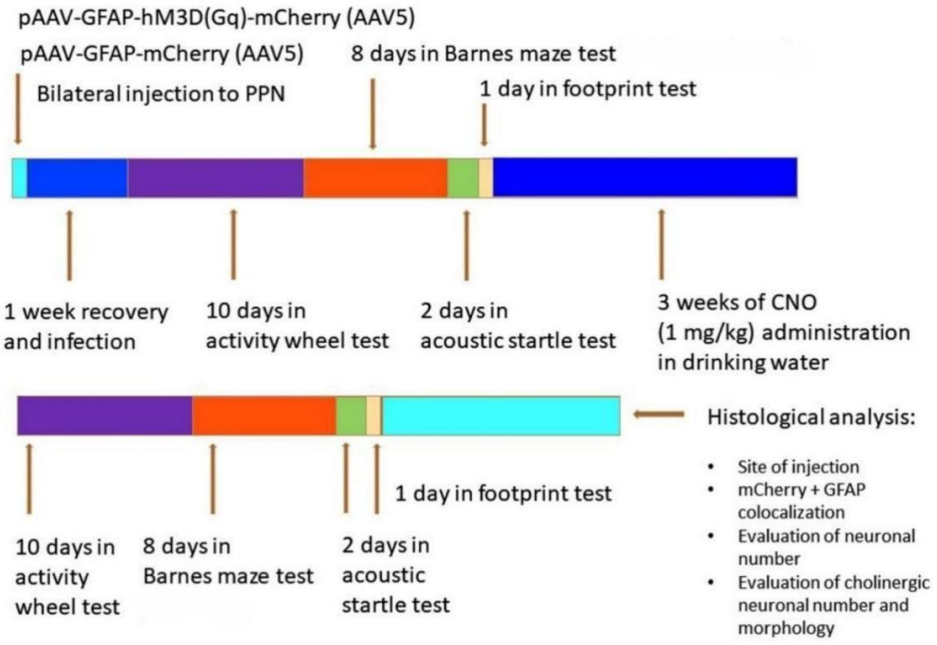

Fig. 13. Experimental approach and sequence of procedure, treatment, and behavioural test.

3.3.1. Two bottle preference tests

This test measured any bias related to low intake or overdose of CNO and compared the consumption of normal tap water with that of CNO water with respect to reward and motivation. In this experiment, mice were placed in cages, each containing a pair of drinking bottles. In the first 3 days of the experiment, both bottles were filled with the same solution,

especially tap water, and the total amount of liquid consumed, measured in millilitres, was recorded within these 3 days duration. Subsequently, for the next 3 days, the bottle labelled in red was filled with tap water with (CNO) at a concentration of (4 µg/ml; 9.6 µM). The mice used in this study were different from those used in the main experiment. (Fig.14)

Fig. 14. two-bottle preference test for CNO. A. Experimental setup with two bottles containing tap water or CNO dissolved in tap water. Paper boxes were used to cover the bottles because of their sensitivity to light.

3.3.2. Activity wheel test

This test was used to assess voluntary physical activity and maximal velocity, and the mice were individually housed in running wheel-equipped cages for 10 days. Data from the initial three-day adaptation period were not included in the analysis. This test helps assess the circadian rhythm of the mice, and how it is influenced by various regions of the CNS that play a role in sleep-wakefulness regulation (Verwey et al., 2013). As discussed previously, cholinergic, and glutamatergic neurons in the PPN have a vital role in initiating and promoting wakefulness. Astrocyte contribution to this mechanism is a strong possibility and the activity wheel test can be used to evaluate it. In this experiment, after a week of habituation without measurements, the mice were exposed to a 24-hour light-dark cycle (6 AM to 6 PM light) for one week. During this time, we measured the number of activity wheel rotations in 10-minute

intervals, the distance travelled in centimetres, and the maximal running velocity in meters per minute (Fig.15).

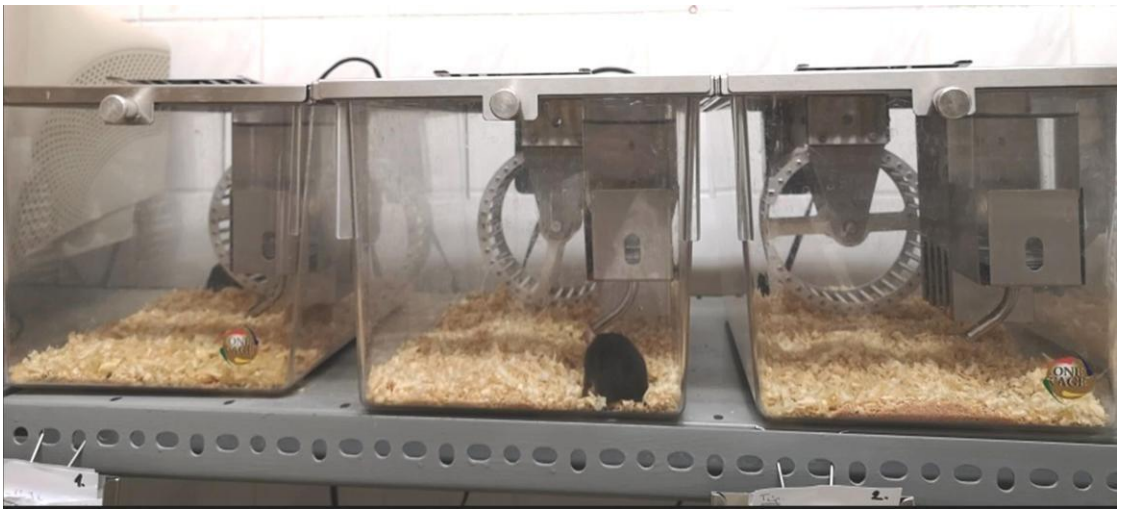

Fig. 15. Indviual Activity wheel staup, mice are housed in cages equipped with a running wheel and maintained under a 24-hour light-dark cycle. Wheel rotations were recorded to determine distance-related measures and to assess the activity levels of the mice.

3.3.3. Barnes maze test

The Barnes maze experiment was performed to evaluate spatial learning and memory. This procedure enables the mice to move from a serial/random search to a spatial learning method that requires functional retention and spatial reference memory (Pitts 2018; Gawel et al. 2019). In this experiment, mice were placed in an elevated circular maze with 20 holes around the perimeter. The maze was illuminated from above via light with a behavioural camera. An escape box was consistently placed beneath one of the holes throughout the experiment.

At the beginning of each measurement, a box was temporarily placed over the mice and then removed to allow exploration. 60 dB white noise was simultaneously applied, the mice were positioned at the centre of the maze, and recording began, continuing until they found the escape box. The experiment consisted of two phases, an acquisition phase, and a probing trial. During the acquisition phase, the mice were placed in the centre of the maze and allowed to freely explore until they found the escape box. If they failed to find the box within 3 min, they were placed inside it for 15 s.

All mice underwent training twice daily for 5 days, with a 1-hour interval between the two trials, under constant white noise. During the probe trial, 3 days after the acquisition phase was complete, the escape box was removed, and mice were placed in the centre and allowed to explore. Eventually, the mice determined the location of the shelter before being placed, and a single trial per mouse was conducted at this phase. To minimise odour interference, the maze was cleaned with disinfectant wipes between each trial. The maze orientation and the surrounding environment remained similar throughout the experiment. We measured the overall distance and duration spent by the mice to find the shelter using ImageJ. The experiment was conducted twice: before and after chronic CNO treatment.

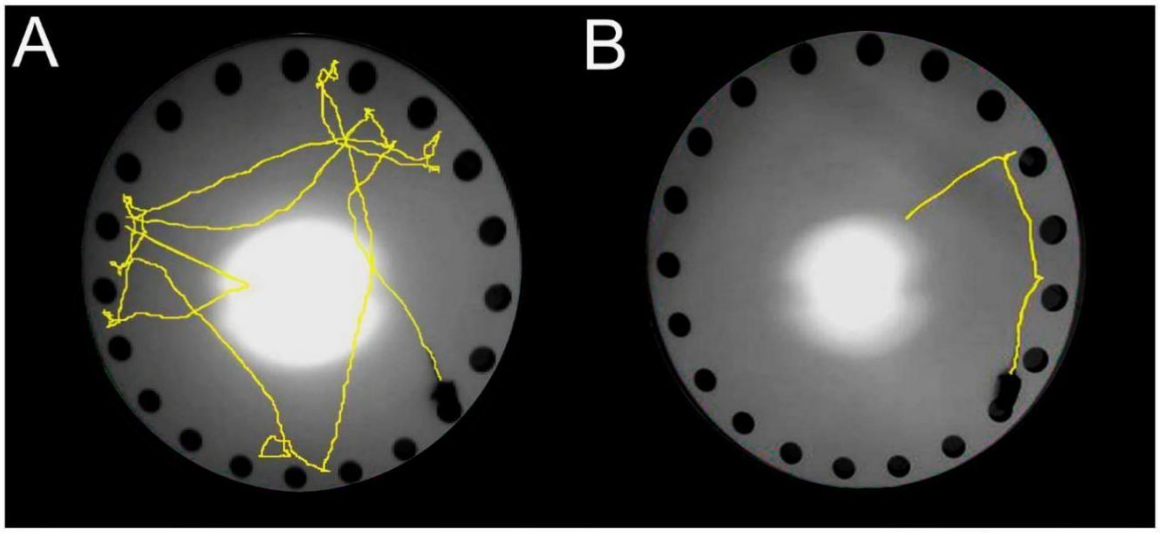

Fig. 16. Barnes maze experiment for assessing spatial learning and memory in mice (A) The mouse is placed on the centre of the platform and allowed to explore until it finds the escape chamber placed underneath the holes. (B) Distance after measurement and analysis using analysis software (Maamrah et al., 2025).

3.3.4. Startle reflex test

The startle reflex test assesses the neurological responses to sudden stimuli. It is commonly used in various clinical settings to evaluate sensory processing and neurological functions. We used a setup that was developed to test the acoustic startle reflex (AR). The setup involved a transducer connected to a perforated plexiglass box, which limited the animal's lateral movement. The mice were habituated to the Plexiglas box, which had been in their cage for one week, during which they often used it as shelter. A constant 60-dB white noise was used

as the background, while a camera recorded the movement of the mouse (Maamrah et al.,2023), with 105 dB noise, administered five times consecutively at 1-minute intervals, induced the acoustic startle response and measured short-term habituation.

The amplitude of the initial startle response, average of five responses, and short-term habituation were measured. Short-term habituation was identified by a decrease in amplitude across the five measured responses (Catharine et al., 2009).

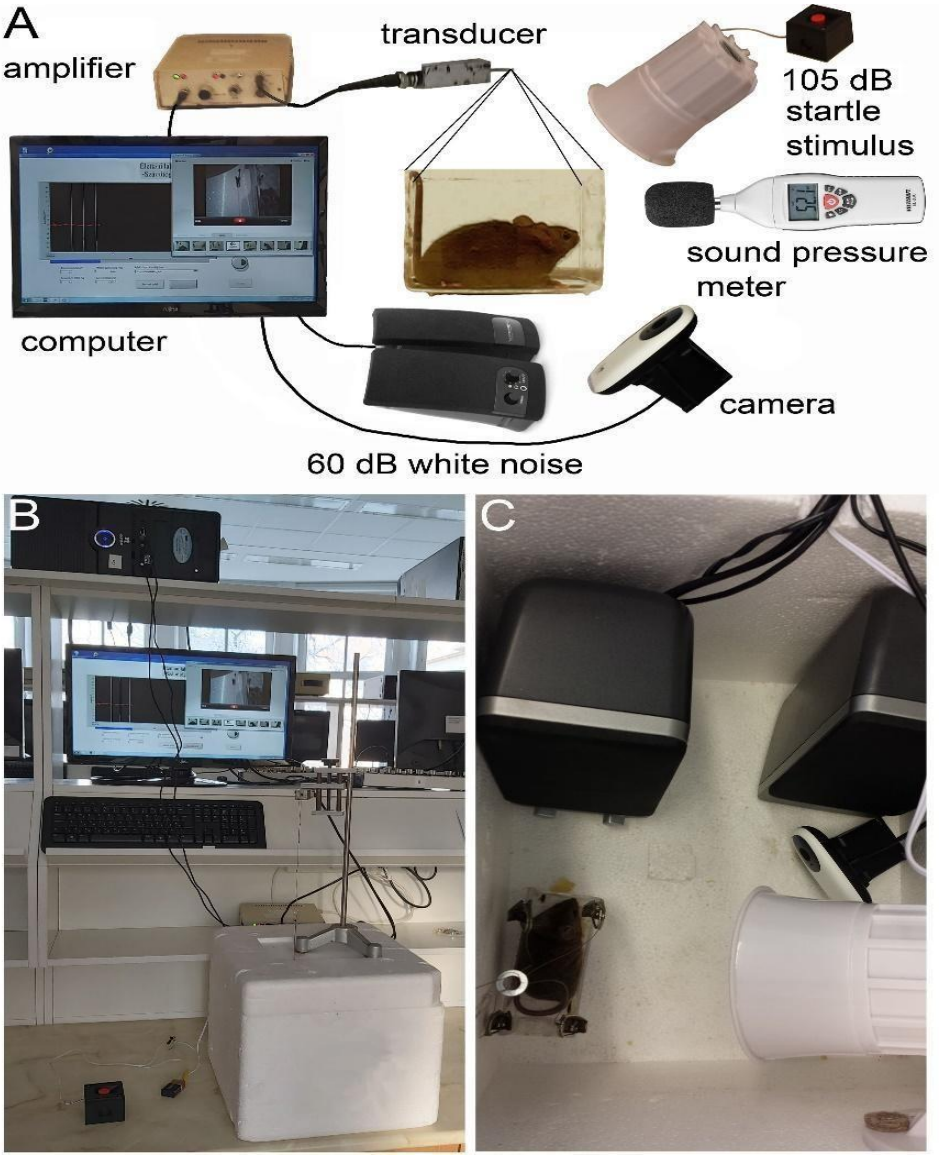

Fig. 17. Investigation of the acoustic startle reflex. (A) The mouse was placed in a box hanging from the transducer device. A 60 dB white noise was used, and 105 dB noise was employed 5 times with 1-minute gaps to initiate the startle reflex in the mouse. The movement of the box was picked up by the transducer which was amplified and measured on a computer program as the amplitude. (B) The setup was confined to a Styrofoam box with a tripod holder placed on top to hold the hanging box. (C) Top view of the setup inside the box.

3.3.5. Footprint test

The footprint test in mice is primarily used to assess locomotor activity and analyze gait patterns (evaluate motor coordination, balance, and measure changes in muscle tone and gait), which are key functions regulated by the pedunculopontine nucleus. The setup involved a blank white piece of paper placed on a clean smooth surface, an escape box positioned 50 cm away from the starting point at the top of the paper, and two cardboards walls surrounding both sides of the paper. A separate piece of cardboard was physically positioned along the bottom edge of the paper during the experiment to prevent mice from escaping. The result was a one-way path to the shelter with no exits from any other side; the path measured 45-50 cm in length, but only the middle 30 cm was used for the analysis.

A test procedure involves taking a mouse from its cage and placing it on the paper surface, allowing it to move towards the vessel positioned on the upper section of the paper. Following this habituation phase, they were removed from the shelter, the front paws of the mouse were labelled with red food dye, and the hind paws were labelled with blue food dye (Szilas Maxcolor, Szilasfood, Kistarcsa, Hungary). Stride length, sway length, and stance length of the forepaws and hind paws were measured in centimetres (Girirajan et al., 2008).

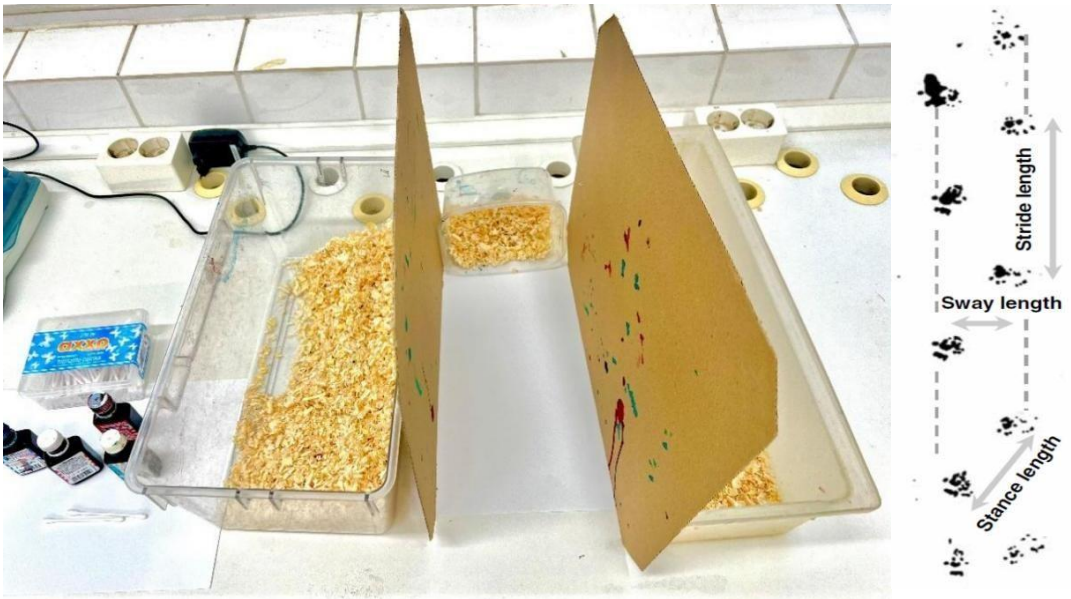

Fig. 18. Footprint test: The front and hind feet of mice are painted in red and blue, respectively. The mice were then allowed to run from one end of a blank piece of paper to the other end where a shelter box was placed. The

test was performed before and after CNO treatment. The stride length, overlap, and width between footprints were measured, as labelled in the figure. Further calculation of the hind-to-front width ratio was performed to better describe the change in muscle tone and gait after CNO treatment.

3.4. Immunohistochemistry

After completion of the behavioural measurements, transcardial perfusion was performed on the mice to assess the injection site and mCherry labelling. Brain samples were sliced to a thickness of 50 µm using a vibratome (Campden Instruments, Loughborough, UK), and free-floating slices were fixed in 4% PFA for histological analysis. A slice thickness of 50 µm is appropriate for light microscopy visualisation, whereas a thickness of approximately 50 nm is frequently appropriate for electron microscopy (Pivak et al., 2023). The process started with washing the free-floating slices three times for 10 min each in Tris-Buffered Saline (TBS). TBS, an isotonic and non-toxic buffer, is frequently used in several biochemical methods to maintain a consistent pH (Ferreira et al., 2015). The TBS solution used in the IHC method can be prepared by dissolving commercially available TBS pouches or tablets, then the blocking that required incubating the brain slices for 60 minutes at room temperature in a solution including 10% donkey serum and 0.5% Triton-X 100 in TBS.

This solution was used to block non-specific binding sites. Triton-X 100, a non-ionic surfactant, is commonly used to lyse cells for component extraction or to permeabilise cellular membranes (Koley and Bard, 2010).

This permeabilization step facilitates enhanced antibody penetration and staining. Subsequently, primary antibody staining was performed. Then, rabbit anti-NeuN primary antibody, diluted 1:1000 in a solution containing 1% serum and 0.5% Triton-X 100 in TBS, was incubated with the tissue slices for 48 h at 4°C. NeuN is commonly used in immunohistochemistry to label neurons in brain tissue sections (Gusel'nikova and Korzhevskiy, 2015). The brain slices from each mouse group have been identified as negative controls, in which no primary antibody was applied. This indicated that any detectable signal resulted from specific binding rather than non-specific interactions.

After the application of the secondary antibody, the slices were washed with TBS. The secondary antibody solution, including donkey anti-rabbit Alexa Fluor 488 diluted 1:1000 in 1% serum and 0.5% Triton-X 100 in TBS, was added to all slices, including negative controls, and incubated for 24 h at 4°C. Alexa Fluor 488 is a highly sensitive and distinct fluorescent dye suited for cellular visualization under a microscope (Thermo Fisher Scientific; absorption 495 nm, emission 519 nm). The indirect labelling used in this experiment improved the signal and immunoreactivity relative to direct labelling. After an additional wash, the samples were stained with DAPI (absorption 358 nm, emission 461 nm), a fluorescent dye that accentuates DNA by adhering to regions abundant in thymine and adenine. Under ultraviolet light in a fluorescence microscope, DAPI shows a blue or cyan illumination, facilitating the visualization of the nuclei. This step was essential for the identification of nuclei in the later counting of neurons.

The immunohistochemical process ended with the visualization by a confocal microscope in a dark room. Brain slices from both mouse groups were collected using a neuron-counting procedure. To confirm that mCherry was expressed in GFAP-positive cells, the tissue samples were stained with anti-GFAP and a blue fluorescent secondary antibody. The other samples were used for cell counting. In experiments on ChAT-tdTomato mice, NeuN (a neuronal marker) was labeled with a green fluorescent antibody. For wild-type mice, NeuN was labeled with a blue fluorescent antibody, and choline acetyltransferase (ChAT) was labeled with a green fluorescent antibody.

3.5. Statistics

The mean ± SEM has been applied for all data. Normality tests were used to evaluate the datasets normal distribution, and the student's t-test was used to determine statistical significance (the level of significance: $p < 0.05$).

4. Results

4.1. Post-injection site evaluation

In the KCNQ study, the injection site, and the regions of mCherry expression were evaluated post hoc for mice that underwent viral injection. First, the mice were transcardially perfused with 4% paraformaldehyde and a vibratome (Campden, Loughborough, UK) that was used to cut 80-µm slices and then post-fixed for 24-h. Slices were scanned with a confocal microscope (Zeiss LSM 700 Live; Carl Zeiss AG, Oberkochen, Germany) mounted on a coverslip using mounting media containing 4',6 diamidino-phenylindol. The injection target was the pedunculopontine nucleus (PPN), which was located 4.26-4.96 mm caudal to the bregma. However, mCherry expression in astrocytes extends beyond the PPN, including the neighbouring regions.

Many brainstem regions showed expression, including the dorsal one-third of the oral pontine reticular nucleus, middle region of the mesencephalic reticular formation, and retrorubral field and nucleus. Also contributing to these processes are the precuneiform nucleus (PrCnF), the lateral and ventrolateral periaqueductal grey, the lateral side of the dorsal raphe nucleus, the medial paralemniscal nucleus, the microcellular tegmental nucleus, and the ventral portion of the cuneiform nucleus. (Paxinos and Watson 2013; Fig.19).

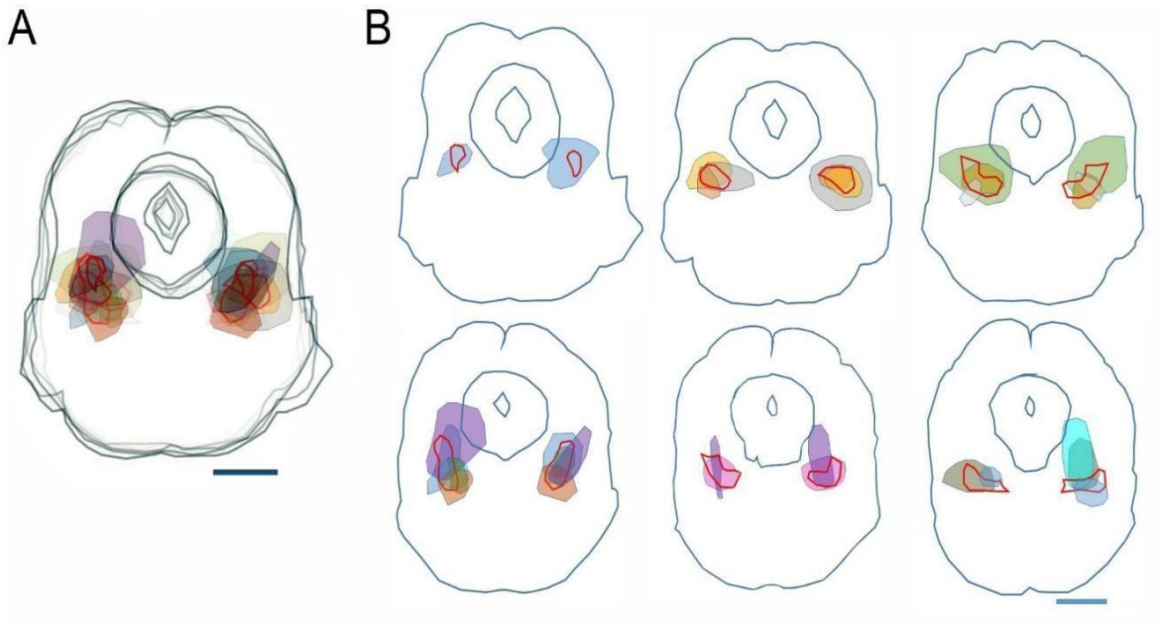

Fig. 19. Regions of astrocytic mCherry expression in the mesopontine region A. Composite image of 6 coronal mesencephalic sections represented in panel B. Individual coronal sections ranging from 4.26 to 4.96 mm caudal to the bregma, by 160 µm. Gray lines: contours of the brainstem, aqueduct, and periaqueductal gray. Red contours: pedunculopontine nucleus. Coloured regions: Specific locations of bilateral mCherry expression. Scale bar: 1 mm.

4.1.1. Two bottle preference test

During the preliminary experiment, a two-bottle preference experiment was conducted to evaluate mouse water consumption and the effects of CNO dissolution. No significant variation in consumption was observed while using tap water in both leakage-free bottles (left bottle: 15.9 ± 8.8 ml/3 days; right bottle: 24.6 ± 10.1 ml/3 days; n.s.). Daily water consumption was 6.75 ml. Based on the average weight of the first four mice (26.96 ± 2.93 g, a CNO concentration of 4 µg/ml was calculated for a daily dosage of 1 mg per body kg. the comparison between one bottle containing tap water and another with 9.6 µM (4 µg/ml) CNO dihydrochloride, no significant difference in consumption was observed (tap water: 18.66 ± 3.84 ml/3 days; CNO: 20 ± 6.93 ml/3 days).

The CNO concentration in the drinking water was first determined to achieve a consumption of 1 mg/kg based on the available data. However, the average body weight of the further 16 mice was 25.7 ± 3.33 g; thus, the calculated daily CNO exposure was slightly higher as planned (1.04 mg/kg). Therefore, no preference for or avoidance of CNO consumption is observed.

followed a similar strategy for chronic administration of CNO in drinking water (Zhan et al., 2019).

4.1.2. Activity wheel test

In the DREADD group, mice exhibited increased restlessness during the resting period (when the cages were lit), whereas the control group remained unaffected (Fig. 20). In the control group, inactivity levels showed no significant change in darkness after CNO drinking and light (resting period: Fig. 20A-B). Likewise, the daily travel distances in mCherry-expressing mice remained unchanged (Fig. 20C). Additionally, CNO treatment did not alter the maximal running speed in the control after CNO (Fig. 20D).

In the hM3D(Gq)-expressing DREADD group, some activity measures showed changes (Fig. 20E). The proportion of inactivity during the active phase (darkness) did not change significantly (Fig 25. F). However, during illumination (resting period), the resting time significantly decreased (Fig 25F). Total activity remained unaffected (Fig. 20F). Similar to the controls, daily running distances in the DREADD group after CNO were unchanged (Fig. 20G). Notably, CNO treatment significantly increased the maximal running speed in DREADD mice during the luminated (resting) period (Fig. 20H). Table 3, that showed all statistical numbers in control and DREADD groups.

Table 3: The statistical analysis that showed the effects of DREADD activation on inactivity, travel distance, and running speed in mice.

Measure	Phase	Control (mCherry) Before	Control (mCherry) After	DREADD (hM3Dq) Before	DREADD (hM3Dq) After	Significant Change
Inactivity (%)	Darkness	23 ± 5.7	30.8 ± 4.9	24.1 ± 3	31.3 ± 2	No
	Light	80.7 ± 3.8	77.5 ± 5	81.3 ± 1.4	74.3 ± 2	**Yes (p = 0.02)**
	Total	52 ± 2.3	54 ± 3	52.7 ± 1.6	52.8 ± 1.9	No
Daily Travel Distance (m/day)	Darkness	6215 ± 1602	5540 ± 1255	7713 ± 3076	5259 ± 369	No
	Light	117 ± 107	81.5 ± 72	63.6 ± 21	169.1 ± 79.2	No
	Total	6347 ± 1607	5522 ± 1228	7776.6 ± 3083	5428 ± 354	No
Max Running Speed (m/min)	Darkness	25.6 ± 1.66	25.3 ± 3.1	24.7 ± 2.89	27.47 ± 2.05	No
	Light	3.9 ± 2	4.3 ± 1.6	2.77 ± 1.61	8.45 ± 1.99	**Yes**

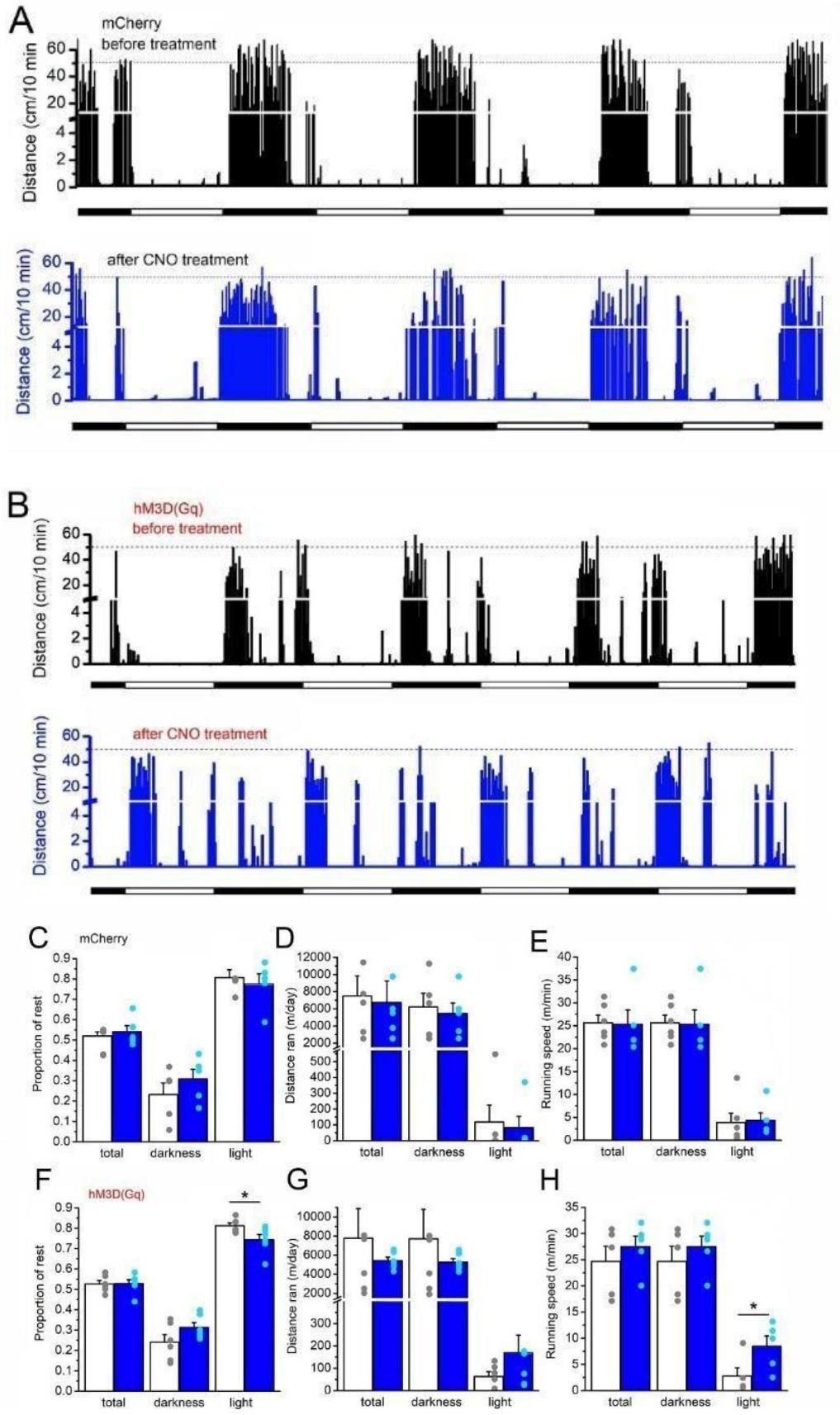

Fig. 20. Mesopontine astrocytic overactivation disrupts circadian activity in mice. Control Group (mCherry-expressing mice): A The activity pattern of a control mouse (before CNO: black bars; after CNO: blue bars) shows distances moved (cm) in 10-minute bins. The light/dark cycle is indicated below (hollow = light; black = dark). B. Resting time proportions (total, darkness, light) before (hollow bars, gray dots) and after CNO (blue bars, light

blue dots) remained unchanged (average ± SEM shown). C. The daily running distances before and after the CNO showed no significant differences. D. The maximal running speed was also unaffected by CNO treatment. DREADD Group (hM3D(Gq)- expressing mice): E. Activity patterns (similar to panel A) revealed altered behaviour. F. Resting time during the light (resting) period significantly decreased after CNO ($p < 0.05$), whereas darkness and total inactivity remained unchanged. G. Daily running distance was not significantly altered. H. Notably, the maximum running speed increased during the light period after the CNO ($p < 0.05$).

Visualization: Panels F-H are like the statistical layouts of B-D, significance (* $p < 0.05$).

4.1.3. Barnes maze test

In the Barnes maze task, we examined the effect of astrocyte overstimulation on spatial memory and learning. We found there are no notable differences between the control group (expressing mCherry) and DREADD group (expressing hM3D(Gq)). Before the administration of CNO, both groups showed similar spatial memory formation (Fig. 21A-C). After the 10th learning session as well as following CNO treatment and a new round of 10 training sessions, performance remained comparable between the two groups. Specifically, before CNO, the control group traveled 1938.6 ± 706.2 cm, while the DREADD group covered 906 ± 189.3 cm by the end of training. After CNO administration, the control group moved 4978.7 ± 1409 cm, and the DREADD group moved 4463.6 ± 959 cm. After the second training series, the control group’s distance was 1166.1 ± 240.3 cm, and the DREADD group's distance was 2136 ± 894 cm (Fig. 21C).

These results suggest that astrocyte overstimulation did not significantly alter spatial memory or learning performance in this experiment (Table 4).

Table 4: Comparative distance metrics (cm) across training phases in control and DREADD mice in the barnes maze.

Training Phase (End of 10 Sessions)	Control (mCherry)	DREADD (hM3Dq)	Significant Difference?
Before CNO	1938.6 ± 706.2	906 ± 189.3	No
After CNO	4978.7 ± 1409	4463.6 ± 959	No
After Second Training Series	1166.1 ± 240.3	2136 ± 894	No

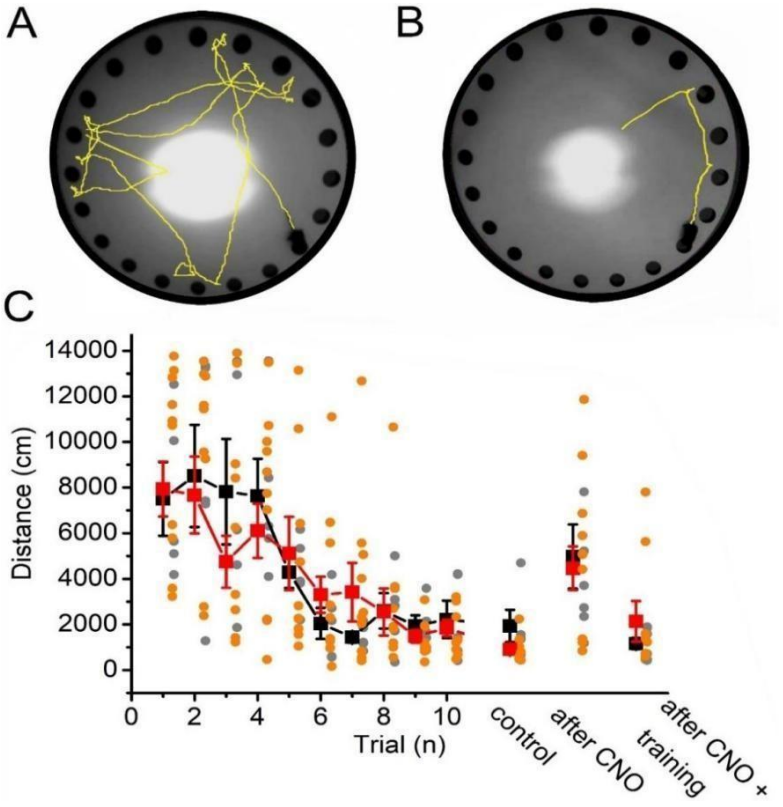

Fig. 21. Astrocytic overactivation in the mesopontine region does not impair spatial memory. A-B. The mouse's movement path (yellow) to the shelter in the Barnes maze test is shown before (A) and after training (B). C. The graph compares the distances travelled during training trials, measured at three time points: After 3 days ("control"), Immediately following CNO consumption, After a second round of training. Data representation: Red squares (average ± SEM) and orange dots (individual hM3D(Gq) mice) for the DREADD group. Black squares

(average ± SEM) and gray dots (individual mCherry control mice) represent the control group. The results indicated no significant differences in spatial memory performance between the two groups.

4.1.4. Acoustic startle test

The amplitude of the acoustic startle reflex and its short-term habituation were also examined (Fig. 22A-B). After normalizing the post-CNO responses to the pre- treatment condition, the DREADD group showed a significantly reduced first relative amplitude compared with the control group (first amplitude: control group with CNO treatment, 133 ± 23%; DREADD group with CNO treatment, 68 ± 12%; $p = 0.012$). Similarly, the mean normalized amplitude of the five simultaneously recorded startle responses was significantly decrease in the DREADD group than in the control group (average amplitude: control group with CNO treatment, 109.8 ± 8.5%; DREADD group with CNO treatment, 93.1 ± 19.4%; $p = 0.006$; Fig. 22C). In the control (mCherry) group, the first startle amplitude was 14.6 ± 2.7 mN under baseline conditions and increased to 18.2 ± 3.3 mN after CNO administration.

In the DREADD group, the mean first amplitude was 26.2 ± 3.3 mN before decreasing to 16.5 ± 2.9 mN following CNO treatment ($p = 0.021$; Fig. 22D-E). However, the subsequent amplitudes remained constant. In summary, chronic astrocytic stimulation reduced the initial acoustic startle reflex but did not significantly alter short-term habituation. The statistical analysis of control and DREADD on Table 5.

Table 5: Quantitative comparison of startle amplitude and habituation in controls and. DREADD mice after CNO treatment.

Group	Condition	1st Startle Amplitude	Avg. of 5 Startle Responses	Statistical Significance
Control	Post-CNO (normalized)	133 ± 23%	109.8 ± 8.5%	-
DREADD	Post-CNO (normalized)	68 ± 12%	93.1 ± 19.4%	1st: **p = 0.012**Avg: **p = 0.006**
Control	Pre-CNO (raw)	14.6 ± 2.7 mN	-	-
Control	Post-CNO (raw)	18.2 ± 3.3 mN	-	-
DREADD	Pre-CNO (raw)	26.2 ± 3.3 mN	-	-
DREADD	Post-CNO (raw)	16.5 ± 2.9 mN	-	**p = 0.021**
Conclusion	-	↓ Initial reflex in DREADD group	No significant habituation difference	-

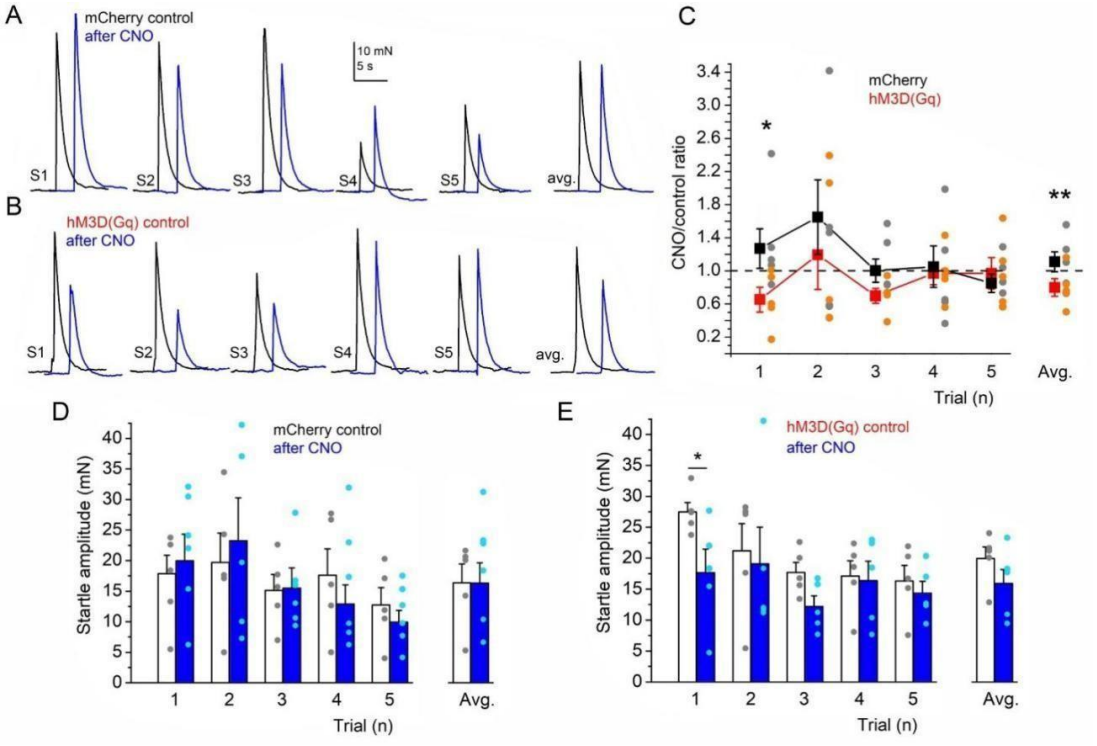

Fig. 22. Chronic astrocyte activation reduces the amplitude of the acoustic startle reflex. A. Representative startle traces from mCherry-expressing control mice, showing repeated trials at 1-minute intervals (S1–S5) and their average before (black) and after CNO treatment (blue). B. Representative startle traces from hM3D(Gq)-expressing mice, displayed in the same format as in panel A. C. Statistical comparison of startle amplitudes after CNO treatment, normalized to pre-treatment values (CNO/control ratio), across five consecutive trials and their average. Red traces: mean ± SEM for hM3D(Gq)-expressing mice. Orange dots: Individual data points. Black traces: mean

± SEM for mCherry-expressing controls. Gray dots: individual data points. D. Statistical comparison of startle amplitudes before (hollow bars: mean ± SEM, gray dots: individual data) and after CNO treatment (blue bars: mean ± SEM, light blue dots: individual data) across five trials and their average in mCherry- expressing controls. E. Statistical comparison of startle amplitudes before and after CNO treatment in hM3D(Gq)-expressing mice, presented in the same format as panel D * $p < 0.05$.

Interestingly, in the KCNQ4 knockout experiment, the strength of the startle response was greater for all five stimuli tested. The difference was statistically significant for the first, fourth, and fifth stimuli (wild type: 1st: P = 0.007; 4th: P = 0.035; 5th: P = 0.028).

Table 6: Startle response amplitudes across five stimuli in Wild-Type and KCNQ4 knockout mice.

Stimulus	Wild-Type (mN)	Knockout (mN)	p-value
1st	23.22 ± 3.74	49.96 ± 7.15	**p = 0.007**
2nd	22.22 ± 6.47	42.02 ± 8.65	-
3rd	21.86 ± 4.23	42.62 ± 9.26	-
4th	18.3 ± 6.13	41.15 ± 7.75	**p = 0.035**
5th	12.52 ± 4.14	30.99 ± 6.19	**p = 0.028**
Average	19.76 ± 2.14	41.27 ± 4.97	**p = 0.0025**

The average startle response across all five stimuli was also significantly different between the two groups (wild type: 19. 76 ± 2.14 mN; knockout: 41.27 ± 4.97 mN; p = 0.0025;(Fig. 23A-E). The startle response during repeated stimuli did not decrease over time in either the normal or knockout mice (Fig. 23F).

Table 7: Startle response amplitudes across five stimuli and habituation in Wild-type and KCNQ4 knockout mice.

Group	Habituation (normalized to 1st)	Average Ratio
Wild-Type	2nd: 1.04 ± 0.24 3rd: 1.12 ± 0.29 4th: 0.954 ± 0.37 5th: 0.84 ± 0.29	1.02 ± 0.18
Knockout	2nd: 0.86 ± 0.09 3rd: 1.00 ± 0.27 4th: 1.03 ± 0.27 5th: 0.84 ± 0.29	0.95 ± 0.14
Conclusion	Knockouts had significantly stronger startle responses. No significant habituation in either group	

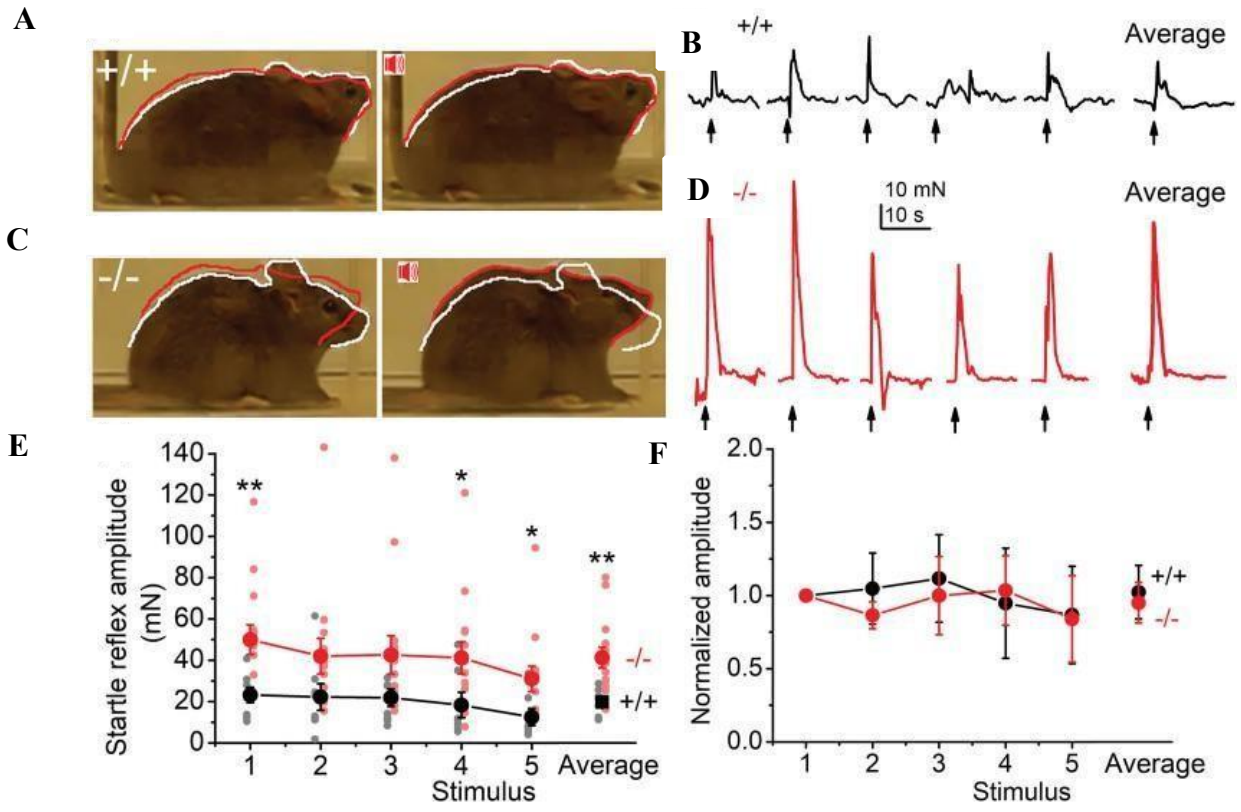

Fig. 23. Deletion of the KCNQ4 subunit strengthens the acoustic startle reflex. A. Shows how a normal mouse (+/+) looks before (left) and during (right) a startle response. The white outline is before, and the red outline is during. B. Shows five startle responses in a row and their average for a normal mouse. C. Shows how a KCNQ4 knockout mouse (−/−) looks before and during a startle response, similar to panel

A. D. Shows the startle responses in a row and their average for a KCNQ4 knockout mouse. E. Comparison of startle reflex strength between normal mice (black) and knockout mice (red). Gray dots represent individual data

points for normal mice, and pink dots represent knockout mice. F. Shows the startle reflex strength after being adjusted based on the first measurement (black for normal, red for knockout). *P < 0.05 and **P < 0.01 indicate statistically significant differences. KCNQ4 is a potassium voltage-gated channel subfamily Q member 4.

Following experiments of the KCNQ study, we investigated a situation in which the startle network might be overly active (hyperexcitability). We used five mice that had a special tag (pAAV-hSyn-mCherry) in the neurons of the caudal pontine reticular nucleus (PnC) and the brain areas that send signals to it. These areas included the ventral cochlear nucleus, principal sensory trigeminal nucleus, superior paraolivary nucleus, lateral and medial superior olive, laterodorsal tegmental nucleus, dorsal raphe nucleus, central nucleus of the inferior colliculus, reticulotegmental nucleus, latero- and medioventral nucleus of the pons, dorsal, intermediate, and ventral nucleus of the lateral lemniscus, and pedunculopontine nucleus (Fig. 24A-B).

For the control, another five mice that had only the mCherry tag in the same brain area were used (Fig. 24C-F.). We then examined the strength of the startle reflex after injecting with either normal saline or clozapine-N-oxide (CNO). In mice with only the mCherry tag, CNO did not cause any significant change in the strength of their startle reflexes (Fig. 24G). However, in the mice that expressed hM3D(Gq), we saw a significant increase in the strength of the first startle response after CNO injection ($P = 0.009$ for the 1st response; averages: 18.19 ± 3.13 with saline and 28.08 ± 7.83 mN with CNO; Fig. 24H). When we compared the strength of the first startle response after CNO treatment between mCherry-only mice and hM3D-expressing mice, the hM3D(Gq)-expressing mice showed a significantly stronger startle response ($p = 0.028$; Fig. 24I).

In hM3D(Gq)-expressing mice that received CNO, their startle responses quickly weakened with repeated stimuli. When we compared their responses during CNO treatment to their responses to the saline injection, we observed a significant jump in the strength of the first startle in the hM3D(Gq) mice ($p = 0.04$), but then this strength rapidly decreased for the following stimuli (1st: 5.17 ± 1.67, 2nd: 1.25 ± 0.31, 3rd: 1.41 ± 0.52, 4th: 1.29 ± 0.45, 5th: 2.5 ± 0.68; average: 1.82 ± 0.4).

Table 8: Startle amplitudes and habituation in mcherry and hM3D(Gq)mice after CNO and saline injections targeting neurons of the caudal pontine reticular nucleus (PnC).

Group	Injection	1st Startle (mN)	Average (mN)	Statistical Comparison
mCherry	Saline	13.78 ± 4.93	18.47 ± 3.09	-
mCherry	CNO	17.47 ± 6.29	25.59 ± 4.85	-
hM3D(Gq)	Saline	14.85 ± 3.98	18.19 ± 3.13	-
hM3D(Gq)	CNO	**42.05 ± 9.26**	**28.08 ± 7.83**	**p = 0.009** (1st vs saline) **p = 0.028** (vs mCherry)

Group	Habituation (Normalized)	Average Ratio
hM3D(Gq) + CNO	2nd: 1.25 ± 0.31 3rd: 1.41 ± 0.52 4th: 1.29 ± 0.45 5th: 2.5 ± 0.68	1.82 ± 0.40
mCherry + CNO	2nd: 1.34 ± 0.64 3rd: 1.88 ± 0.29 4th: 1.52 ± 0.25 5th: 1.87 ± 0.55	1.55 ± 0.24
Conclusion	hM3D(Gq) mice showed stronger initial reflex and rapid short-term habituation after CNO, unlike controls	

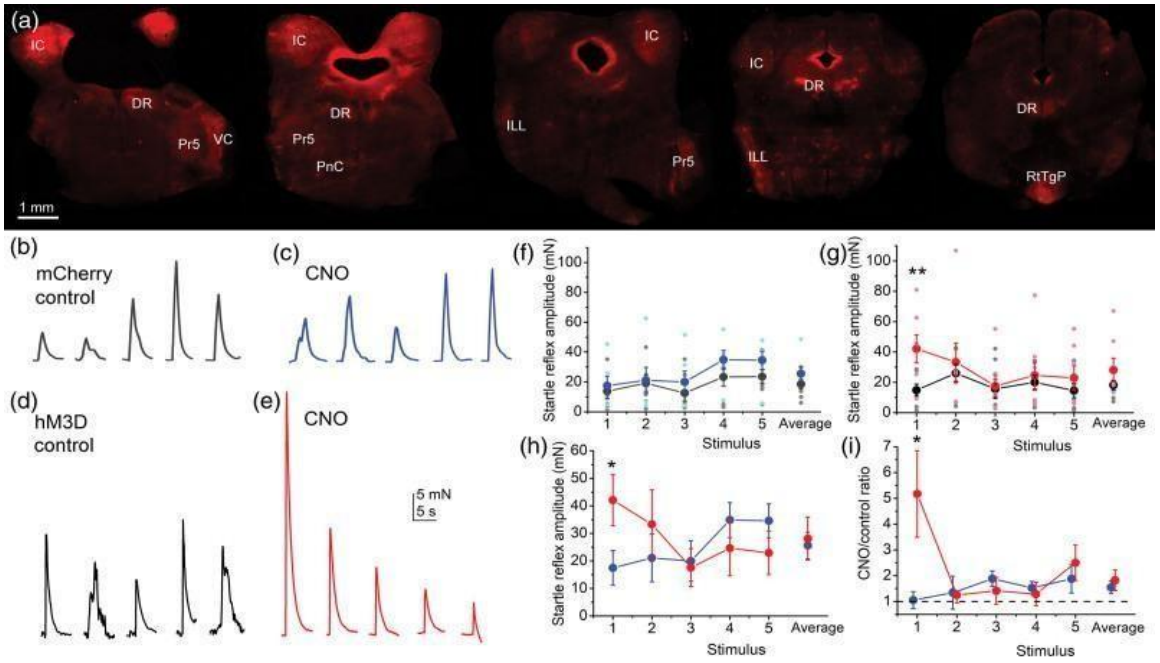

Fig. 24. Chemogenetic activation of the PnC and the nuclei projecting to it cause a similar increase in the amplitude of the acoustic startle. A. Shows where the injections were made and where the mCherry tag was expressed. B, C. Show five startle responses in a row for a mouse with only the mCherry tag, both normal (black) and after receiving a CNO injection (blue). D, E. Show the startle responses for a mouse expressing hM3D, both normally (black), while CNO was active (red). F. Comparison of the strength of startle responses in mice with only mCherry (black before CNO, blue during CNO; gray dots are individual data before, light blue dots are individual data with CNO). G. Strength of startle responses in mice expressing hM3D (black before CNO, red during CNO; gray dots are individual data before, pink dots are individual data with CNO). H. Comparison of the average startle responses after CNO treatment in mCherry-expressing mice (blue) and hM3D-expressing mice (red). I. Shows the average ratios of startle responses with CNO compared to normal conditions for mCherry- (blue) and hM3D- expressing mice (red). CNO, clozapine-N-oxide; DLL, dorsal nucleus of the lateral lemniscus; DR, dorsal raphe nucleus; hM3D, human M3 muscarinic; IC, inferior colliculus; ILL, intermediate nucleus of the lateral lemniscus; LDT, laterodorsal tegmental nucleus; PnC, pontine caudal nucleus; PnR, pontine raphe nucleus; Pr5, principal trigeminal nucleus; SOC, superior olivary complex; SPTG, subpeduncular tegmental nucleus; VC, ventral cochlear nucleus.

This quick weakening of the response was not observed in the control mice that only had the mCherry tag (1st: 1.05 ± 0.33, 2nd: 1.34 ± 0.64, 3rd: 1.88 ± 0.29, 4th: 1.52 ± 0.25, 5th: 1.87 ± 0.55; average: 1.55 ± 0.24). The initial startle strengths of mCherry- only and hM3D mice were significantly different ($p = 0.04$; Fig. 24G).

4.1.5. Gait alterations

In this experiment, we examined gait parameters, such as stride length, sway length, and stance length (Fig. 25A-C). The control group, which expressed mCherry, showed no changes in these measurements after CNO administration compared to baseline (front limb: stride length—5.39 ± 0.3 cm before vs. 5.27 ± 0.4 cm after; sway length— 1.84 ± 0.19 cm before vs. 1.53 ± 0.15 cm after; stance length—3.67 ± 0.18 cm before vs. 3.99 ± 0.4 cm after; hind limb: stride length—5.27 ± 0.35 cm before vs. 5.33 ± 0.46 cm after; sway length—2.41 ± 0.15 cm before vs. 2.39 ± 0.17 cm after; stance length—

3.61 ± 0.13 cm before vs. 3.83 ± 0.27 cm after; Fig. 25D-F).

However, in the DREADD group—where mesopontine astrocytes expressed hM3D(Gq)—all measured parameters increased significantly after CNO treatment (front limb: stride length—4.3 ± 0.22 cm before vs. 5.88 ± 0.25 cm after, $p = 0.000116$; sway length—1.37 ± 0.1 cm before vs. 2.03 ± 0.18 cm after, $p = 0.0028$; stance length—3.13 ± 0.21 cm before vs. 3.86 ± 0.13 cm after, $p = 0.0053$; hind limb: stride length—4.4 ± 0.18 cm before vs. 6.22 ± 0.16 cm after, $p < 0.00001$; sway length—2.33 ± 0.12 cm before vs. 3.26 ± 0.18 cm after, $p = 0.00039$; stance length—3.39 ± 0.12 cm before vs. 5.13 ± 0.19 cm after, $p < 0.00001$; Fig. 35A-B, G-I). Stastical comparison between Control (mCherry) and DREADD (hM3D(Gq)) on Table 9.

Table 9: Gait parameter increases in DREADD mice after CNO treatment compared to stable measures in controls (n.s = not significant).

Limb	Parameter	Group	Before CNO (cm)	After CNO (cm)	p-value
Front	Stride Length	Control (mCherry)	5.39 ± 0.30	5.27 ± 0.40	n.s.
		DREADD (hM3D(Gq))	4.30 ± 0.22	5.88 ± 0.25	**0.000116**
	Sway Length	Control (mCherry)	1.84 ± 0.19	1.53 ± 0.15	n.s.
		DREADD (hM3D(Gq))	1.37 ± 0.10	2.03 ± 0.18	**0.0028**
	Stance Length	Control (mCherry)	3.67 ± 0.18	3.99 ± 0.40	n.s.
		DREADD (hM3D(Gq))	3.13 ± 0.21	3.86 ± 0.13	**0.0053**
Hind	Stride Length	Control (mCherry)	5.27 ± 0.35	5.33 ± 0.46	n.s.
		DREADD (hM3D(Gq))	4.40 ± 0.18	6.22 ± 0.16	**< 0.00001**
	Sway Length	Control (mCherry)	2.41 ± 0.15	2.39 ± 0.17	n.s.
		DREADD (hM3D(Gq))	2.33 ± 0.12	3.26 ± 0.18	**0.00039**
	Stance Length	Control (mCherry)	3.61 ± 0.13	3.83 ± 0.27	n.s.
		DREADD (hM3D(Gq))	3.39 ± 0.12	5.13 ± 0.19	**< 0.00001**

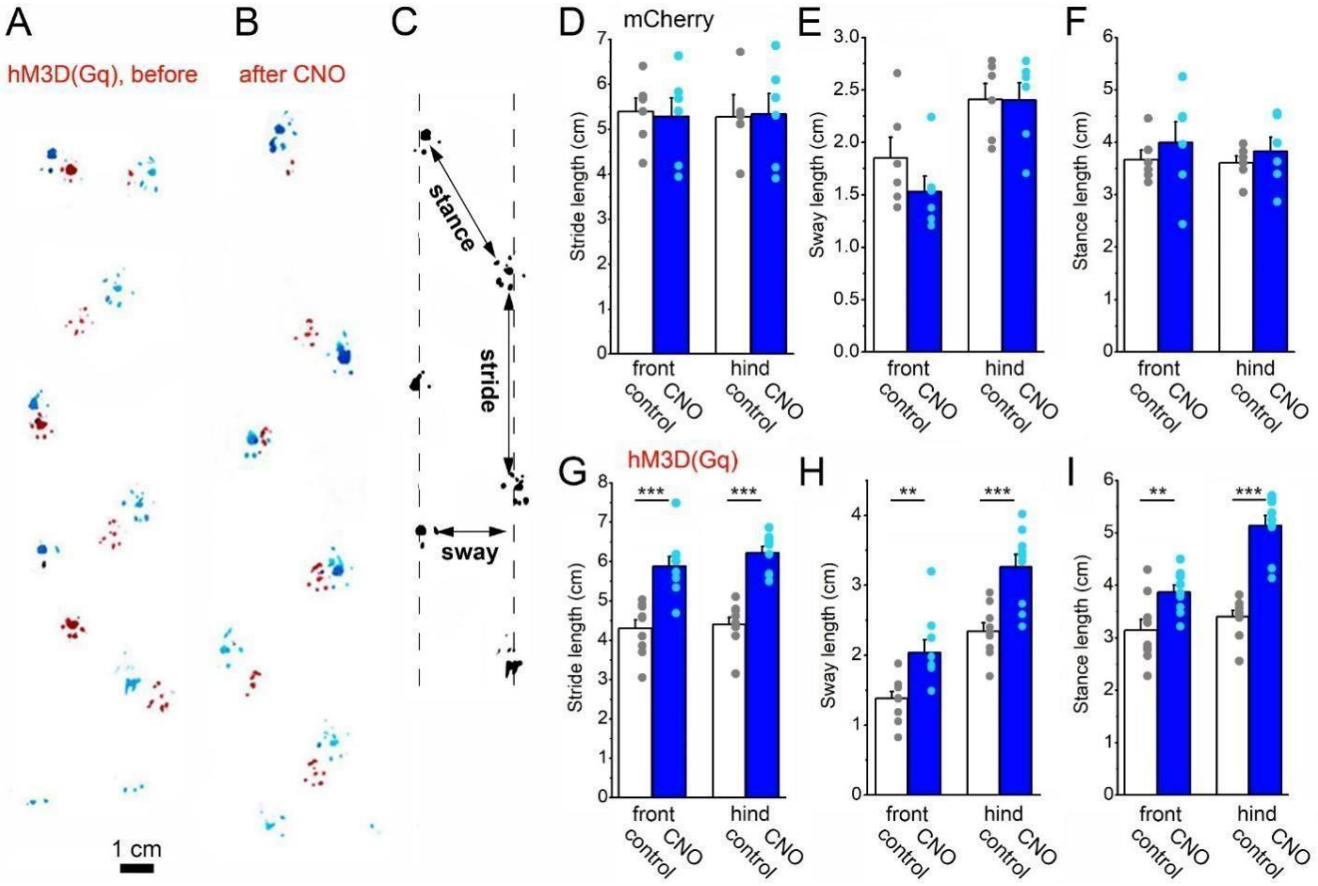

Fig. 25. Changes in movement patterns following astrocyte overactivation. A-B. Example footprint traces from an hM3D(Gq) mouse before (A) and after (B) CNO administration. Hindpaws are marked in blue and front paws are marked in red. C. Diagram illustrating how footprint parameters were measured. D-F. Bar graphs comparing stride, sway, and stance lengths in mCherry control mice before (hollow bars: mean ± SEM; grey dots: individual values) and after CNO (blue bars: mean ± SEM; light blue dots: individual values). G-I. Equivalent analysis for hM3D(Gq)-expressing mice was identical to that for (D- F). Asterisks denote significance: **p < 0.01, ***p < 0.001.

4.2. Histological analysis

To assess the injection site and the affected brain regions, we quantified cholinergic neurons, non-cholinergic neurons, and astrocytes using immunohistochemical markers. Cholinergic neurons were identified by ChAT immunopositivity combined with NeuN labelling, whereas non-cholinergic neurons showed NeuN positivity without ChAT expression. Astrocytes were defined based on mCherry expression. Cell counts were performed bilaterally at the injection site within a standardized 0.43 × 0.43 mm square centered on the PPN (see Fig. 26C, D).

The analysis revealed comparable anatomical locations between groups: the counting region

measured 4.5 ± 0.09 mm caudal to bregma in control mice (expressing only mCherry in astrocytes) versus 4.54 ± 0.08 mm in DREADD mice (co-expressing mCherry and chemogenetic actuators), with no statistically significant difference in positioning (Fig. 27A). This methodological consistency confirmed that the experimental groups were evaluated under equivalent neuroanatomical conditions.

Following chronic CNO administration, quantitative analysis revealed distinct cellular changes in the groups. Control animals exhibited 58.62 ± 6.2 cholinergic neurons, 512.89 ± 28.72 non-cholinergic neurons, and 70.61 ± 10.02 astrocytes per mm². In contrast, the DREADD group showed significantly reduced numbers: 31.89 ± 7.03 cholinergic neurons (54.4% of controls, $p = 0.0054$) and 389.06 ± 31.9 non-cholinergic neurons (75.8% of controls, $p = 0.0049$). Astrocyte counts in DREADD mice (78.19 ± 12.17/mm²) represented 110.7% of control values ($p = 0.32$), demonstrating no statistically significant change (Fig. 27B). These findings indicate that prolonged astrocytic activation preferentially affects cholinergic populations, while sparing glial cells.

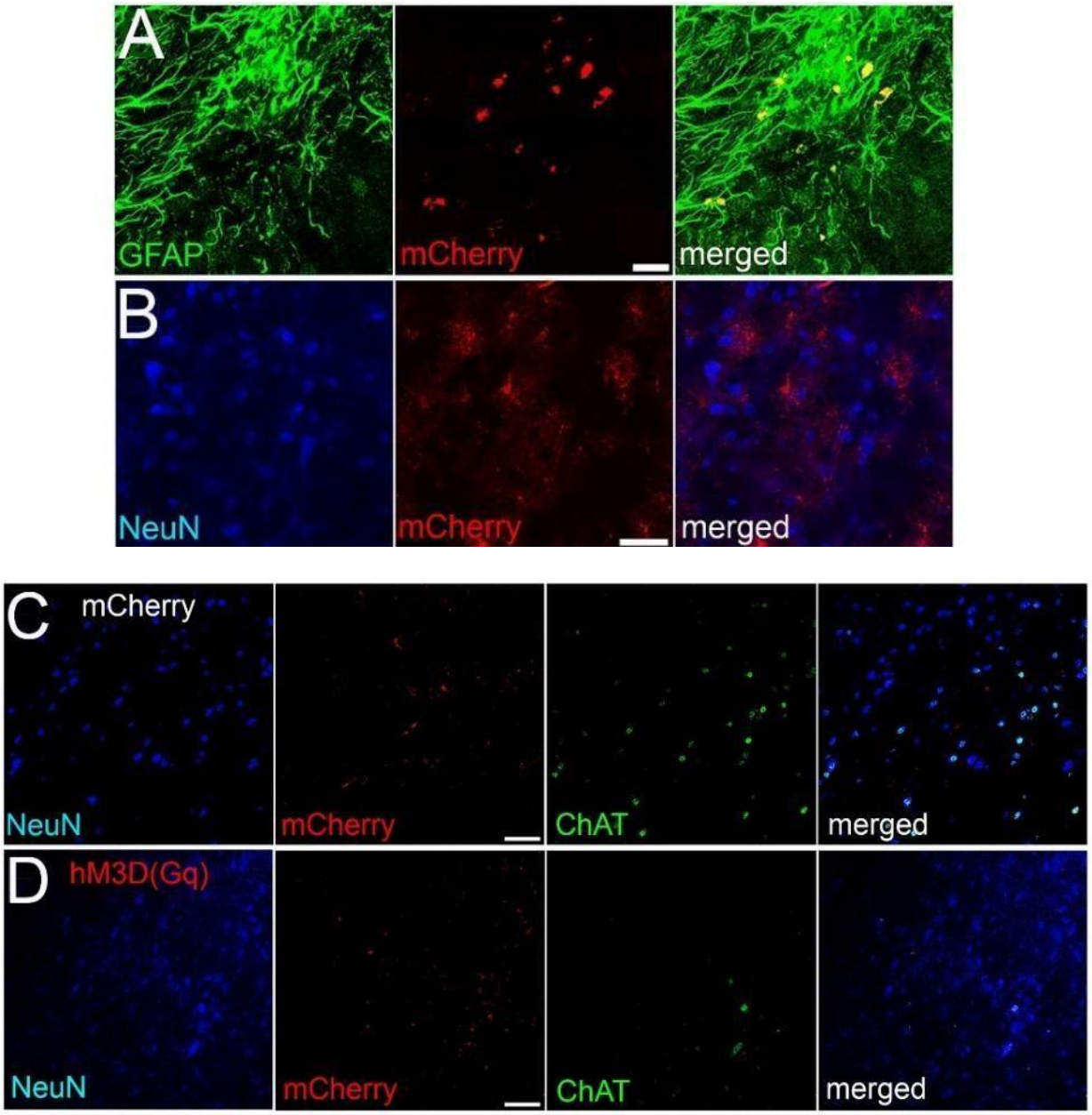

Fig. 26. Evaluation of injection sites and long-term neuronal changes. A. single z-stack image demonstrating GFAP immunostaining (green) overlapping with mCherry expression (red), with a merged view on the right. Scale bar: 20 µm. B. Another z-stack image shows NeuN labelling (blue) without colocalization with mCherry (red), as confirmed in the merged image. Scale bar: 20 µm. C. In control mice (mCherry-expressing), cholinergic (ChAT+, green) and non-cholinergic (NeuN+, blue) neuron counts were assessed after chronic CNO treatment and behavioural tests. Merged imaging combines NeuN, mCherry, and ChAT signals. D. Similarly, in DREADD mice (hM3D(Gq)-expressing), neuronal counts were analyzed post-treatment, with merged images displaying NeuN, mCherry, and ChAT labeling. Scale bars: 50 µm.

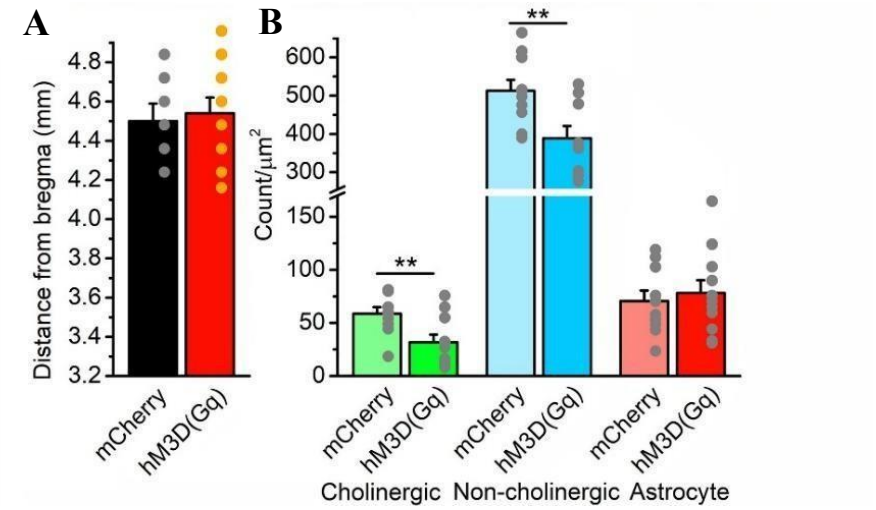

Fig. 27. The injection site locations (caudal to bregma, mm) were statistically compared between the control (mCherry, black bars ± SEM; gray dots) and DREADD mice (hM3D(Gq), red bars ± SEM; orange dots). F. Neuronal counts after CNO treatment were compared: cholinergic neurons (control: light green, DREADD: green), non-cholinergic neurons (control: light blue, DREADD: blue), and astrocytes (control: pink, DREADD: red). Bars show the mean ± SEM; gray dots represent individual data. ** $p < 0.01$.

5. Discussion

Summarizing our findings in this project, chronic chemogenetic activation of astrocytes in the pedunculopontine nucleus and nearby mesopontine regions led to a decrease in acoustic startle reflex amplitude and an increase in locomotion speed during the resting period. Additionally, gait alterations were observed, but spatial memory remained unaffected. These findings may be attributed to a significant reduction in neuronal populations: cholinergic neurons decreased to 54% of the control levels, and non-cholinergic neurons dropped to 76% of the control levels (the control mice received identical CNO treatment and underwent the same surgical procedure injection as the DREADD group). If neuronal loss was primarily due to the injection's physical trauma or fluid volume, both groups would show similar levels of damage. The observed differential loss in the DREADD group indicated that injection-related physical damage was not the primary cause of neuronal degeneration.

Thus, chronic astrocytic overstimulation, with subsequent neuronal loss, resulted in motor and circadian rhythm disturbances similar to brainstem-related symptoms seen in progressive supranuclear palsy, suggesting a possible role for astrocytic overactivation in the development of this disease. Later histological analysis showed a significant loss of cholinergic neurons in the group with long-term artificial astrocyte activation compared to the control group, which received the same CNO treatment but did not show astrocyte overactivation (Maamrah et al., 2025).

The important role of potassium voltage-gated channel (KCNQ) in regulating of startle reflex, we found KCNQ4 knockout mice exhibited a significantly exaggerated acoustic startle reflex and showed minimal habituation compared to wild-type mice. This heightened startle response, which differs from other forms of startle hyperexcitability, is attributed to both cochlear damage and altered neuronal excitability within the startle networks resulting from KCNQ4 subunit deletion (Maamrah et al., 2023).

5.1. Actions of astrocytic activation on the PPN

In earlier studies using in vitro slice electrophysiology and imaging, we identified an astrocyte-

mediated mechanism shared across multiple neuromodulatory systems, including the cholinergic, cannabinoid, serotonergic, and partly orexinergic pathways (Kőszeghy et al., 2015; Kovács et al., 2017, 2019; Kovács and Pál, 2017). We observed that astrocyte activation—whether triggered by neuromodulators or optogenetics—led to distinct neuronal responses: one subgroup of neurons hyperpolarized and reduced firing via group I mGluRs, while another subgroup depolarized and increased firing via group II mGluRs (Kőszeghy et al., 2015; Kovács et al., 2017). The third group did not respond to astrocyte stimulation. Another regulatory mechanism involves the extrasynaptic GluN2B-containing NMDARs. When "slow inward currents" (SICs) had a low baseline frequency, neuromodulators consistently increased their occurrence. Conversely, if SICs were initially frequent, the same neuromodulators would suppress them. This effect results from NMDAR activation, followed by desensitisation and subsequent reactivation (Kovács and Pál, 2017).

Although these findings were obtained in vitro, their potential physiological or pathological relevance remains unclear. To further understand this, we targeted astrocytes in vivo using behavioural experiments to assess how astrocyte overactivation might influence functions linked to the mesencephalic locomotor region (MLR) and nearby brain areas using DREADD chemogenetic activation. Chemogenetic activation is considered a good tool to target astrocytes and investigate their role in different brain areas. Previous studies using chemogenetic activation of astrocytes in different brain regions have shown varied behavioural effects. The acute Gq-DREADD stimulation of astrocytes in the hippocampus and medial prefrontal cortex enhanced memory and learning (Wang et al. 2022, Delcourte et al. 2023; Adamsky et al. 2018). Similarly, acute astrocyte activation in the nucleus accumbens alters reward processing and addictive behaviours (Scofield et al., 2015; Bull et al., 2014), promotes goal-directed over habitual actions in the striatum (Kang et al., 2020), and reduces fear responses in the amygdala (Martin et al., 2017). Additionally, acute chemogenetic stimulation of pontine astrocytes suppresses REM sleep and decreases the number of REM time (Kurogi et al., 2024).

Chronic chemogenetic activation of hippocampal astrocytes—applied over periods ranging from 7 days to lifelong— produces effects that differ from neuronal activation, influencing fear memory differently (Suthard et al., 2023). The outcomes of excitotoxicity are inconsistent; in some cases, it triggers astrocyte morphological changes and a neuroinflammatory state linked to cognitive impairment (Kim et al., 2024), while in others, it counteracts kainate-induced metabolic hyperactivity, protecting against excitotoxic damage and memory decline (Martin et al., 2024).

Progressive supranuclear palsy (PSP) is a neurodegenerative disorder characterised by motor symptoms such as Parkinson's disease. It involves gait and postural disturbances, along with cognitive and behavioural impairments, such as dementia, REM sleep- related motor abnormalities, and loss of the acoustic startle reflex (Jellinger, 2025; Gironell et al., 2003). This disease is marked by the accumulation of tau protein in neurons, astrocytes, and oligodendrocytes. In the early stages, tau pathology primarily affects the brainstem and subcortical neurons, which later spread to cortical regions as the disease progresses (Kovacs et al., 2020).

5.2. Alterations of the acoustic startle reflex

Startle reflex changes are related to cochlear damage caused by aging, noise, or drugs (Chen et al., 2013; Salloum et al., 2014; Xiong et al., 2017; Zhang et al., 2022b). Minimal damage increases this reflex, and severe damage reduces it (Zhang et al., 2022b). KCNQ4 knockout mice and DFNA2 patients have 60 dB progressive hearing loss due to outer (and lesser inner) hair cell degeneration (Carignano et al., 2019). These specific channels are noteworthy because they are activated by membrane potentials that are more negative than the threshold required for an action potential. Additionally, neural KCNQ channels are crucial for epilepsy treatment and hold promise as therapeutic targets for various neurological conditions, including chronic and neuropathic pain, deafness, and mental disorders. Previous studies suggested that KCNQ4 plays a role in startle, supported by its overlap with brainstem startle structures (Kharkovets et al., 2006) and its presence in the pedunculopontine nucleus (Azzopardi et al., 2018;

Bayasgalan et al., 2021). In addition to cochlear damage, KCNQ4 loss causes hyperexcitability of the brainstem nuclei. A chemogenetic model mimicking brainstem hyperexcitability (without cochlear damage) showed a similar increase in the initial startle but stronger short-term habituation in KCNQ4 knockout animals.

These differences might be due to cochlear damage in knockout animals and more affected nuclei. CNO itself may also slightly inhibit startle growth (MacLaren et al., 2016). KCNQ4 deletion was long considered 'nonsyndromic' hearing loss, but elevated mechanosensitivity (Heidenreich et al., 2011), and altered circadian rhythm adaptation (Bayasgalan et al., 2021). The exaggerated acoustic startle response in KCNQ4-deleted animals results from both cochlear damage and brainstem hyperexcitability (Maamrah et al. 2023).

5.3. Memory and gait alterations

The excitotoxicity of the PPN by astrocytes (primarily affecting non-cholinergic neurons) has been shown to cause learning impairments (Wilson et al., 2009; MacLaren et al., 2016) and attention deficits (Cyr et al., 2014). Similar to progressive supranuclear palsy, cognitive disruptions, including memory and attention problems have been observed (Jellinger et al., 2025). Furthermore, sleep and circadian rhythm disturbances may contribute to memory dysfunction (Palagini et al., 2020). Given these findings, we chose the Barnes maze test, which minimizes stress compared to the fear conditioning or forced swim tests, to assess cognitive function. Our results revealed no differences between control and DREADD-treated groups, aligning with previous evidence that cholinergic neuron loss does not severely impair memory. Additionally, since the number of non-cholinergic neurons (which may influence cognitive performance) remained stable during our experiments, this further supports the absence of memory- related deficits in our model.

Analysis of footprint patterns revealed increases in all measured parameters, including stride, stance, and sway length, for both the front and hind paws. Previous studies have shown that the loss of PPN cholinergic neurons leads to significant motor impairments, including rear paw slips and disrupted gait precision (MacLaren et al., 2018; King et al., 2021). Several

neurological conditions alter stride and sway length, including hyperekplexia (characterized by heightened muscle tone), and Alzheimer's disease models exhibit shorter strides and narrower step widths (Hirzel et al., 2006; Nyul-Toth et al., 2021), with the latter also showing reduced walking speed. By contrast, PSP presents with shorter strides and wider step widths (Egerton et al., 2012). Our findings, which showed an overall increase in footprint measures, do not align with these disease patterns. One possible explanation is that stride length correlates directly with movement speed (Herbin et al., 2004), and our activity-wheel tests confirmed faster locomotion. Thus, the observed changes may reflect a mix of PSP-like features (such as increased sway length) and the effects of increased walking speed (leading to longer strides).

5.4. Alterations of neuronal numbers as the background of the behavioral changes

Previous studies have shown that excitotoxic damage to the posterior PPN causes learning impairments and changes in locomotor behaviour (Wilson et al., 2009; Alderson et al., 2008). These effects were later revealed to be due to alterations in non- cholinergic neurones, as the depletion of cholinergic neurons did not produce the same deficits (MacLaren et al., 2016). Rodent models of brainstem-related PSP symptoms have been developed by targeting the cholinergic brainstem regions (MacLaren et al., 2018; King et al., 2021). First, selective depletion of PPN cholinergic neurons in PSP motor symptoms reduces acoustic startle responses and movement impairments, such as disrupted gait control (MacLaren et al., 2018). Second, the expression of tau protein in PPN-induced tau pathology leads to the loss of cholinergic neurons in the PPN and dopaminergic cell death in the substantia nigra, which produces symptoms consistent with earlier findings (King et al., 2021).

We addressed this gap by demonstrating that chronic astrocyte activation can induce symptoms similar to those of PSP and PPN excitotoxicity. Chronic overactivation of astrocytes resulted in an almost 50% reduction in cholinergic neurons and a significant decline in non-cholinergic neurons, whereas the number of astrocytes remained unchanged. This effect may be explained

by chemogenetic astrocyte stimulation triggering glutamate release (Csemer et al., 2023), which then induces tonic depolarization in PPN neurons expressing group II metabotropic glutamate receptors (Kőszeghy et al., 2015; Kovács et al., 2017) and phasic depolarization through extrasynaptic NMDA receptor activation (Kovács and Pál, 2017).

However, because only some neurons have group I mGluRs, leading to hyperpolarization, and others show no tonic current response, not all neurons in the area are equally susceptible to excessive astrocyte activity (Kőszeghy et al., 2015; Kovács et al., 2017). One of the key effects of chronic astrocytic activation in the MLR and surrounding areas is a reduction in the acoustic startle reflex, which is regulated by the PPN. Optogenetic activation of cholinergic neurons increases this reflex, whereas non- cholinergic neurons likely help control it through prepulse inhibition (Azzopardi et al., 2018). Supporting this, selective damage to PPN cholinergic neurons or tau protein buildup in these cells has been shown to reduce startle reflex amplitude (MacLaren et al., 2018; King et al., 2021).

Chronic activation of midbrain astrocytes leads to disruption of circadian patterns. The mice showed increased movement during their normal resting period, along with faster peak movement speeds. These changes may stem from disturbances in the sleep regulation. Sudies found that acute chemogenetic stimulation of pontine astrocytes reduces REM sleep and shortens REM episodes (Kurogi et al., 2024), and our primary target was the PPN, a key area controlling REM sleep and wakefulness (Mena-Segovia and Bolam, 2017), which may explain our observations.

Astrocytes have been shown to affect movement in various disease states. For instance, acute chemogenetic activation of astrocytes using Gi-coupled DREADDs improved movement impairment in a mouse model of Parkinson's disease (Evans et al., 2025). Interestingly, chronic chemogenetic stimulation of serotonergic neurons in the dorsal raphe produces circadian motor changes similar to our findings: increased activity during the light (resting) phase and reduced movement in the dark (active) phase (Urban et al., 2016). These parallels could stem from the known role of the dorsal raphe in regulating activity cycles, or they might

result from indirect raphe neuron activation (via PPN-mediated effects) or direct stimulation (because DREADD expression partially overlaps with the dorsal raphe).

5.5. Limitations of the study

While our study clearly showed that astrocyte overactivation leads to significant motor changes, several limitations should be considered when interpreting the results. First, although we targeted astrocyte activation primarily in the MLR (centered on the PPN), mCherry labelling was not strictly confined to this region; adjacent areas also showed expression. However, the fact that we observed a sharp reduction in ChAT+ neurons without significant changes in NeuN labelling suggests that cholinergic neuron loss likely drove these behavioural effects. That said, functional alterations in neurons or astrocytes (independent of cell count) may also play a role.

Second, CNO administration relied on voluntary drinking guided by preliminary water intake measurements. Although less precise than forced methods such as daily intraperitoneal injections or CNO depot formulations, this approach minimized stress and avoided confounding behavioural effects from handling-related anxiety or abdominal discomfort. While our voluntary CNO administration protocol may have introduced some variability, we recognize that precise dosing could yield more consistent results with reduced standard errors, potentially indicating that our reported effects are conservative estimates. Similar oral CNO delivery methods were successfully employed in previous studies (Zhan et al. 2019).

A third consideration is CNO's known off-target effects in naive animals. At our working concentration (1 mg/kg), CNO was shown to diminish acoustic startle responses and modify sleep architecture by altering NREM-REM transition latencies (MacLaren et al., 2016; Traut et al., 2023). Higher doses (5-10 mg/kg) have been reported to suppress amphetamine-induced hyperactivity and disrupt NREM/REM sleep cycles without affecting baseline locomotion (MacLaren et al., 2016; Traut et al., 2023; Gomez et al., 2017). To mitigate these confounds, our experimental design was rigorously controlled for CNO/clozapine effects by comparing DREADD-expressing mice with operated controls receiving identical CNO treatments but

lacking DREADDs. Importantly, control animals showed no startle response reduction or significant gait/circadian alterations, suggesting that our observed phenotypes stem from targeted astrocyte activation rather than pharmacological artefacts. We potentially underestimated the actions of PnC and startle network hyperexcitability on the startle reflex, as CNO decreased the startle amplitude.

It is probable that DREADD expression is not limited to the PPN area and that other regions have been affected as well, even though AAV viral injection of DREADDs is the best option for achieving a more localised effect. To solve this issue as effectively as possible, stereotaxic equipment, post hoc histological examination, and elimination of mice with limited expression were used. As previously established, the acoustic startle reflex can be affected by CNO alone, regardless of DREADD expression (MacLaren et al., 2016). Importantly, although the most probable cause of cholinergic neuron loss in the background of behavioural findings is an excitotoxic lesion related to gliotransmitters released from overstimulated astrocytes, an alternative explanation is cholinergic neuronal degradation due to loss of physical support from astrocytes.

5.6. Conclusions and clinical implications

This study successfully addressed its primary aims, providing critical insights into the functional role of astrocytes in the PPN and developing animal model for PSP.

1. Regarding to astrocytic overstimulation within the PPN using chemogenetic tools to precisely investigate the functional role of astrocytes within the PPN. This aim was effectively achieved. The research employed a chemogenetic approach utilizing the hM3D(Gq) system to selectively overstimulate astrocytes within the PPN. The findings demonstrated that prolonged astrocyte overactivation in the PPN, likely through excitotoxic mechanisms, lead to a reduction in cholinergic neuron numbers. Beyond cell loss, functional changes in neuronal activity were observed, contributing to behavioral shifts. Specifically, the study proposed that altered mGluR- and NMDAR-dependent signaling in mesopontine circuits triggered disruptions in circadian

movement patterns, sensory processing, and muscle tone changes. This precise targeting of PPN astrocytes, as intended, allowed for the investigation of their contribution to physiological processes, revealing their previously underappreciated role in PSP progression.

2. Creating an animal model of PSP, that causes damage to the PPN was successfully accomplished. Our study developed an animal model of PSP by inducing astrocyte overactivation in the PPN. Specifically, this model demonstrated that astrocyte activation alone can reproduce comparable deficits to those seen in PSP, including cholinergic neuron loss and behavioral changes resembling brainstem-related symptoms of PSP (e.g., disruptions in movement, sensory processing, and muscle tone). This contrasts with previous PSP models focusing solely on cholinergic neuron loss or beta-amyloid accumulation, thereby establishing beneficial tool for examining the pathophysiology of PSP and identifying potential treatments. The observed decrease in the startle reflex, a characteristic clinical feature of PSP, further validates this model.
3. The KCNQ4 study investigated the impact of KCNQ4 subunit loss on the startle reflex and brainstem hyperexcitability, its conclusion directly informed the understanding of the PPN's role in the observed deficits and the relevance to PSP.
4. In conclusion, this project effectively utilized chemogenetic tools to illuminate the significant role of PPN astrocytes in neurodegeneration and behavioral alterations relevant to PSP. By demonstrating that astrocyte activation alone can induce PSP-like deficits, the study not only achieved its stated aims but also opened new avenues for therapeutic intervention targeting astrocytes to potentially slow disease progression.

In future research, should invistagate pharmacological agents like the GluN2B NMDA receptor antagonist memantine to target the affected neural pathways to assist in identifying the cause. If the cause is truly excitotoxic in nature due to excessive glutamate release from

astrocytes, the use of memantine will ameliorate symptoms and decreases the reduction in neuronal populations.

6. References

1. Abbott NJ. Astrocyte-endothelial interactions and blood-brain barrier permeability. J Anat. 2002 Jun;200(6):629-38. doi: 10.1046/j.1469-7580.2002.00064.x. PMID: 12162730; PMCID: PMC1570746.

2. Adamsky A, Kol A, Kreisel T, Doron A, Ozeri-Engelhard N, Melcer T, Refaeli R, Horn H, Regev L, Groysman M, London M, Goshen I. Astrocytic activation generates de novo neuronal potentiation and memory enhancement. Cell. 2018 Jun 28;174(1):59-71.e14. doi: 10.1016/j.cell.2018.05.002. Epub 2018 May 24. PMID: 29804835.

3. Alderson HL, Latimer MP, Winn P. A functional dissociation of the anterior and posterior pedunculopontine tegmental nucleus: excitotoxic lesions have differential effects on locomotion and the response to nicotine. Brain Struct Funct. 2008 Sep;213(1-2):247-53. doi: 10.1007/s00429-008- 0174-4. Epub 2008 Feb 12. PMID: 18266007; PMCID: PMC2522332.

4. Alexander GM, Rogan SC, Abbas AI, Armbruster BN, Pei Y, Allen JA, Nonneman RJ, Hartmann J, Moy SS, Nicolelis MA, McNamara JO, Roth BL. Remote control of neuronal activity in transgenic mice expressing evolved G protein-coupled receptors. Neuron. 2009 Jul 16;63(1):27-
39. doi: 10.1016/j.neuron.2009.06.014. PMID: 19607790; PMCID: PMC2751885.

5. Allen NJ, Eroglu C. Cell Biology of Astrocyte-synapse interactions. Neuron. 2017 Nov 1;96(3):697-708. doi: 10.1016/j.neuron.2017.09.056. PMID: 29096081; PMCID: PMC5687890.

6. Amédée T, Robert A, Coles JA. Potassium homeostasis and glial energy metabolism. Glia. 1997 Sep;21(1):46-55. doi: 10.1002/(sici)1098-1136(199709)21:1<46:aid-glia5>3.0.co;2-#. PMID: 9298846.

7. Andermann F, Andermann E. Startle disorders of man: hyperekplexia, jumping and startle epilepsy. Brain Dev. 1988;10(4):213-22. doi: 10.1016/s0387-7604(88)80001-9. PMID: 3064625.

8. Araque A, Carmignoto G, Haydon PG, Oliet SH, Robitaille R, Volterra A. Gliotransmitters travel in time and space. Neuron. 2014 Feb 19;81(4):728-39. doi: 10.1016/j.neuron.2014.02.007. PMID: 24559669; PMCID: PMC4107238.

9. Araque A, Parpura V, Sanzgiri RP, Haydon PG. Tripartite synapses: glia, the unacknowledged partner. Trends Neurosci. 1999 May;22(5):208-15. doi: 10.1016/s0166-2236(98)01349-6. PMID: 10322493.

10. Armbruster BN, Li X, Pausch MH, Herlitze S, Roth BL. Evolving the lock to fit the key to create a family of G protein-coupled receptors potently activated by an inert ligand. Proc Natl Acad Sci U S A. 2007 Mar 20;104(12):5163-8. doi: 10.1073/pnas.0700293104. Epub 2007 Mar 2. PMID: 17360345; PMCID: PMC1829280.

11. Armbruster BN, Roth BL. Mining the receptorome. J Biol Chem. 2005 Feb 18;280(7):5129-32. doi: 10.1074/jbc.R400030200. Epub 2004 Dec 8. PMID: 15590622.

12. Atasoy D, Betley JN, Su HH, Sternson SM. Deconstruction of a neural circuit for hunger. Nature. 2012 Aug 9;488(7410):172-7. doi: 10.1038/nature11270. PMID: 22801496; PMCID: PMC3416931.

13. Azzopardi E, Louttit AG, DeOliveira C, Laviolette SR, Schmid S. The role of cholinergic midbrain neurons in startle and prepulse inhibition. J Neurosci. 2018 Oct 10;38(41):8798-8808. doi: 10.1523/JNEUROSCI.0984-18.2018. Epub 2018 Aug 31. PMID: 30171090; PMCID: PMC6596090.

14. Bakker MJ, van Dijk JG, van den Maagdenberg AM, Tijssen MA. Startle syndromes. Lancet Neurol. 2006 Jun;5(6):513-24. doi: 10.1016/S1474-4422(06)70470-7. PMID: 16713923.

15. Bayasgalan T, Stupniki S, Kovács A, Csemer A, Szentesi P, Pocsai K, Dionisio L, Spitzmaul G, Pál B. Alteration of mesopontine cholinergic function by the lack of KCNQ4 subunit. Front Cell Neurosci. 2021 Jul 26;15:707789. doi: 10.3389/fncel.2021.707789. PMID: 34381336; PMCID: PMC8352570.

16. Bayasgalan T, Stupniki S, Kovács A, Csemer A, Szentesi P, Pocsai K, Dionisio L, Spitzmaul G, B P. The KCNQ4-mediated M-current regulates the circadian rhythm in mesopontine cholinergic neurons. bioRxiv; 2020. doi: 10.1101/2020.09.11.293423. PPR:PPR213640.

17. Bazargani N, Attwell D. Astrocyte calcium signaling: the third wave. Nat Neurosci. 2016 Feb;19(2):182-9. doi: 10.1038/nn.4201. PMID: 26814587.

18. Bedard MA, Aghourian M, Legault-Denis C, Postuma RB, Soucy JP, Gagnon JF, Pelletier A, Montplaisir J. Brain cholinergic alterations in idiopathic REM sleep behaviour disorder: a PET imaging study with 18F-FEOBV. Sleep Med. 2019 Jun;58:35-41. doi: 10.1016/j.sleep.2018.12.020. Epub 2019 Jan 6. PMID: 31078078.

19. Belelli D, Harrison NL, Maguire J, Macdonald RL, Walker MC, Cope DW. Extrasynaptic GABAA receptors: form, pharmacology, and function. J Neurosci. 2009 Oct 14;29(41):12757-63. doi: 10.1523/JNEUROSCI.3340-09.2009. PMID: 19828786; PMCID: PMC2784229.

20. Benarroch EE. Pedunculopontine nucleus: functional organization and clinical implications. Neurology. 2013 Mar 19;80(12):1148-55. doi: 10.1212/WNL.0b013e3182886a76. PMID: 23509047.

21. Bevan MD, Bolam JP. Cholinergic, GABAergic, and glutamate-enriched inputs from the mesopontine tegmentum to the subthalamic nucleus in the rat. J Neurosci. 1995 Nov;15(11):7105-
20. doi: 10.1523/JNEUROSCI.15-11-07105.1995. PMID: 7472465; PMCID: PMC6578076.

22. Bohnen NI, Kanel P, Zhou Z, Koeppe RA, Frey KA, Dauer WT, Albin RL, Müller MLTM. Cholinergic system changes of falls and freezing of gait in Parkinson's disease. Ann Neurol. 2019 Apr;85(4):538-549. doi: 10.1002/ana.25430. Epub 2019 Mar 13. PMID: 30720884; PMCID: PMC6450746.

23. Bohnen NI, Müller ML, Koeppe RA, Studenski SA, Kilbourn MA, Frey KA, Albin RL. History of falls in Parkinson disease is associated with reduced cholinergic activity. Neurology. 2009 Nov 17;73(20):1670-6. doi: 10.1212/WNL.0b013e3181c1ded6. PMID: 19917989; PMCID: PMC2788804.

24. Boxer AL, Yu JT, Golbe LI, Litvan I, Lang AE, Höglinger GU. Advances in progressive supranuclear palsy: new diagnostic criteria, biomarkers, and therapeutic approaches. Lancet Neurol. 2017 Jul;16(7):552-563. doi: 10.1016/S1474-4422(17)30157-6. Epub 2017 Jun 13. PMID:
28653647; PMCID: PMC5802400.

25. Boyd JD. Cytoarchitecture of the human brain stem. J Anat. 1955 Jul;89(Pt 3):424. PMCID: PMC1244773.

26. Boyden ES, Zhang F, Bamberg E, Nagel G, Deisseroth K. Millisecond-timescale, genetically targeted optical control of neural activity. Nat Neurosci. 2005 Sep;8(9):1263-8. doi: 10.1038/nn1525. Epub 2005 Aug 14. PMID: 16116447.

27. Brown DA, Passmore GM. Neural KCNQ (Kv7) channels. Br J Pharmacol. 2009 Apr;156(8):1185-95. doi: 10.1111/j.1476-5381.2009.00111.x. Epub 2009 Mar 9. PMID: 19298256; PMCID: PMC2697739.

28. Bull C, Freitas KC, Zou S, Poland RS, Syed WA, Urban DJ, Minter SC, Shelton KL, Hauser KF, Negus SS, Knapp PE, Bowers MS. Rat nucleus accumbens core astrocytes modulate reward and the motivation to self-administer ethanol after abstinence. Neuropsychopharmacology. 2014 Nov;39(12):2835-45. doi: 10.1038/npp.2014.135. Epub 2014 Jun 6. PMID: 24903651; PMCID: PMC4200494.

29. Caggiano V, Leiras R, Goñi-Erro H, Masini D, Bellardita C, Bouvier J, Caldeira V, Fisone G, and Kiehn O (2018). Midbrain circuits that set locomotor speed and gait selection. Nature 553, 455–
460. 10.1038/nature25448.

30. Carignano C, Barila EP, Rías EI, Dionisio L, Aztiria E, Spitzmaul G. Inner hair cell and neuron degeneration contribute to hearing loss in a DFNA2-like mouse model. Neuroscience. 2019 Jul 1;410:202-216. doi: 10.1016/j.neuroscience.2019.05.012. Epub 2019 May 16. PMID: 31102762.

31. Charvériat M, Naus CC, Leybaert L, Sáez JC, Giaume C. Connexin-dependent neuroglial networking as a new therapeutic target. Front Cell Neurosci. 2017 Jun 26;11:174. doi: 10.3389/fncel.2017.00174. PMID: 28694772; PMCID: PMC5483454.

32. Chen G, Lee C, Sandridge SA, Butler HM, Manzoor NF, Kaltenbach JA. Behavioral evidence for possible simultaneous induction of hyperacusis and tinnitus following intense sound exposure. J Assoc Res Otolaryngol. 2013 Jun;14(3):413-24. doi: 10.1007/s10162-013-0375-2. Epub 2013 Feb
26. PMID: 23440516; PMCID: PMC3642276.

33. Choi SS, Lee HJ, Lim I, Satoh J, Kim SU. Human astrocytes: secretome profiles of cytokines and chemokines. PLoS One. 2014 Apr 1;9(4):e92325. doi: 10.1371/journal.pone.0092325. PMID: 24691121; PMCID: PMC3972155.

34. Chung KA, Lobb BM, Nutt JG, Horak FB. Effects of a central cholinesterase inhibitor on reducing falls in Parkinson disease. Neurology. 2010 Oct 5;75(14):1263-9. doi: 10.1212/WNL.0b013e3181f6128c. Epub 2010 Sep 1. PMID: 20810998; PMCID: PMC3013493.

35. Cicirelli G, Impedovo D, Dentamaro V, Marani R, Pirlo G, D'Orazio TR. Human Gait Analysis in Neurodegenerative Diseases: A Review. IEEE J Biomed Health Inform. 2022 Jan;26(1):229-242. doi: 10.1109/JBHI.2021.3092875. Epub 2022 Jan 19. PMID: 34181559.

36. Clarkson AN, Huang BS, Macisaac SE, Mody I, Carmichael ST. Reducing excessive GABA- mediated tonic inhibition promotes functional recovery after stroke. Nature. 2010 Nov 11;468(7321):305-9. doi: 10.1038/nature09511. Epub 2010 Nov 3. PMID: 21048709; PMCID: PMC3058798.

37. Colangelo AM, Alberghina L, Papa M. Astrogliosis as a therapeutic target for neurodegenerative diseases. Neurosci Lett. 2014 Apr 17;565:59-64. doi: 10.1016/j.neulet.2014.01.014. Epub 2014 Jan 20. PMID: 24457173.

38. Comella CL. Sleep disorders in Parkinson's disease: an overview. Mov Disord. 2007 Sep;22 Suppl 17:S367-73. doi: 10.1002/mds.21682. PMID: 18175398.

39. Cope DW, Di Giovanni G, Fyson SJ, Orbán G, Errington AC, Lorincz ML, Gould TM, Carter DA, Crunelli V. Enhanced tonic GABAA inhibition in typical absence epilepsy. Nat Med. 2009 Dec;15(12):1392-8. doi: 10.1038/nm.2058. Epub 2009 Nov 22. PMID: 19966779; PMCID: PMC2824149.

40. Csemer A, Kovács A, Maamrah B, Pocsai K, Korpás K, Klekner Á, Szücs P, Nánási PP, Pál B. Astrocyte- and NMDA receptor-dependent slow inward currents differently contribute to synaptic plasticity in an age-dependent manner in mouse and human neocortex. Aging Cell. 2023 Sep;22(9):e13939. doi: 10.1111/acel.13939. Epub 2023 Jul 25. PMID: 37489544; PMCID:

PMC10497838.

41. Cyr M, Parent MJ, Mechawar N, Rosa-Neto P, Soucy JP, Clark SD, Aghourian M, Bedard MA. Deficit in sustained attention following selective cholinergic lesion of the pedunculopontine tegmental nucleus in rat, as measured with both post-mortem immunocytochemistry and in vivo PET imaging with [^{18}F]fluoroethoxybenzovesamicol. Behav Brain Res. 2015 Feb 1;278:107-14. doi: 10.1016/j.bbr.2014.09.021. Epub 2014 Sep 22. PMID: 25257103.

42. Dallérac G, Rouach N. Astrocytes as new targets to improve cognitive functions. Prog Neurobiol. 2016 Sep;144:48-67. doi: 10.1016/j.pneurobio.2016.01.003. Epub 2016 Mar 8. PMID: 26969413.

43. Datta S, Maclean RR. Neurobiological mechanisms for the regulation of mammalian sleep-wake behavior: reinterpretation of historical evidence and inclusion of contemporary cellular and molecular evidence. Neurosci Biobehav Rev. 2007;31(5):775-824. doi: 10.1016/j.neubiorev.2007.02.004. Epub 2007 Mar 12. PMID: 17445891; PMCID: PMC1955686.

44. Dautan D, Hacioğlu Bay H, Bolam JP, Gerdjikov TV, Mena-Segovia J. Extrinsic sources of cholinergic innervation of the striatal complex: a whole-brain mapping analysis. Front Neuroanat. 2016 Jan 22;10:1. doi: 10.3389/fnana.2016.00001. PMID: 26834571; PMCID: PMC4722731.

45. Dautan D, Huerta-Ocampo I, Witten IB, Deisseroth K, Bolam JP, Gerdjikov T, Mena-Segovia J. A major external source of cholinergic innervation of the striatum and nucleus accumbens originates in the brainstem. J Neurosci. 2014 Mar 26;34(13):4509-18. doi: 10.1523/JNEUROSCI.5071- 13.2014. PMID: 24671996; PMCID: PMC3965779.

46. Dautan D, Kovács A, Bayasgalan T, Diaz-Acevedo MA, Pal B, Mena-Segovia J. Modulation of motor behavior by the mesencephalic locomotor region. Cell Rep. 2021 Aug 24;36(8):109594. doi: 10.1016/j.celrep.2021.109594. PMID: 34433068; PMCID: PMC8641693.

47. Dautan D, Souza AS, Huerta-Ocampo I, Valencia M, Assous M, Witten IB, Deisseroth K, Tepper JM, Bolam JP, Gerdjikov TV, Mena-Segovia J. Segregated cholinergic transmission modulates dopamine neurons integrated in distinct functional circuits. Nat Neurosci. 2016 Aug;19(8):1025-33. doi: 10.1038/nn.4335. Epub 2016 Jun 27. PMID: 27348215; PMCID: PMC5086413.

48. Davis M. Neurochemical modulation of sensory-motor reactivity: acoustic and tactile startle reflexes. Neurosci Biobehav Rev. 1980 Summer;4(2):241-63. doi: 10.1016/0149-7634(80)90016-0. PMID: 6106916.

49. Delcourte S, Bouloufa A, Rovera R, Bétry C, Abrial E, Dkhissi-Benyahya O, Heinrich C, Marcy G, Raineteau O, Haddjeri N, Lucas G, Etiévant A. Chemogenetic activation of prefrontal astroglia enhances recognition memory performance in rat. Biomed Pharmacother. 2023 Oct;166:115384. doi: 10.1016/j.biopha.2023.115384. Epub 2023 Aug 31. PMID: 37657260.

50. Delmas P, Brown DA. Pathways modulating neural KCNQ/M (Kv7) potassium channels. Nat Rev Neurosci. 2005 Nov;6(11):850-62. doi: 10.1038/nrn1785. PMID: 16261179.

51. Dong S, Rogan SC, Roth BL. Directed molecular evolution of DREADDs: a generic approach to creating next-generation RASSLs. Nat Protoc. 2010 Mar;5(3):561-73. doi: 10.1038/nprot.2009.239. Epub 2010 Feb 25. PMID: 20203671.

52. Dreissen YE, Bakker MJ, Koelman JH, Tijssen MA. Exaggerated startle reactions. Clin Neurophysiol. 2012 Jan;123(1):34-44. doi: 10.1016/j.clinph.2011.09.022. Epub 2011 Oct 26. PMID: 22033030.

53. Dreissen YE, Tijssen MA. The startle syndromes: physiology and treatment. Epilepsia.

2012 Dec;53 Suppl 7:3-11. doi: 10.1111/j.1528-1167.2012.03709.x. PMID: 23153204.

54. Egerton T, Williams DR, Iansek R. Comparison of gait in progressive supranuclear palsy, Parkinson's disease and healthy older adults. BMC Neurol. 2012 Oct 2;12:116. doi: 10.1186/1471- 2377-12-116. PMID: 23031506; PMCID: PMC3517411.

55. Ellwanger J, Geyer MA, Braff DL. The relationship of age to prepulse inhibition and habituation of the acoustic startle response. Biol Psychol. 2003 Mar;62(3):175-95. doi: 10.1016/s0301-0511(02)00126-6. PMID: 12633977.

56. Ertuglu LA, Aydin A, Kumru H, Valls-Sole J, Opisso E, Cecen S, Türker KS. Jendrassik maneuver effect on spinal and brainstem reflexes. Exp Brain Res. 2019 Dec;237(12):3265-3271. doi: 10.1007/s00221-019-05668-y. Epub 2019 Oct 24. PMID: 31650212.

57. Eulenburg V, Gomeza J. Neurotransmitter transporters expressed in glial cells as regulators of synapse function. Brain Res Rev. 2010 May;63(1-2):103-12. doi: 10.1016/j.brainresrev.2010.01.003. Epub 2010 Jan 26. PMID: 20097227.

58. Evans WR, Baskar SS, Vellore A, Costa ARCE, Jacob C, Ravoori S, Arigbe A, Huda R. Chemogenetic control of striatal astrocytes improves parkinsonian motor deficits in mice. Glia. 2025 Jun;73(6):1188-1202. doi: 10.1002/glia.24679. Epub 2025 Feb 4. PMID: 39902809; PMCID: PMC12012328.

59. Feng MC, Courtney CG, Mather M, Dawson ME, Davison GC. Age-related affective modulation of the startle eyeblink response: older adults startle most when viewing positive pictures. Psychol Aging. 2011 Sep;26(3):752-60. doi: 10.1037/a0023110. PMID: 21463060; PMCID: PMC3168692.

60. Garcia-Rill, E. (2015). Waking and the reticular activating system in health and disease, 978-0- 12-801385-4. doi.org/10.1016/C2014-0-00011-1.

61. Gerber U, Gee CE, Benquet P. Metabotropic glutamate receptors: intracellular signaling pathways. Curr Opin Pharmacol. 2007 Feb;7(1):56-61. doi: 10.1016/j.coph.2006.08.008. Epub 2006 Oct 19. PMID: 17055336.

62. Girirajan S, Patel N, Slager RE, Tokarz ME, Bucan M, Wiley JL, Elsea SH. How much is too much? Phenotypic consequences of Rai1 overexpression in mice. Eur J Hum Genet. 2008 Aug;16(8):941-54. doi: 10.1038/ejhg.2008.21. Epub 2008 Feb 20. PMID: 18285828.

63. Gironell A, Kulisevsky J, Roig C, Pascual-Sedano B, Rodríguez-Fornells A, Otermin P. Diagnostic potential of acoustic startle reflex, acoustic blink reflex, and electro-oculography in progressive supranuclear palsy: a prospective study. Mov Disord. 2003 Nov;18(11):1273-9. doi: 10.1002/mds.10529. PMID: 14639667.

64. Golob EJ, Miranda GG, Johnson JK, Starr A. Sensory cortical interactions in aging, mild cognitive impairment, and Alzheimer's disease. Neurobiol Aging. 2001 Sep-Oct;22(5):755-63. doi: 10.1016/s0197-4580(01)00244-5. PMID: 11705635.

65. Gomez JL, Bonaventura J, Lesniak W, Mathews WB, Sysa-Shah P, Rodriguez LA, Ellis RJ, Richie CT, Harvey BK, Dannals RF, Pomper MG, Bonci A, Michaelides M. Chemogenetics revealed: DREADD occupancy and activation via converted clozapine. Science. 2017 Aug 4;357(6350):503-507. doi: 10.1126/science.aan2475. PMID: 28774929; PMCID: PMC7309169.

66. Gómez-Gonzalo M, Martin-Fernandez M, Martínez-Murillo R, Mederos S, Hernández-Vivanco A, Jamison S, Fernandez AP, Serrano J, Calero P, Futch HS, Corpas R, Sanfeliu C, Perea G, Araque
A. Neuron-astrocyte signaling is preserved in the aging brain. Glia. 2017 Apr;65(4):569-580. doi: 10.1002/glia.23112. Epub 2017 Jan 28. PMID: 28130845; PMCID: PMC5314210.

67. Gonçalves-Ribeiro J, Pina CC, Sebastião AM, Vaz SH. Glutamate transporters in

hippocampal LTD/LTP: not just prevention of excitotoxicity. Front Cell Neurosci. 2019 Aug 6;13:357. doi: 10.3389/fncel.2019.00357. PMID: 31447647; PMCID: PMC6691053.

68. Gutiérrez R, Heinemann U. Co-existence of GABA and Glu in the hippocampal granule cells: implications for epilepsy. Curr Top Med Chem. 2006;6(10):975-8. doi: 10.2174/156802606777323692. PMID: 16787272.

69. Hallanger AE, Levey AI, Lee HJ, Rye DB, Wainer BH. The origins of cholinergic and other subcortical afferents to the thalamus in the rat. J Comp Neurol. 1987 Aug 1;262(1):105-24. doi: 10.1002/cne.902620109. PMID: 2442206.

70. Hama H, Hara C, Yamaguchi K, Miyawaki A. PKC signaling mediates global enhancement of excitatory synaptogenesis in neurons triggered by local contact with astrocytes. Neuron. 2004 Feb 5;41(3):405-15. doi: 10.1016/s0896-6273(04)00007-8. PMID: 14766179.

71. Hansen HH, Waroux O, Seutin V, Jentsch TJ, Aznar S, Mikkelsen JD. Kv7 channels: interaction with dopaminergic and serotonergic neurotransmission in the CNS. J Physiol. 2008 Apr 1;586(7):1823-32. doi: 10.1113/jphysiol.2007.149450. Epub 2008 Jan 3. PMID: 18174210; PMCID: PMC2375731.

72. Harrison FE, Hosseini AH, McDonald MP. Endogenous anxiety and stress responses in water maze and Barnes maze spatial memory tasks. Behav Brain Res. 2009 Mar 2;198(1):247-51. doi: 10.1016/j.bbr.2008.10.015. Epub 2008 Oct 18. PMID: 18996418; PMCID: PMC2663577.

73. Hartman DE. Wechsler adult intelligence scale IV (WAIS IV): return of the gold standard. Neuropsychol. 2009;16(1):85-7. doi: 10.1080/09084280802644466. PMID: 19205953.

74. Heidenreich M, Lechner SG, Vardanyan V, Wetzel C, Cremers CW, De Leenheer EM, Aránguez G, Moreno-Pelayo MÁ, Jentsch TJ, Lewin GR. KCNQ4 K(+) channels tune mechanoreceptors for normal touch sensation in mouse and man. Nat Neurosci. 2011 Nov 20;15(1):138-45. doi: 10.1038/nn.2985. PMID: 22101641.

75. Héja L, Barabás P, Nyitrai G, Kékesi KA, Lasztóczi B, Toke O, Tárkányi G, Madsen K, Schousboe A, Dobolyi A, Palkovits M, Kardos J. Glutamate uptake triggers transporter-mediated GABA release from astrocytes. PLoS One. 2009 Sep 24;4(9):e7153. doi: 10.1371/journal.pone.0007153. PMID: 19777062; PMCID: PMC2744931.

76. Héja L, Karacs K, Kardos J. Role for GABA and Glu plasma membrane transporters in the interplay of inhibitory and excitatory neurotransmission. Curr Top Med Chem. 2006;6(10):989-95. doi: 10.2174/156802606777323656. PMID: 16787274.

77. Henneberger C, Papouin T, Oliet SH, Rusakov DA. Long-term potentiation depends on release of D-serine from astrocytes. Nature. 2010 Jan 14;463(7278):232-6. doi: 10.1038/nature08673. PMID: 20075918; PMCID: PMC2807667.

78. Herbin M, Gasc JP, Renous S. Symmetrical and asymmetrical gaits in the mouse: patterns to increase velocity. J Comp Physiol A Neuroethol Sens Neural Behav Physiol. 2004 Nov;190(11):895-906. doi: 10.1007/s00359-004-0545-0. Epub 2004 Sep 24. PMID: 15449091.

79. Hernández-Martín N, Martínez MG, Bascuñana P, Fernández de la Rosa R, García-García L, Gómez F, Solas M, Martín ED, Pozo MA. Astrocytic Ca2+ activation by chemogenetics mitigates the effect of kainic acid-induced excitotoxicity on the hippocampus. Glia. 2024 Dec;72(12):2217- 2230. doi: 10.1002/glia.24607. Epub 2024 Aug 26. PMID: 39188024.

80. Herrera-Solís A, Vásquez KG, Prospéro-García O. Acute and subchronic administration of anandamide or oleamide increases REM sleep in rats. Pharmacol Biochem Behav. 2010 Mar;95(1):106-12. doi: 10.1016/j.pbb.2009.12.014. Epub 2010 Jan 7. PMID: 20056119.

81. Hirsch EC, Graybiel AM, Duyckaerts C, Javoy-Agid F. Neuronal loss in the

pedunculopontine tegmental nucleus in Parkinson disease and in progressive supranuclear palsy. Proc Natl Acad Sci U S A. 1987 Aug;84(16):5976-80. doi: 10.1073/pnas.84.16.5976. PMID: 3475716; PMCID: PMC298986.

82. Hirzel K, Müller U, Latal AT, Hülsmann S, Grudzinska J, Seeliger MW, Betz H, Laube B. Hyperekplexia phenotype of glycine receptor alpha1 subunit mutant mice identifies Zn(2+) as an essential endogenous modulator of glycinergic neurotransmission. Neuron. 2006 Nov 22;52(4):679-
90. doi: 10.1016/j.neuron.2006.09.035. PMID: 17114051.

83. Huang Y., Wang S., Wang Q., Zheng C., Yang F., Wei L., Zhou X., Wang Z. Glutamatergic circuits in the pedunculopontine nucleus modulate multiple motor functions. Neurosci. Bull. 2024;40:1713–1731. doi: 10.1007/s12264-024-01314-y.

84. Iivonen H, Nurminen L, Harri M, Tanila H, Puoliväli J. Hypothermia in mice tested in Morris water maze. Behav Brain Res. 2003 May 15;141(2):207-13. doi: 10.1016/s0166-4328(02)00369-8. PMID: 12742257.

85. Isaias IU, Dipaola M, Michi M, Marzegan A, Volkmann J, Rodocanachi Roidi ML, Frigo CA, Cavallari P. Gait initiation in children with Rett syndrome. PLoS One. 2014 Apr 17;9(4):e92736. doi: 10.1371/journal.pone.0092736. PMID: 24743294; PMCID: PMC3990480.

J. F. Emard, J. P. Thouez, and D. Gauvreau, “neurodegenerative diseases and risk factors: A literature review,” Social Sci. Med., vol. 40, no. 6, pp. 847–858, 1995.

86. Jankovic J, Tintner R. Dystonia and parkinsonism. Parkinsonism relat disord. 2001 Oct;8(2):109-21. doi: 10.1016/s1353-8020(01)00025-6. PMID: 11489676.

87. Jellinger K. The pedunculopontine nucleus in Parkinson's disease, progressive supranuclear palsy and Alzheimer's disease. J Neurol Neurosurg Psychiatry. 1988 Apr;51(4):540-3. doi: 10.1136/jnnp.51.4.540. PMID: 3379428; PMCID: PMC1032970.

88. Jellinger KA. Pathomechanisms of neuropsychiatric disturbances in atypical parkinsonian disorders: a current view. J Neural Transm (Vienna). 2025 Apr;132(4):495-518. doi: 10.1007/s00702-025-02890-7. Epub 2025 Feb 15. PMID: 39954076.

89. Jha MK, Kim JH, Song GJ, Lee WH, Lee IK, Lee HW, An SSA, Kim S, Suk K. Functional dissection of astrocyte-secreted proteins: implications in brain health and diseases. Prog Neurobiol. 2018 Mar;162:37-69. doi: 10.1016/j.pneurobio.2017.12.003. Epub 2017 Dec 13. PMID: 29247683.

90. Juncos JL, Hirsch EC, Malessa S, Duyckaerts C, Hersh LB, Agid Y. Mesencephalic cholinergic nuclei in progressive supranuclear palsy. Neurology. 1991 Jan;41(1):25-30. doi: 10.1212/wnl.41.1.25. PMID: 1985290.

91. Kang S, Hong SI, Lee J, Peyton L, Baker M, Choi S, Kim H, Chang SY, Choi DS. Activation of astrocytes in the dorsomedial striatum facilitates transition from habitual to goal-directed reward- seeking behavior. Biol Psychiatry. 2020 Nov 15;88(10):797-808. doi: 10.1016/j.biopsych.2020.04.023. Epub 2020 May 6. PMID: 32564901; PMCID: PMC7584758.

92. Kelland MD, Asdourian D. Pedunculopontine tegmental nucleus-induced inhibition of muscle activity in the rat. Behav Brain Res. 1989 Sep 1;34(3):213-34. doi: 10.1016/s0166-4328(89)80103-2. PMID: 2789701.

93. Kenneth D. Miller, David J. C. MacKay; The Role of constraints in hebbian learning. Neural Comput 1994; 6 (1): 100–126. doi: org/10.1162/neco.1994.6.1.100.

94. Kezunovic N, Urbano FJ, Simon C, Hyde J, Smith K, Garcia-Rill E. Mechanism behind gamma band activity in the pedunculopontine nucleus. Eur J Neurosci. 2011 Aug;34(3):404-15.

doi: 10.1111/j.1460-9568.2011.07766.x. Epub 2011 Jul 4. PMID: 21722210; PMCID: PMC3671604.

95. Kharkovets T, Dedek K, Maier H, Schweizer M, Khimich D, Nouvian R, Vardanyan V, Leuwer R, Moser T, Jentsch TJ. Mice with altered KCNQ4 K+ channels implicate sensory outer hair cells in human progressive deafness. EMBO J. 2006 Feb 8;25(3):642-52. doi: 10.1038/sj.emboj.7600951. Epub 2006 Jan 26. PMID: 16437162; PMCID: PMC1383535.

96. Kharkovets T, Hardelin JP, Safieddine S, Schweizer M, El-Amraoui A, Petit C, Jentsch TJ. KCNQ4, a K+ channel mutated in a form of dominant deafness, is expressed in the inner ear and the central auditory pathway. Proc Natl Acad Sci U S A. 2000 Apr 11;97(8):4333-8. doi: 10.1073/pnas.97.8.4333. PMID: 10760300; PMCID: PMC18242.

97. Kim JH, Michiko N, Choi IS, Kim Y, Jeong JY, Lee MG, Jang IS, Suk K. Aberrant activation of hippocampal astrocytes causes neuroinflammation and cognitive decline in mice. PLoS Biol. 2024 Jul 11;22(7):e3002687. doi: 10.1371/journal.pbio.3002687. PMID: 38991663; PMCID: PMC11239238.

98. King G, Veros KM, MacLaren DAA, Leigh MPK, Spernyak JA, Clark SD. Human wildtype tau expression in cholinergic pedunculopontine tegmental neurons is sufficient to produce PSP-like behavioural deficits and neuropathology. Eur J Neurosci. 2021 Nov;54(10):7688-7709. doi: 10.1111/ejn.15496. Epub 2021 Nov 2. PMID: 34668254; PMCID: PMC9355171.

99. Koch M. The neurobiology of startle. Prog Neurobiol. 1999 Oct;59(2):107-28. doi: 10.1016/s0301-0082(98)00098-7. PMID: 10463792.

100. Kol A, Adamsky A, Groysman M, Kreisel T, London M, Goshen I. Astrocytes contribute to remote memory formation by modulating hippocampal-cortical communication during learning. Nat Neurosci. 2020 Oct;23(10):1229-1239. doi: 10.1038/s41593-020-0679-6. Epub 2020 Aug 3. PMID: 32747787; PMCID: PMC7611962.

101. Kőszeghy Á, Kovács A, Bíró T, Szücs P, Vincze J, Hegyi Z, Antal M, Pál B. Endocannabinoid signaling modulates neurons of the pedunculopontine nucleus (PPN) via astrocytes. Brain Struct Funct. 2015 Sep;220(5):3023-41. doi: 10.1007/s00429-014-0842-5. Epub 2014 Jul 10. PMID: 25009314.

102. Kotagal V, Albin RL, Müller ML, Koeppe RA, Chervin RD, Frey KA, Bohnen NI. Symptoms of rapid eye movement sleep behavior disorder are associated with cholinergic denervation in Parkinson disease. Ann Neurol. 2012 Apr;71(4):560-8. doi: 10.1002/ana.22691. PMID: 22522445; PMCID: PMC3727906.

103. Kovács A, Baksa B, Bayasgalan T, Szentesi P, Csemer A, Pál B. Orexinergic actions modify occurrence of slow inward currents on neurons in the pedunculopontine nucleus. Neuroreport. 2019 Oct 9;30(14):933-938. doi: 10.1097/WNR.0000000000001298. PMID: 31469725.

104. Kovács A, Bordás C, Bíró T, Hegyi Z, Antal M, Szücs P, Pál B. Direct presynaptic and indirect astrocyte-mediated mechanisms both contribute to endocannabinoid signaling in the pedunculopontine nucleus of mice. Brain Struct Funct. 2017 Jan;222(1):247-266. doi: 10.1007/s00429-016-1214-0. Epub 2016 May 11. PMID: 27169390.

105. Kovács A, Bordás C, Pál B. Cholinergic and endocannabinoid neuromodulatory effects overlap on neurons of the pedunculopontine nucleus of mice. Neuroreport. 2015 Mar 25;26(5):273-
8. doi: 10.1097/WNR.0000000000000342. PMID: 25730677.

106. Kovács A, Pál B. Astrocyte-dependent slow inward currents (SICs) participate in neuromodulatory mechanisms in the pedunculopontine nucleus (PPN). Front Cell Neurosci. 2017 Feb 1;11:16. doi: 10.3389/fncel.2017.00016. PMID: 28203147; PMCID: PMC5285330.

107. Kovacs GG, Lukic MJ, Irwin DJ, Arzberger T, Respondek G, Lee EB, Coughlin D, Giese A, Grossman M, Kurz C, McMillan CT, Gelpi E, Compta Y, van Swieten JC, Laat LD, Troakes C, Al-Sarraj S, Robinson JL, Roeber S, Xie SX, Lee VM, Trojanowski JQ, Höglinger GU. Distribution patterns of tau pathology in progressive supranuclear palsy. Acta Neuropathol. 2020 Aug;140(2):99-119. doi: 10.1007/s00401-020-02158-2. Epub 2020 May 7. PMID: 32383020; PMCID: PMC7360645.

108. Krashes MJ, Shah BP, Koda S, Lowell BB. Rapid versus delayed stimulation of feeding by the endogenously released AgRP neuron mediators GABA, NPY, and AgRP. Cell Metab. 2013 Oct 1;18(4):588-95. doi: 10.1016/j.cmet.2013.09.009. PMID: 24093681; PMCID: PMC3822903.

109. Krencik R, Weick JP, Liu Y, Zhang ZJ, Zhang SC. Specification of transplantable astroglial subtypes from human pluripotent stem cells. Nat Biotechnol. 2011 May 22;29(6):528-34. doi: 10.1038/nbt.1877. PMID: 21602806; PMCID: PMC3111840.

110. Krencik R, Zhang SC. Directed differentiation of functional astroglial subtypes from human pluripotent stem cells. Nat Protoc. 2011 Oct 13;6(11):1710-7. doi: 10.1038/nprot.2011.405. PMID: 22011653; PMCID: PMC3198813.

111. Krut' VG, Kalinichenko AL, Maltsev DI, Jappy D, Shevchenko EK, Podgorny OV, Belousov VV. Optogenetic and chemogenetic approaches for modeling neurological disorders in vivo. Prog Neurobiol. 2024 Apr;235:102600. doi: 10.1016/j.pneurobio.2024.102600. Epub 2024 Mar 26. PMID: 38548126.

112. Kumru H, Kofler M, Valls-Solé J, Portell E, Vidal J. Brainstem reflexes are enhanced following severe spinal cord injury and reduced by continuous intrathecal baclofen. Neurorehabil Neural Repair. 2009 Nov;23(9):921-7. doi: 10.1177/1545968309335979. Epub 2009 May 19. PMID: 19454623.

113. Kunkel MT, Peralta EG. Identification of domains conferring G protein regulation on inward rectifier potassium channels. Cell. 1995 Nov 3;83(3):443-9. doi: 10.1016/0092-8674(95)90122-1. PMID: 8521474.

114. Kurogi Y, Sanagi T, Ono D, Tsunematsu T. Chemogenetic activation of astrocytes modulates sleep-wakefulness states in a brain region-dependent manner. Sleep Adv. 2024 Dec 17;5(1):zpae091. doi: 10.1093/sleepadvances/zpae091. PMID: 39717113; PMCID: PMC11664484.

115. Lang PJ, Bradley MM, Cuthbert BN. Emotion, attention, and the startle reflex. Psychol Rev. 1990 Jul;97(3):377-95. PMID: 2200076.

116. Le Duc J, Fournier P, Hébert S. Modulation of Prepulse Inhibition and Startle Reflex by Emotions: A Comparison between Young and Older Adults. Front Aging Neurosci. 2016 Feb 23;8:33. doi: 10.3389/fnagi.2016.00033. PMID: 26941643; PMCID: PMC4763063.

117. Lewerenz J, Maher P. Chronic glutamate toxicity in neurodegenerative diseases-what is the evidence? Front Neurosci. 2015 Dec 16;9:469. doi: 10.3389/fnins.2015.00469. PMID: 26733784; PMCID: PMC4679930.

118. Li D, Agulhon C, Schmidt E, Oheim M, Ropert N. New tools for investigating astrocyte-to-neuron communication. Front Cell Neurosci. 2013 Oct 29;7:193. doi: 10.3389/fncel.2013.00193. PMID: 24194698; PMCID: PMC3810613.

119. Liang SL, Carlson GC, Coulter DA. Dynamic regulation of synaptic GABA release by the glutamate-glutamine cycle in hippocampal area CA1. J Neurosci. 2006 Aug 16;26(33):8537-48. doi: 10.1523/JNEUROSCI.0329-06.2006. PMID: 16914680; PMCID: PMC2471868.

120. Liddelow SA, Guttenplan KA, Clarke LE, Bennett FC, Bohlen CJ, Schirmer L, Bennett ML, Münch AE, Chung WS, Peterson TC, Wilton DK, Frouin A, Napier BA, Panicker N, Kumar

M, Buckwalter MS, Rowitch DH, Dawson VL, Dawson TM, Stevens B, Barres BA. Neurotoxic reactive astrocytes are induced by activated microglia. Nature. 2017 Jan 26;541(7638):481-487. doi: 10.1038/nature21029. Epub 2017 Jan 18. PMID: 28099414; PMCID: PMC5404890.

121. Liegeois-Chauvel C, Morin C, Musolino A, Bancaud J, Chauvel P. Evidence for a contribution of the auditory cortex to audiospinal facilitation in man. Brain. 1989 Apr;112 (Pt 2):375-91. doi: 10.1093/brain/112.2.375. PMID: 2650802.

122. Lin JC, Ho WH, Gurney A, Rosenthal A. The netrin-G1 ligand NGL-1 promotes the outgrowth of thalamocortical axons. Nat Neurosci. 2003 Dec;6(12):1270-6. doi: 10.1038/nn1148. Epub 2003 Nov 2. PMID: 14595443.

123. Lo EH, Rosenberg GA. The neurovascular unit in health and disease: introduction. Stroke. 2009 Mar;40(3 Suppl):S2-3. doi: 10.1161/STROKEAHA.108.534404. Epub 2008 Dec 8. PMID: 19064779; PMCID: PMC2811575.

124. Maamrah B, Pocsai K, Bayasgalan T, Csemer A, Pál B. KCNQ4 potassium channel subunit deletion leads to exaggerated acoustic startle reflex in mice. Neuroreport. 2023 Mar 1;34(4):232-237. doi: 10.1097/WNR.0000000000001883. Epub 2023 Feb 6. PMID: 36789839; PMCID: PMC10399928.

125. Maamrah B, Pocsai K, Hoang BM, Abdelhadi A, Al-Khafaji MQ, Csemer A, Sokvári C, Szentesi P, Pál B. chronic chemogenetic activation of astrocytes in the murine mesopontine region leads to disturbances in circadian activity and movement. Int J Mol Sci. 2025 May 16;26(10):4793. doi: 10.3390/ijms26104793. PMID: 40429935; PMCID: PMC12111845.

126. MacLaren DA, Browne RW, Shaw JK, Krishnan Radhakrishnan S, Khare P, España RA, Clark SD. Clozapine N-Oxide administration produces behavioral effects in long-evans rats: implications for designing DREADD experiments. eNeuro. 2016 Nov 1;3(5):ENEURO.0219- 16.2016. doi: 10.1523/ENEURO.0219-16.2016. PMID: 27822508; PMCID: PMC5089539.

127. MacLaren DAA, Ljungberg TL, Griffin ME, Clark SD. Pedunculopontine tegmentum cholinergic loss leads to a progressive decline in motor abilities and neuropathological changes resembling progressive supranuclear palsy. Eur J Neurosci. 2018 Dec;48(12):3477-3497. doi: 10.1111/ejn.14212. Epub 2018 Nov 9. PMID: 30339310.

128. Malessa S, Gaymard B, Rivaud S, Cervera P, Hirsch E, Verny M, Duyckaerts C, Agid Y, Pierrot-Deseilligny C. Role of pontine nuclei damage in smooth pursuit impairment of progressive supranuclear palsy: a clinical-pathologic study. Neurology. 1994 Apr;44(4):716-21. doi: 10.1212/wnl.44.4.716. PMID: 8164832.

129. Malessa S, Hirsch EC, Cervera P, Javoy-Agid F, Duyckaerts C, Hauw JJ, Agid Y. Progressive supranuclear palsy: loss of choline-acetyltransferase-like immunoreactive neurons in the pontine reticular formation. Neurology. 1991 Oct;41(10):1593-7. doi: 10.1212/wnl.41.10.1593. PMID: 1922800.

130. Marion MH, Qurashi M, Marshall G, Foster O. Is REM sleep behaviour disorder (RBD) a risk factor of dementia in idiopathic Parkinson's disease? J Neurol. 2008 Feb;255(2):192-6. doi: 10.1007/s00415-008-0629-9. Epub 2008 Jan 29. PMID: 18217187.

131. Martinez-Gonzalez C, Bolam JP, Mena-Segovia J. Topographical organization of the pedunculopontine nucleus. Front Neuroanat. 2011 Apr 5;5:22. doi: 10.3389/fnana.2011.00022. PMID: 21503154; PMCID: PMC3074429.

132. Martin-Fernandez M, Jamison S, Robin LM, Zhao Z, Martin ED, Aguilar J, Benneyworth MA, Marsicano G, Araque A. Synapse-specific astrocyte gating of amygdala-related behavior. Nat Neurosci. 2017 Nov;20(11):1540-1548. doi: 10.1038/nn.4649. Epub 2017 Sep 25. PMID: 28945222; PMCID: PMC5903286.

133. Mederos S, Sánchez-Puelles C, Esparza J, Valero M, Ponomarenko A, Perea G. GABAergic signaling to astrocytes in the prefrontal cortex sustains goal-directed behaviors. Nat Neurosci. 2021 Jan;24(1):82-92. doi: 10.1038/s41593-020-00752-x. Epub 2020 Dec 7. PMID: 33288910.

134. Mena-Segovia J, Bolam JP. Rethinking the pedunculopontine nucleus: from cellular organization to function. Neuron. 2017 Apr 5;94(1):7-18. doi: 10.1016/j.neuron.2017.02.027. PMID: 28384477.

135. Mena-Segovia, J., & Bolam, J. P. (2017). Rethinking the Pedunculopontine Nucleus: From Cellular Organization to Function. Neuron, 94(1), 7-18.

136. Mestre TA, Sidiropoulos C, Hamani C, Poon YY, Lozano AM, Lang AE, Moro E. Long-term double-blinded unilateral pedunculopontine area stimulation in Parkinson's disease. Mov Disord. 2016 Oct;31(10):1570-1574. doi: 10.1002/mds.26710. PMID: 27392513.

137. Mitchell IJ, Clarke CE, Boyce S, Robertson RG, Peggs D, Sambrook MA, Crossman AR. Neural mechanisms underlying parkinsonian symptoms based upon regional uptake of 2- deoxyglucose in monkeys exposed to 1-methyl-4-phenyl-1,2,3,6-tetrahydropyridine. Neuroscience. 1989;32(1):213-26. doi: 10.1016/0306-4522(89)90120-6. PMID: 2586750.

138. Murillo-Rodríguez E. The role of the CB1 receptor in the regulation of sleep. Prog Neuropsychopharmacol Biol Psychiatry. 2008 Aug 1;32(6):1420-7. doi: 10.1016/j.pnpbp.2008.04.008. Epub 2008 Apr 18. PMID: 18514375.

139. Nagai J, Yu X, Papouin T, Cheong E, Freeman MR, Monk KR, Hastings MH, Haydon PG, Rowitch D, Shaham S, Khakh BS. Behaviorally consequential astrocytic regulation of neural circuits. Neuron. 2021 Feb 17;109(4):576-596. doi: 10.1016/j.neuron.2020.12.008. Epub 2020 Dec
31. PMID: 33385325; PMCID: PMC7897322.

140. Nawaratne V, Leach K, Suratman N, Loiacono RE, Felder CC, Armbruster BN, Roth BL, Sexton PM, Christopoulos A. New insights into the function of M4 muscarinic acetylcholine receptors gained using a novel allosteric modulator and a DREADD (designer receptor exclusively activated by a designer drug). Mol Pharmacol. 2008 Oct;74(4):1119-31. doi: 10.1124/mol.108.049353. Epub 2008 Jul 15. PMID: 18628403.

141. Nichols CD, Roth BL. Engineered G-protein Coupled Receptors are Powerful Tools to Investigate Biological Processes and Behaviors. Front Mol Neurosci. 2009 Oct 23;2:16. doi: 10.3389/neuro.02.016.2009. PMID: 19893765; PMCID: PMC2773177.

142. Novak CM, Burghardt PR, Levine JA. The use of a running wheel to measure activity in rodents: relationship to energy balance, general activity, and reward. Neurosci Biobehav Rev. 2012 Mar;36(3):1001-1014. doi: 10.1016/j.neubiorev.2011.12.012. Epub 2012 Jan 2. PMID:
22230703; PMCID: PMC4455940.

143. Nyul-Toth A, DelFavero J, Mukli P, Tarantini A, Ungvari A, Yabluchanskiy A, Csiszar A, Ungvari Z, Tarantini S. Early manifestation of gait alterations in the Tg2576 mouse model of Alzheimer's disease. Geroscience. 2021 Aug;43(4):1947-1957. doi: 10.1007/s11357-021-00401-6. Epub 2021 Jun 23. PMID: 34160781; PMCID: PMC8492885.

144. Orr AG, Hsiao EC, Wang MM, Ho K, Kim DH, Wang X, Guo W, Kang J, Yu GQ, Adame A, Devidze N, Dubal DB, Masliah E, Conklin BR, Mucke L. Astrocytic adenosine receptor A2A and Gs-coupled signaling regulate memory. Nat Neurosci. 2015 Mar;18(3):423-34. doi: 10.1038/nn.3930. Epub 2015 Jan 26. PMID: 25622143; PMCID: PMC4340760.

145. P. A. Lewis and J. E. Spillane, The Molecular and Clinical Pathology of Neurodegenerative Disease. Academic Press, 2019.

146. Palagini L, Geoffroy PA, Miniati M, Perugi G, Biggio G, Marazziti D, Riemann D. Insomnia, sleep loss, and circadian sleep disturbances in mood disorders: a pathway toward neurodegeneration and neuroprogression? A theoretical review. CNS Spectr. 2022 Jun;27(3):298-
308. doi: 10.1017/S1092852921000018. Epub 2021 Jan 11. PMID: 33427150.

147. Pantoni MM, Carmack SA, Hammam L, Anagnostaras SG. Dopamine and norepinephrine transporter inhibition for long-term fear memory enhancement. Behav Brain Res. 2020 Jan 27; 378:112266. doi: 10.1016/j.bbr.2019.112266. Epub 2019 Sep 30. PMID: 31580915.

148. Penfield, W. (Ed.). (1932). Cytology and cellular pathology of the nervous system (Vol. 2). Hoeber. (Includes Río Hortega's chapter on neuroglia).

149. Pereira EA, Muthusamy KA, De Pennington N, Joint CA, Aziz TZ. Deep brain stimulation of the pedunculopontine nucleus in Parkinson's disease. Preliminary experience at Oxford. Br J Neurosurg. 2008;22 Suppl 1:S41-4. doi: 10.1080/02688690802448335. PMID: 19085352.

150. Phatnani H, Maniatis T. Astrocytes in neurodegenerative disease. Cold Spring Harb Perspect Biol. 2015 Apr 15;7(6):a020628. doi: 10.1101/cshperspect.a020628. PMID: 25877220; PMCID: PMC4448607.

151. Pienaar IS, Gartside SE, Sharma P, De Paola V, Gretenkord S, Withers D, Elson JL, Dexter DT. Pharmacogenetic stimulation of cholinergic pedunculopontine neurons reverses motor deficits in a rat model of Parkinson's disease. Mol Neurodegener. 2015 Sep 23;10:47. doi: 10.1186/s13024-015-0044-5. PMID: 26394842; PMCID: PMC4580350.

152. Pisani A, Bernardi G, Ding J, Surmeier DJ. Re-emergence of striatal cholinergic interneurons in movement disorders. Trends Neurosci. 2007 Oct;30(10):545-53. doi: 10.1016/j.tins.2007.07.008. Epub 2007 Sep 29. PMID: 17904652.

153. Plaha P, Gill SS. Bilateral deep brain stimulation of the pedunculopontine nucleus for Parkinson's disease. Neuroreport. 2005 Nov 28;16(17):1883-7. doi: 10.1097/01.wnr.0000187637. 20771.a0. PMID: 16272872.

154. Popov A, Brazhe A, Denisov P, Sutyagina O, Li L, Lazareva N, Verkhratsky A, Semyanov A. Astrocyte dystrophy in ageing brain parallels impaired synaptic plasticity. Aging Cell. 2021 Mar;20(3):e13334. doi: 10.1111/acel.13334. Epub 2021 Mar 6. PMID: 33675569; PMCID: PMC7963330.

155. Porsolt RD, Le Pichon M, Jalfre M. Depression: a new animal model sensitive to antidepressant treatments. Nature. 1977 Apr 21;266(5604):730-2. doi: 10.1038/266730a0. PMID: 559941.

156. Rasmussen R, Nicholas E, Petersen NC, Dietz AG, Xu Q, Sun Q, Nedergaard M. Cortex-wide changes in extracellular potassium ions parallel brain state transitions in awake behaving mice. Cell Rep. 2019 Jul 30;28(5):1182-1194.e4. doi: 10.1016/j.celrep.2019.06.082. PMID: 31365863; PMCID: PMC6790006.

157. Reuveny E, Slesinger PA, Inglese J, Morales JM, Iñiguez-Lluhi JA, Lefkowitz RJ, Bourne HR, Jan YN, Jan LY. Activation of the cloned muscarinic potassium channel by G protein beta gamma subunits. Nature. 1994 Jul 14;370(6485):143-6. doi: 10.1038/370143a0. PMID: 8022483.

158. Ridet JL, Malhotra SK, Privat A, Gage FH. Reactive astrocytes: cellular and molecular cues to biological function. Trends Neurosci. 1997 Dec;20(12):570-7. doi: 10.1016/s0166- 2236(97)01139-9. Erratum in: Trends Neurosci 1998 Feb;21(2):80. PMID: 9416670.

159. Ringman JM, Simmons JH. Treatment of REM sleep behavior disorder with

donepezil: a report of three cases. Neurology. 2000 Sep 26;55(6):870-1. doi: 10.1212/wnl.55.6.870. PMID: 10994012.

160. Riva P, Battaglia C, Venturin M. Emerging role of genetic alterations affecting exosome biology in neurodegenerative diseases. Int J Mol Sci. 2019 Aug 23;20(17):4113. doi: 10.3390/ijms20174113. PMID: 31450727; PMCID: PMC6747137.

161. Robillard KN, Lee KM, Chiu KB, MacLean AG. Glial cell morphological and density changes through the lifespan of rhesus macaques. Brain Behav Immun. 2016 Jul;55:60-69. doi: 10.1016/j.bbi.2016.01.006. Epub 2016 Feb 2. PMID: 26851132; PMCID: PMC4899176.

162. Rose CR, Felix L, Zeug A, Dietrich D, Reiner A, Henneberger C. Astroglial glutamate signaling and uptake in the hippocampus. Front Mol Neurosci. 2018 Jan 17;10:451. doi: 10.3389/fnmol.2017.00451. PMID: 29386994; PMCID: PMC5776105.

163. Roseberry TK, Lee AM, Lalive AL, Wilbrecht L, Bonci A, and Kreitzer AC (2016). Cell-Type-Specific Control of Brainstem Locomotor Circuits by Basal Ganglia. Cell 164, 526–537. 10.1016/j.cell.2015.12.037.

164. Roth BL. DREADDs for neuroscientists. Neuron. 2016 Feb 17;89(4):683-94. doi: 10.1016/j.neuron.2016.01.040. PMID: 26889809; PMCID: PMC4759656.

165. Roth RH, Ding JB. From Neurons to cognition: Technologies for precise recording of neural activity underlying behavior. BME Front. 2020 Dec 25;2020:7190517. doi: 10.34133/2020/7190517. PMID: 37849967; PMCID: PMC10521756.

166. Sakai K, Koyama Y. Are there cholinergic and non-cholinergic paradoxical sleep-on neurones in the pons? Neuroreport. 1996 Nov 4;7(15-17):2449-53. doi: 10.1097/00001756-199611040-00009. PMID: 8981401.

167. Salloum RH, Yurosko C, Santiago L, Sandridge SA, Kaltenbach JA. Induction of enhanced acoustic startle response by noise exposure: dependence on exposure conditions and

testing parameters and possible relevance to hyperacusis. PLoS One. 2014 Oct 31;9(10):e111747. doi: 10.1371/journal.pone.0111747. PMID: 25360877; PMCID: PMC4216136.

168. Santello M, Toni N, Volterra A. Astrocyte function from information processing to cognition and cognitive impairment. Nat Neurosci. 2019 Feb;22(2):154-166. doi: 10.1038/s41593- 018-0325-8. Epub 2019 Jan 21. PMID: 30664773.

169. Sasse LK, Gamer M, Büchel C, Brassen S. Selective control of attention supports the positivity effect in aging. PLoS One. 2014 Aug 5;9(8):e104180. doi: 10.1371/journal.pone.0104180. PMID: 25093459; PMCID: PMC4122404.

170. Savtchouk I, Volterra A. Gliotransmission: Beyond black-and-white. J Neurosci. 2018 Jan 3;38(1):14-25. doi: 10.1523/JNEUROSCI.0017-17.2017. PMID: 29298905; PMCID: PMC6705815.

171. Schmidt BZ, Lehmann M, Gutbier S, Nembo E, Noel S, Smirnova L, Forsby A, Hescheler J, Avci HX, Hartung T, Leist M, Kobolák J, Dinnyés A. In vitro acute and developmental neurotoxicity screening: an overview of cellular platforms and high-throughput technical possibilities. Arch Toxicol. 2017 Jan;91(1):1-33. doi: 10.1007/s00204-016-1805-9. Epub 2016 Aug
4. PMID: 27492622.

172. Scofield MD, Boger HA, Smith RJ, Li H, Haydon PG, Kalivas PW. Gq-DREADD selectively initiates glial glutamate release and inhibits cue-induced cocaine seeking. Biol Psychiatry. 2015 Oct 1;78(7):441-51. doi: 10.1016/j.biopsych.2015.02.016. Epub 2015 Feb 24. PMID: 25861696; PMCID: PMC4547911.

173. Semyanov A, Walker MC, Kullmann DM, Silver RA. Tonically active GABA A receptors: modulating gain and maintaining the tone. Trends Neurosci. 2004 May;27(5):262-9. doi: 10.1016/j.tins.2004.03.005. PMID: 15111008.

174. Sherwin CM. Voluntary wheel running: a review and novel interpretation. Anim Behav. 1998 Jul;56(1):11-27. doi: 10.1006/anbe.1998.0836. PMID: 9710457.

175. Shik ML, Orlovskiĭ GN, Severin FV. Organizatsiia lokomotornoĭ sinergii [Organization of locomotor synergism]. Biofizika. 1966;11(5):879-86. Russian. PMID: 6000596.

176. Shik ML, Severin FV, Orlovskiĭ GN. Upravlenie khod'boĭ i begom posredstvom elektricheskoĭ stimulatsii srednego mozga [Control of walking and running by means of electric stimulation of the midbrain]. Biofizika. 1966;11(4):659-66. Russian. PMID: 6000625.

177. Sladeczek F, Pin JP, Récasens M, Bockaert J, Weiss S. Glutamate stimulates inositol phosphate formation in striatal neurones. Nature. 1985 Oct 24-30;317(6039):717-9. doi: 10.1038/317717a0. PMID: 2865680.

178. Somogyi J. Functional significance of co-localization of GABA and Glu in nerve terminals: a hypothesis. Curr Top Med Chem. 2006;6(10):969-73. doi: 10.2174/156802606777323737. PMID: 16787271.

179. Squire LR. Memory systems of the brain: a brief history and current perspective. Neurobiol Learn Mem. 2004 Nov;82(3):171-7. doi: 10.1016/j.nlm.2004.06.005. PMID: 15464402.

180. Steele Jc, Richardson Jc, Olszewski J. Progressive supranuclear palsy. A heterogeneous degeneration involving the brain stem, basal ganglia and cerebellum with vertical gaze and pseudobulbar palsy, nuchal dystonia and dementia. Arch Neurol. 1964 Apr;10:333-59. doi: 10.1001/archneur.1964.00460160003001. PMID: 14107684.

181. Steriade M, Dossi RC, Paré D, Oakson G. Fast oscillations (20-40 Hz) in thalamocortical systems and their potentiation by mesopontine cholinergic nuclei in the cat. Proc Natl Acad Sci U S A. 1991 May 15;88(10):4396-400. doi: 10.1073/pnas.88.10.4396. PMID: 2034679; PMCID: PMC51666.

182. Sugiyama H, Ito I, Hirono C. A new type of glutamate receptor linked to inositol phospholipid metabolism. Nature. 1987 Feb 5-11;325(6104):531-3. doi: 10.1038/325531a0. PMID: 2880300.

183. Suthard RL, Jellinger AL, Surets M, Shpokayte M, Pyo AY, Buzharsky MD, Senne RA, Dorst K, Leblanc H, Ramirez S. Chronic Gq activation of ventral hippocampal neurons and astrocytes differentially affects memory and behavior. Neurobiol Aging. 2023 May;125:9-31. doi: 10.1016/j.neurobiolaging.2023.01.007. Epub 2023 Jan 31. PMID: 36801699.

184. Takakusaki K., Chiba R., Nozu T., Okumura T. Brainstem control of locomotion and muscle tone with special reference to the role of the mesopontine tegmentum and medullary reticulospinal systems. J. Neural Transm. 2016;123:695–729. doi: 10.1007/s00702-015-1475-4.

185. Takano T, Han X, Deane R, Zlokovic B, Nedergaard M. Two-photon imaging of astrocytic Ca2+ signaling and the microvasculature in experimental mice models of Alzheimer's disease. Ann N Y Acad Sci. 2007 Feb;1097:40-50. doi: 10.1196/annals.1379.004. PMID: 17413008.

186. Traut J, Mengual JP, Meijer EJ, McKillop LE, Alfonsa H, Hoerder-Suabedissen A, Song SH, Fehér KD, Riemann D, Molnar Z, Akerman CJ, Vyazovskiy VV, Krone LB. Effects of clozapine-N-oxide and compound 21 on sleep in laboratory mice. Elife. 2023 Mar 9;12:e84740. doi: 10.7554/eLife.84740. PMID: 36892930; PMCID: PMC9998087.

187. Tye KM, Deisseroth K. Optogenetic investigation of neural circuits underlying brain disease in animal models. Nat Rev Neurosci. 2012 Mar 20;13(4):251-66. doi: 10.1038/nrn3171. PMID: 22430017; PMCID: PMC6682316.

188. Urban DJ, Zhu H, Marcinkiewcz CA, Michaelides M, Oshibuchi H, Rhea D, Aryal DK, Farrell MS, Lowery-Gionta E, Olsen RH, Wetsel WC, Kash TL, Hurd YL, Tecott LH, Roth BL. Elucidation of the behavioral program and neuronal network encoded by dorsal raphe serotonergic neurons. Neuropsychopharmacology. 2016 Apr;41(5):1404-15. doi: 10.1038/npp.2015.293. Epub 2015 Sep 18. PMID: 26383016; PMCID: PMC4793125.

189. Verkhratsky A, Nedergaard M. Physiology of astroglia. Physiol Rev. 2018 Jan 1;98(1):239-389. doi: 10.1152/physrev.00042.2016. PMID: 29351512; PMCID: PMC6050349.

190. Vincent SR, Satoh K, Armstrong DM, Fibiger HC. Substance P in the ascending cholinergic reticular system. Nature. 1983 Dec 15-21;306(5944):688-91. doi: 10.1038/306688a0. PMID: 6197654.

191. Volterra A, Meldolesi J. Astrocytes, from brain glue to communication elements: the revolution continues. Nat Rev Neurosci. 2005 Aug;6(8):626-40. doi: 10.1038/nrn1722. PMID: 16025096.

192. Wang HL, Morales M. Pedunculopontine and laterodorsal tegmental nuclei contain distinct populations of cholinergic, glutamatergic and GABAergic neurons in the rat. Eur J Neurosci. 2009 Jan;29(2):340-58. doi: 10.1111/j.1460-9568.2008.06576.x. PMID: 19200238; PMCID: PMC3833361.

193. Wang X, Li Y, Zhao J, Yu J, Zhang Q, Xu F, Zhang Y, Zhou Q, Yin C, Hou Z, Wang Q. Activation of astrocyte Gq pathway in hippocampal CA1 region attenuates anesthesia/surgery induced cognitive dysfunction in aged mice. Front Aging Neurosci. 2022 Nov 11;14:1040569. doi: 10.3389/fnagi.2022.1040569. PMID: 36437995; PMCID: PMC9692004.

194. Weinberger M, Hamani C, Hutchison WD, Moro E, Lozano AM, Dostrovsky JO. Pedunculopontine nucleus microelectrode recordings in movement disorder patients. Exp Brain Res. 2008 Jun;188(2):165-74. doi: 10.1007/s00221-008-1349-1. Epub 2008 Mar 18. PMID: 18347783.

195. Wilson DI, MacLaren DA, Winn P. Bar pressing for food: differential consequences of lesions to the anterior versus posterior pedunculopontine. Eur J Neurosci. 2009 Aug;30(3):504-13. doi: 10.1111/j.1460-9568.2009.06836.x. Epub 2009 Jul 15. PMID: 19614747.

196. Xiong B, Alkharabsheh A, Manohar S, Chen GD, Yu N, Zhao X, Salvi R, Sun W. Hyperexcitability of inferior colliculus and acoustic startle reflex with age-related hearing loss. Hear Res. 2017 Jul;350:32-42. doi: 10.1016/j.heares.2017.03.011. Epub 2017 Mar 27. PMID: 28431308; PMCID: PMC9083438.

197. Yiou E, Caderby T, Delafontaine A, Fourcade P, Honeine JL. Balance control during gait initiation: State-of-the-art and research perspectives. World J Orthop. 2017 Nov 18;8(11):815- 828. doi: 10.5312/wjo.v8.i11.815. PMID: 29184756; PMCID: PMC5696609.

198. Zhang C, Ding D, Sun W, Hu BH, Manohar S, Salvi R. Time- and frequency-dependent changes in acoustic startle reflex amplitude following cyclodextrin-induced outer and inner cell loss. Hear Res. 2022b Mar 1;415:108441. doi: 10.1016/j.heares.2022.108441. Epub 2022 Jan 15. PMID: 35065507.

199. Zhang J, Wang M, Wei B, Shi J, Yu T. Research progress in the study of startle reflex to disease states. Neuropsychiatr Dis Treat. 2022a Feb 24;18:427-435. doi: 10.2147/NDT.S351667. PMID: 35237036; PMCID: PMC8884703.

200. Zhang Y, Barres BA. Astrocyte heterogeneity: an underappreciated topic in

neurobiology. Curr Opin Neurobiol. 2010 Oct;20(5):588-94. doi: 10.1016/j.conb.2010.06.005. Epub 2010 Jul 23. PMID: 20655735.

201. Zweig RM, Whitehouse PJ, Casanova MF, Walker LC, Jankel WR, Price DL. Loss of pedunculopontine neurons in progressive supranuclear palsy. Ann Neurol. 1987 Jul;22(1):18-25. doi: 10.1002/ana.410220107. PMID: 3631916.

7. Summary

Our previous in vitro research demonstrated that neuromodulatory actions on astrocytes in the mesopontine region can lead to tonic excitability changes dependent on metabotropic glutamate and N-methyl-D-aspartate receptors. To investigate the in vivo significance of these findings, we conducted a study using chronic chemogenetic activation of mesopontine astrocytes in young adult male mice.

In chronic study, we compared a control group, where mesopontine astrocytes expressed only the mCherry fluorescent tag, to a group expressing the hM3D(Gq) chemogenetic actuator. We conclude that chronic astrocytic activation significantly decreased neuronal numbers in the mesopontine region. Cholinergic neuron numbers were reduced to 54% of control levels, while non-cholinergic neuron numbers dropped to 76%. These findings suggest that chronic astrocytic overactivation, and the subsequent neuronal loss, contributes to disturbances in movement and circadian activity, which resemble brain-related symptomes of PSP. This raises a compelling hypothesis: astrocytic overactivation may play a role in the pathogenesis of PSP.

In KCNQ study, the KCNQ4 is crucial for regulating neuronal excitability, which is involved in the startle reflex. We investigated how the deleted of the KCNQ4 subunit affects the acoustic startle reflex. We found that KCNQ4 knockout mice exhibited a significantly increased acoustic startle reflex. The findings suggest that the amplified startle reflex observed in KCNQ4 knockout animals is likely due to a combination of cochlear damage and altered neuronal excitability within the brain's startle networks.

8. Keywords

Pedunculopontine nucleus (PPN), designer receptor exclusively activated by designer drug (DREEAD), KCNQ4 (Kv7.4), astrocyte, acetylcholine (AC), Mesopontine Regions (MR), non- syndromic hearing loss (DFNA2), acoustic startle reflex (ASR), cuneiform nucleus (CnF).

9. Acknowledgements

I extend my deepest gratitude to the head of department Dr. Csernoch László, individuals and organizations who played pivotal roles in completing my doctoral dissertation.

Supervisor and advisor: I am grateful to my supervisor, Dr. Pál Balázs for his unwavering support, guidance, and feedback throughout this research journey and for allowing me to pursue higher education at the esteemed University of Debrecen. His expertise and encouragement have been instrumental in shaping the direction of my work, and much appreciated for my dissertation advisors (Dr. Botond Gaal, Department of Anatomay, and Dr. Marta Fuzi, Department of Insitute of Behavioural sciences) and special thanks for Prof. Dr. Janos Szollosi.

Family and Friends: Heartfelt appreciation goes to my family for their constant encouragement, understanding, and unwavering belief in my abilities. My mother (Zainab Maamrah), and father (Mr. Imad Maamrah), were the most significant source of motivation for continuing my education and obtaining the highest degree. Post his demise, my family members, including my brother and sisters, backed me up. Their love and support provided the emotional foundation necessary for me to navigate the challenges of doctoral research. With special gratitude, I remember my aunt, (Razzia Maamrah). Though she is no longer with us, her early support was instrumental in initiating during my academic journey, and its impact continues to inspire me.

Colleagues and Research Peers: I am grateful to my colleagues and fellow researchers, Dr Péter Szentesi, Dr Krisztina Pocsai, Dr Andrea Csemer, Ail abdulhadi, , Mustafa Al-Khafaji, Bui Minh, Cintia Sokvári, Ms. Monika Barotane Kovacs who shared their knowledge, insights, and collaborative spirit. The exchange of ideas and discussions greatly enriched the depth and breadth of my research.

Funding Agencies and Institutions: I acknowledge the generous financial support provided by Tempus Public Foundation for funding, scholarships, and resources that facilitated the execution of my research.

Support Staff: A heartfelt acknowledgment to the support staff at the Physiology Department of the University of Debrecen for their assistance in accessing research materials and resources crucial to the completion of this dissertation

This dissertation is a testament to the collaborative effort of many individuals who have contributed to my academic journey. Your support has been immeasurable, and I am deeply grateful for your collective impact on this research.

10. Author Contributions

My primary experimental contributions encompassed comprehensive stereotaxic operations and behavioral tests and their subsequent analysis. Specifically, I performed and analyzed the activity wheel test, which provides insights into general locomotor activity and endurance. I was also responsible for the execution and analysis of the Barnes maze, a valuable tool for assessing spatial learning and memory. Furthermore, I conducted and analyzed the footprint test, offering data on gait patterns and motor coordination, and the startle reflex assessment, which measures sensorimotor gating and reactivity. The analytical work for all these tests was also primarily performed by me. It is important to highlight my critical role in disseminating our findings. I wrote the papers, this comprehensive involvement in the writing process was a significant contribution to the project's success.

Regarding other contributions, A.A. and M.Q.A. were involved in performing the Barnes maze operations, C.S. analyzed the behavioral tests; P.S. supervised the Barnes maze test and the activity wheel test; K.P., A.C. and B.M.H. performed morphological processing of the samples; B.P. initiated the project, analyzed the data.

11. Funding

This work was funded by the National Research Development and Innovation Office (NKFIH-K146873 to B.P.) and the project no. TKP2020-NKA-04, which has been implemented with the support provided from the National Research, Development, and Innovation Fund of Hungary, financed under the 2020-4.1.1-TKP2020 funding scheme. B.M. was supported by the Stipendium Hungaricum PhD programme.

12. List of publications related to dissertation

UNIVERSITY of DEBRECEN

UNIVERSITY AND NATIONAL LIBRARY
UNIVERSITY OF DEBRECEN
H-4002 Egyetem tér 1, Debrecen
Phone: +3652/410-443, email: publikaciok@lib.unideb.hu

Registry number: DEENK//2025.PL
Subject: PhD Publication List

Candidate: Baneen Maamrah
Doctoral School: Doctoral School of Molecular Medicine
MTMT ID: 10087365

List of publications related to the dissertation

1. **Maamrah, B.**, Pocsai, K., Hoang, B. M., Abdelhadi, A., Al-Khafaji, M. Q. M., Csemer, A., Sokvári, C., Szentesi, P., Pál, B.: Chronic Chemogenetic Activation of Astrocytes in the Murine Mesopontine Region Leads to Disturbances in Circadian Activity and Movement.
   Int. J. Mol. Sci. 26 (10), 1-21, 2025.
   DOI: http://dx.doi.org/10.3390/ijms26104793
   IF: 4.9 (2023)

2. **Maamrah, B.**, Pocsai, K., Bayasgalan, T., Csemer, A., Pál, B.: KCNQ4 potassium channel subunit deletion leads to exaggerated acoustic startle reflex in mice.
   Neuroreport. 34 (4), 232-237, 2023.
   DOI: http://dx.doi.org/10.1097/WNR.0000000000001883
   IF: 1.6

List of other publications

3. Csemer, A., Sokvári, C., **Maamrah, B.**, Szabó, L., Korpás, K. L., Pocsai, K., Pál, B.: Pharmacological Activation of Piezo1 Channels Enhances Astrocyte-Neuron Communication via NMDA Receptors in the Murine Neocortex.
   Int. J. Mol. Sci. 25 (7), 3994, 2024.
   DOI: http://dx.doi.org/10.3390/ijms25073994
   IF: 4.9 (2023)

4. Csemer, A., Kovács, A., **Maamrah, B.**, Pocsai, K., Korpás, K. L., Klekner, Á., Szűcs, P., Nánási, P. P., Pál, B.: Astrocyte- and NMDA receptor-dependent slow inward currents differently contribute to synaptic plasticity in an age-dependent manner in mouse and human neocortex. *Aging Cell. 22* (9), e13939, 2023.
DOI: http://dx.doi.org/10.1111/acel.13939
IF: 8

Total IF of journals (all publications): 19,4
Total IF of journals (publications related to the dissertation): 6,5

The Candidate's publication data submitted to the Tudóstér have been validated by DEENK on the basis of the Journal Citation Report (Impact Factor) database.

22 May, 2025